ABSORPTION, FLUORESCENCE AND AMPLIFIED SPONTANEOUS EMISSION

OF BLUE-EMITTING DYES

BY

Christopher Dudley

A thesis submitted in partial fulfillment of
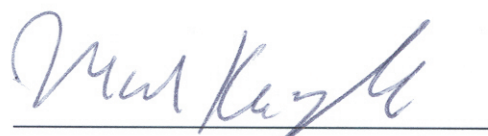
the requirements for the degree of

MASTER OF SCIENCE IN PHYSICS

WASHINGTON STATE UNIVERSITY

Department of Physics

August 2004

To the Faculty of Washington State University:

The members of the Committee appointed to examine the thesis of
CHRISTOPHER DUDLEY find it satisfactory and recommend that it be accepted.

_____
Chair

_____
Matthew S. Mcclure

_____

Acknowledgments

ABSORPTION, FLUORESCENCE AND AMPLIFIED SPONTANEOUS EMISSION OF BLUE-EMITTING DYES

Abstract

By Christopher Dudley, M.S.

Washington State Univsersity

Department of Physics

August 2004

Chair: Mark G. Kuzyk

An acceptor/acceptor conjugated oligomer chromophore, Naval Research Laboratory 303 (NRL303) was rigorously studied in a polymethyl methacrylate (PMMA) matrix. Linear optical studies were conducted with the third harmonic (THG) of an Nd:YAG laser (355nm) and nonlinear studies with the second harmonic (SH) (533nm) and the optical parametric amplification (OPA) wavelengths from a tunable Ti:Saphire laser. The chromophore-doped PMMA matrix strongly fluoresces and is a source of efficient blue light centered around 460nm from amplified spontaneous emission (ASE). Blue emission from this chromophore has higher gain, efficiency and two-photon absorption cross-section (σ_2) than Rhodamine 6G (Rh6G) a benchmark in laser dyes in a solid state system. This chromophore has been successfully made into a blue ASE polymer-fiber light source. A design factor σ_{df} is introduced to investigate the design strategy for making molecules with large TPA cross-section for this class of donor/donor (D/D), acceptor/acceptor (A/A) and acceptor/donor(A/D)chromophore-linked π-centers.

Contents

Appendix 79

List of Tables

List of Figures

Chapter 1

Introduction

Researchers have spent decades trying to develop efficient blue light emitting materials and devices. The search for a viable blue laser has been a driving force of laser research. Blue sources are technologically important both in displays, because blue is a primary color, and in optical storage devices, because the wavelength of blue light is shorter than infra-red or red wavelengths commonly used today in commercial applications. The density of data stored would be three to four times greater for a blue laser over a red laser. Applications for blue light go beyond data storage and displays. Some cancer cells as well as chemical and biological weapons agents are fluorescent when illuminated with blue light. A blue laser printer would have better resolution than current laser printers. Blue lasers coupled to fiber optics could in principle transmit greater bandwidth of information and their use in compact disks and digital videos disk would store more data. Blue lasers should impact applications such as lasers, microscopy, underwater communications and remote sensing as well as organic light emitting diodes and photo/electroluminescent devices. Two-photon absorption applications range from nondestructive microscopy and 3D data storage to optical limiting.

In this work, the dye NRL303 provided by Dr. Oh-Kil Kim from the Naval Research Laboratories was investigated. The generic term dye is defined as a compound that visually appears colored. This occurs from the dye absorbing strongly in parts of the visible spectrum leaving the photons of the colors not absorbed to be seen by the observer.

We are concerned with laser dyes which are similar to common dyes used in food coloring and textiles, but with an absorbtion spectrum that goes beyond just the visible region. Any molecule that has π-electrons (which are highly mobile) with allowable transitions to an excited state can be considered a laser dye. As was shown by Hans Kuhn in the 1940's [36], a π-electron system can be understood by modelling it as a particle in a box: the smaller the conjugation length of the cloud (therefore the smaller the box) the shorter the wavelength of maximum absorption. For a normal "colored" dye, it is the absorption of the dye that is of interest. For a laser dye, the fluorescence wavelength is what is used. In general, laser dyes are excited by optical pumping; however, electron pumping is more amenable to commercial and consumer products. See, for example, the work of Marowsky. [2]

Laser dyes are commonly referred to as chromophores. A chromophore is a chemical group that gives color to a molecule. Most important laser dyes are substituted tricyclic ring structures, such as rhodamine, which has conjugated bonds, (successive single then double bonds), associated with organic dye's typical absorbance in the visible region of the electromagnetic spectrum. Sorokin and Lankard first used a phthalocyanine dye solution to make a laser in 1966. [4] Rhodamine 6G lasing was demonstrated the following year. [5] The large number of commercial dyes that are available has revealed few laser dyes of practical value.

Laser dyes can generally be tuned for operation over a wavelength of 30 to 50nm within the fluorescence band. The lasing wavelength may be tunable for some dyes by varying the dye concentration, solvent (polarity and pH), temperature, or laser cavity parameters. [1, p.11] Over 150 dyes are listed by Maeda [1] to lase between 300 and 500nm. Generally a dye will lase at the wavelength of maximum gain.

Drexhage cataloged over 200 dyes in 1973 [3] and Maeda over 500 in 1984. [1, p.2] Most of the values reported are for dyes in solution. Only about three percent (18 dyes) of the more than 500 dyes reported by Maeda were doped in polymethylmethacrylate (PMMA). Only four dyes of promise were found by Gregg and Thomas in 1969 after screening 1000 commercially available dyes. [8, 3] Dyes that are commercially available are not generally good laser dyes. As such, dye molecules for lasing applications must be carefully designed.

For any dye, stability tends to be a large factor in its usefulness. Most dyes that fluoresce will lase if pumped hard enough provided that the damage threshold of the material is not exceeded.

NRL303 is a conjugated chromophore in the spiro-bifluorene-centered (π-center) acceptor linked (A-π- A) chromophore class of molecules that are known for their electrical and optical properties. [14, 28] Together, the conjugated bridge and electron acceptor pairs increase the optical nonlinearity.

In this work, the laser dye NRL303 was investigated for lasing in the blue region of the visible spectrum and the ability for making a polymer fiber optic laser is demonstrated. In 1963 Wolff & Pressley [6] and also Huffman [7] reported on PMMA polymer lasers sources at 613 and 545nm respectively. Even after 41 years since the first idea of making a polymer laser, there are no commercially available blue fiber lasers. This is understandable since work on blue laser dyes has only recently accelerated, and is limited mostly to commercially available coumarin dyes. In general, dyes in a solid matrix exhibit far less gain than in solvent. So even good dyes identified in solution, often do not lase in dye-doped bulk solid matrix samples.

From this work, NRL303 was found to have an absorbance maximum at 395nm and ASE maximum at 460nm in polymethylmethacrylate (PMMA). This thesis will investigate the ASE gain, efficiency, decay and two photon absorption to determine the two photon cross section. The results will help evaluate a new design scheme for improving these desirable traits in a dye molecule. Only NRL303 in PMMA will be studied since milligram quantities are all that is available from the Naval Research Lab. The usual parallel analysis in solution must be omitted.

Chapter 2

Theory

2.1 Linear Absorbance and Fluorescence

Absorption and fluorescence are well known optical phenomena. Absorbance is defined by

$$A \equiv \log \left(\frac{I_0}{I} \right), \tag{2.1}$$

where I_0 is the intensity incident on the sample and I is the transmitted intensity, which is a function of the depth of material.
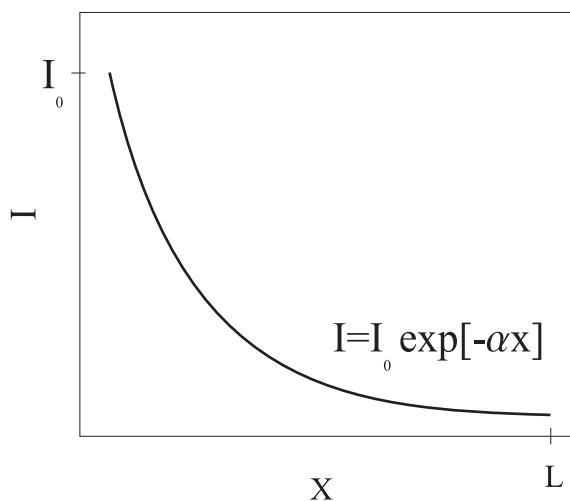
Figure 2.1: Intensity vs depth.

The increase in energy imparted to the electron promotes it to a higher excited state energy. Linear absorption (a one photon process) is independent of incident intensity but

depends on the number or density of available absorbing sites. In a saturable absorption material, the absorption coefficient decreases under high laser energy when all of the molecules in the material are in their excited state.

Since the intensity of light falls off exponentially with the distance propagated through the sample according to $I = I_0 \exp[-\alpha x]$, the relationship between A and the absorption coefficient α is given by,

$$\alpha = \frac{1}{L}\frac{A}{\log e}.$$ (2.2)

The linear absorption cross section σ is defined as the ratio of the absorption coefficient to the number density N,

$$\sigma = \frac{\alpha}{N}.$$ (2.3)

(a) (b) (c)

Nonradiative
Decay To Lowest
Excited State

Excited State

pump

hν
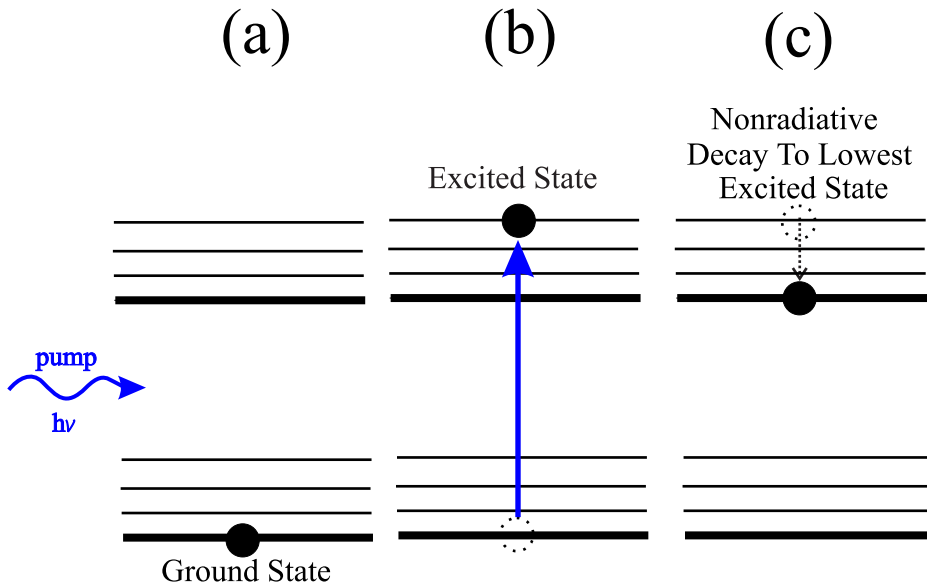
Ground State

Figure 2.2: Absorption of photon. a.) Electron in the ground state, b.) Electron is promoted to an excited state with the energy difference of the photon. c.) Non-radiative decay of the electron to the lowest excited state.

When a photon is absorbed by the sample, the electron is promoted to a higher energy state as shown in Figure 2.2. Absorption of a photon can occur when the photon energy matches the difference between the ground state and one of the excited states. The peak in the absorption spectrum corresponds to ΔE=hν. The subsequent absorbed energy will

be emitted through non-radiative processes or emission or a photon to return the molecule to the ground state. However, if another photon is present, it can stimulate the emission of a photon, causing the system to decay back to the ground state, emitting a photon of the same energy and phase as the stimulating photon. The emitted energy will be less than the absorbed energy if the molecule relaxes non-radiatively to a long lived excited state as shown in Figure 2.2c. The energy difference between the absorbed and emitted photon is called the Stokes shift. As a result, the wavelength of the maximum fluorescence will be longer than the wavelength of maximum absorption.

To understand the energy levels in figure 2.2, we consider a diatomic molecule. S_0 is the electronic ground state and S_1 is the electronic excited state. The curves in figure 2.3 show the energies as a function of the separation of the nuclei. The potential wells of the states S_0 and S_1 can be approximated as harmonic oscillators, whose energies are represented by the closely spaced horizontal lines. These are vibronic states. Since the bond is weaker in the excited state S_1, the equilibrium nuclear distance is larger than the ground state (Figure 2.3).

Potential Energy Curves
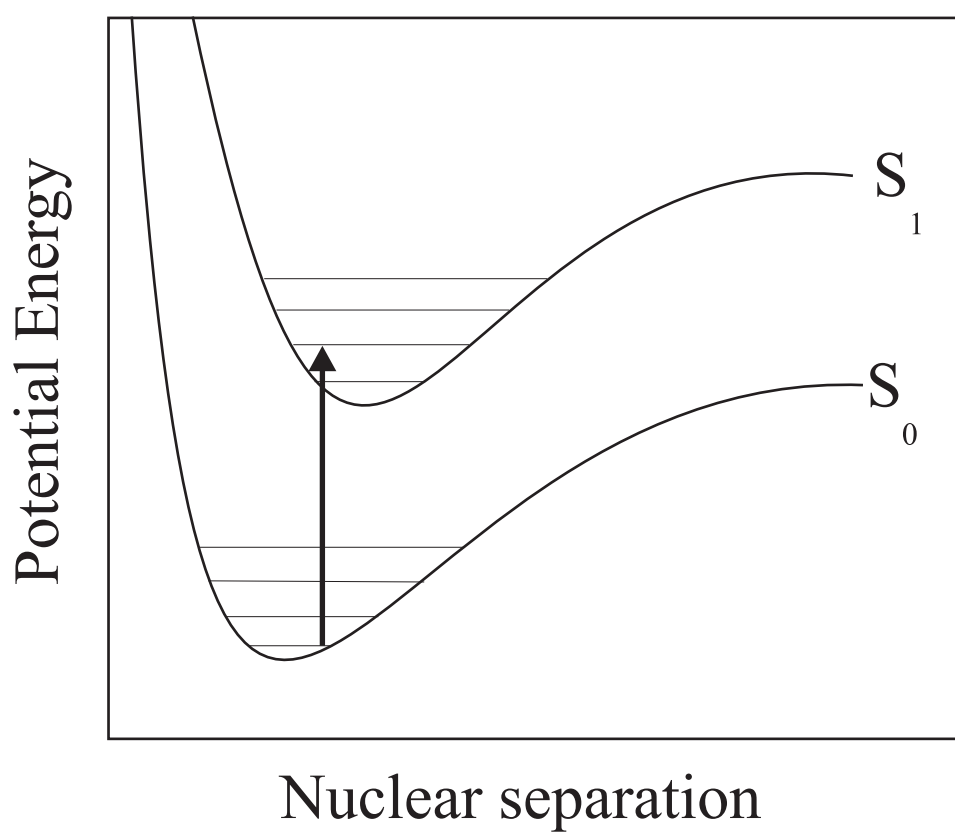
Figure 2.3: Potential Energy Curve for diatomic molecule.

The absorbance spectrum is a fingerprint of the transition from the levels of the ground state S_0 to the Excited State S_1, where the greatest overlap in vibronic state wavefunctions between S_0 and S_1 vibrational levels will have the greater transition peak in the absorbance spectrum. The similarity of the S_0 and S_1 curves leads to a symmetry in the absorbance and fluorescence spectra (Figure 2.4).
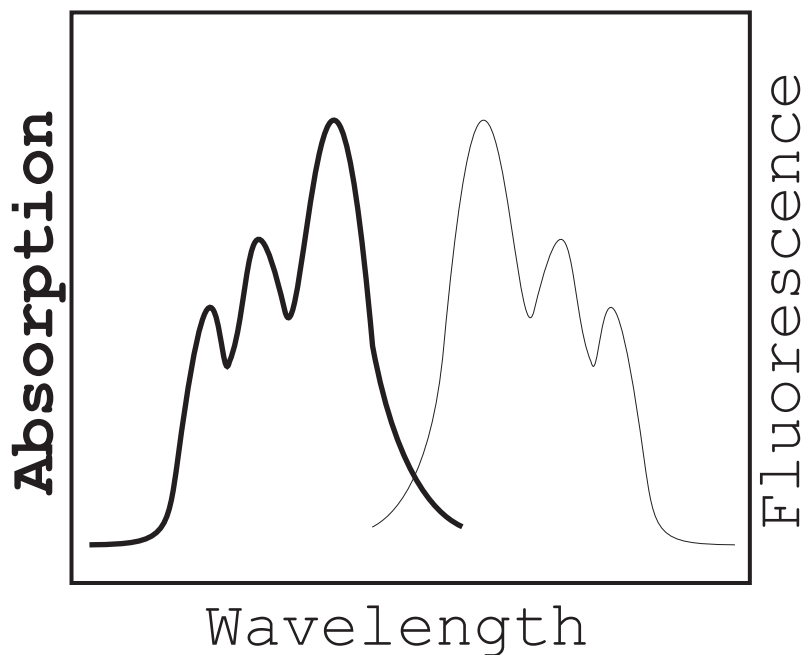
Figure 2.4: Absorption and Fluorescence Spectra.

A laser pump is more efficient than a flash lamp, because its spectrum is narrower and therefore all the light can be tuned to the most efficient absorption wavelength. As little as 1 percent of the flashlamp's energy may be converted but as much as 50 percent of a laser pump can be converted. Secondly, laser pumping has a quicker rise time (on the order of 100ns) and this keeps the population of the triplet state low, where a triplet state is a state having a total spin number equal to one.

2.2 Emission

Once a molecule has absorbed a photon it can emit a photon upon returning to the electronic ground state from the electronic excited state. As with absorbance, the strength of the transition is governed by the transition moment. The related peaks in turn will be the

dominant peaks in the resulting spectrum. Two processes that emit light from a dye molecule are fluorescence, where the emitted photon is from the decay of excited state S_1 to the ground state S_0, and phosphorescence, which is a transition from the triplet state T_1 to the electronic ground state S_0. Most ground states are singlets due to the total spin being zero, cancelled out by pairs of electrons with opposite spin. The direct transition from S_0 to T_1 is forbidden since the value of the spin quantum number S would have to change. Similarly a transition from T_1 to S_0 is slow due to the same reason, resulting in a slow process called phosphorescence. Triplet-triplet absorption bands tend to heavily overlap the fluorescence region. The triplet state has a long lifetime leading to a build up of population inversion. However since the transition from S_0 to T_1 is forbidden, it would require very high dye concentrations for lasing. Fluorescence can be used at relatively low dye concentrations for laser applications. If the triplet state is at a lower energy than S_1, it then competes with the build up of the excited S_1 state, lowering the quantum yield of the fluorescence.

Decay to the lowest level of S_1 is very quick provided that the temperature is low enough to prevent thermal excitation to a higher vibronic level within S_1. The number of excited atoms N where k is the Boltzman's constant is $N_{excited} = N_0 \exp[-\Delta E/kT]$. At room temperature $kT = 2.15 10^{-2} eV$ so the population density of the excited state will be low.

The longevity of different excited states is important to the usefulness of a dye as a laser medium. The typical time scales for these processes are: 1ps from S_2 to S_1 (non-raditative transition), 10ns from S_1 to T_1 (non-raditative transition), 1μs from T_1 to S_0 (phosphorescence) and 1ns from S_1 to S_0 (fluorescence)(Figure 2.5).

2.2.1   Fluorescence

Excitation of a molecule from absorption of a photon or thermal energy promotes the molecule to an excited energy state, setting up the possibility of emission of a photon. The excited molecules may lose energy through a non-radiative process to reach the lowest vibrational level of the excited state. Fluorescence is then the radiative loss of energy as a photon is emitted from a molecule in the excited state returning to the ground state. Since

Excited
Singlet
States

Excited
Triplet
States

Energy Levels

S_2

S_1

nonradiative

Fluorescence

T_2

T_1

S_0 Ground
State

Phosphorescence

$t_{nr} \simeq 1ps$

$t_F \simeq 1ns$

$t_{(S-T)nr} \simeq 10ns$

$t_P \simeq 1\mu s$

—— Absorption

— Fluorescence

– – Phosphorescence
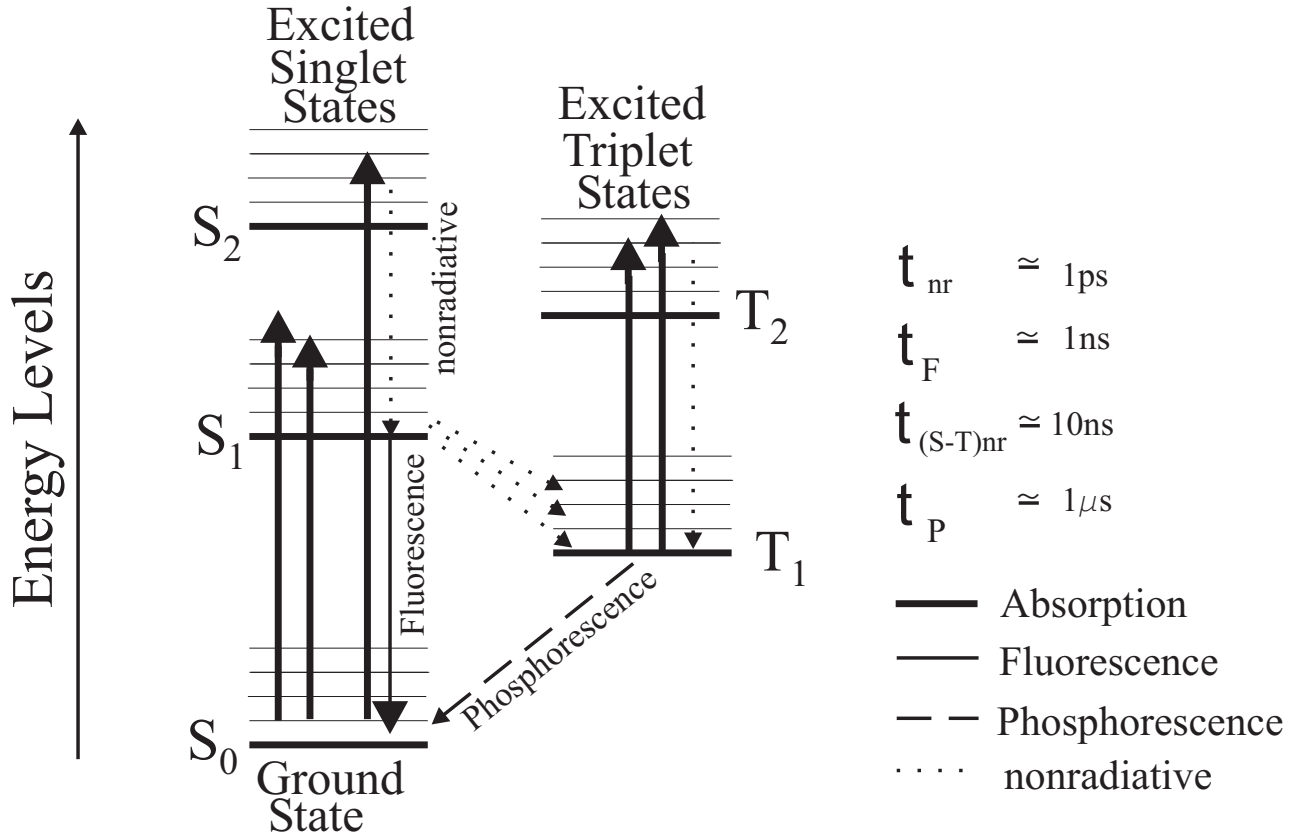
· · · · nonradiative

Figure 2.5: Dye molecule energy states.

a non-radiative loss of energy occurs between the absorption and subsequent fluorescence, the emitted photon is of lower frequency than the absorbed photon producing a red shift between the absorbance and fluorescence spectra.

2.2.2 Stimulated Emission

The ratio between the populations of states S_0 and S_1 is given by,

$$\frac{N_{S_1}}{N_{S_0}} = \exp\left(-\frac{E_{S_1} - E_{S_0}}{kT}\right), \qquad (2.4)$$

where N is the number of molecules in that state, and T the temperature. Since T is typically room temperature, the population of the excited state will be much less the ground state. Optical pumping of a molecule promotes an electron to an excited state. Some of this energy is available for the emission of a photon. Stimulated emission occurs when light stimulates a

dye molecule to emit a coherent photon of the same energy and phase, as shown schematically in figure 2.6.

<div style="text-align:center">(a)   (b)   (c)</div>
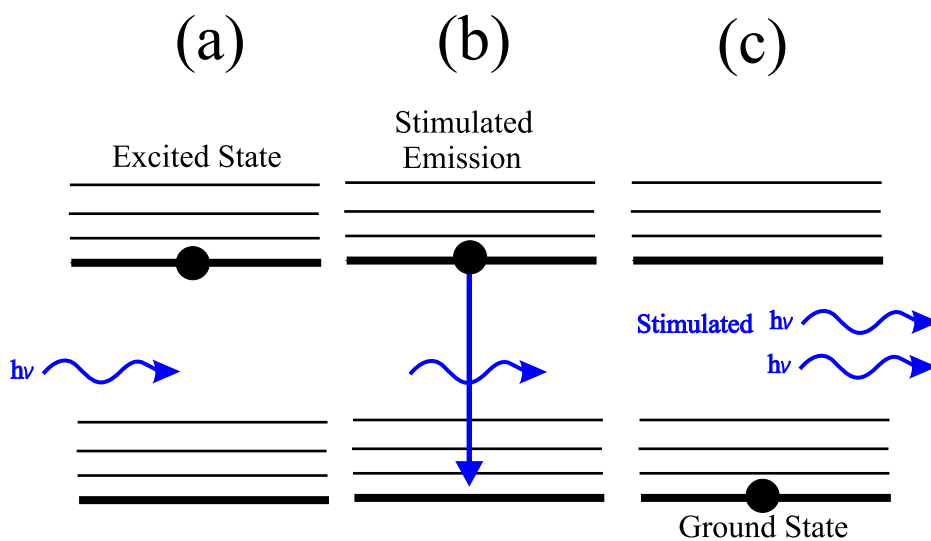
Figure 2.6: Stimulated emission of photon. a.) Electron in the lowest excited state. b.) Photon stimulates emission of a second photon and electron decays to ground state. c.) Electron is in the ground state and there is now a coherent amplification of the original photon.

The stimulated photon will induce another stimulated emission in another molecule and the cycle will continue in a cascade of emission. The state with the lower population will determine if absorption or emission results. This makes apparent the importance of the rise time of a pump pulse. The dipole reacts to the applied pump and the stimulated emission is coherent with the pump. If the purpose of such a procedure is to amplify a separate signal beam, in this regime, spontaneous emission and pump amplification could be unwanted and considered to be noise.

2.2.3   Spontaneous Emission

Spontaneous emission, shown in figure 2.7 will in general be incoherent and emitted randomly in all directions. However if the pump pulse is polarized it will have a preferred emission direction perpendicular to the pump's polarization. Thus, for a source, spontaneous emission will create coherent stimulated emission along its direction of propagation called amplified spontaneous emission (ASE). It should be noted that pump energy and dye concentration

both determine the threshold for ASE. The ASE wavelength will be centered around the part of the fluorescence with the highest gain. ASE appearers in the spectrum as gain narrowing of the fluorescence spectrum occurs since ASE has an exponential dependance the intensity of the incident light.
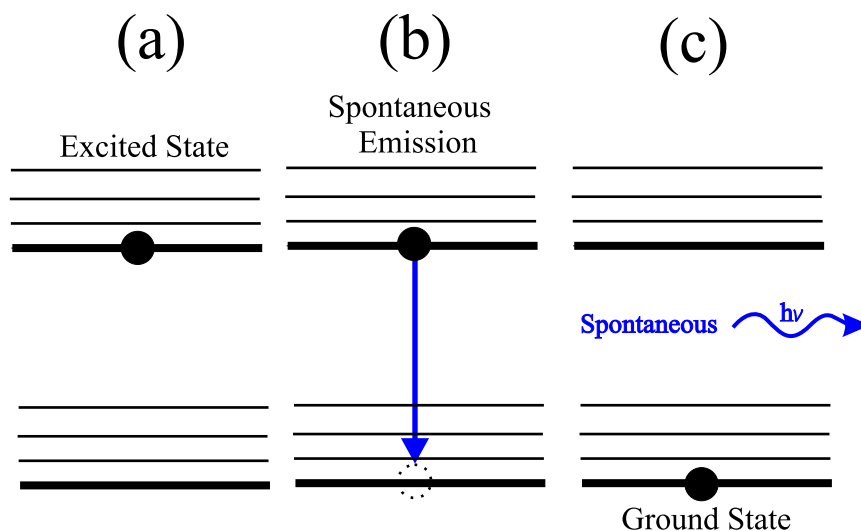
Figure 2.7: Spontaneous emission of a photon. a.) Electron in the lowest excited state. b.) Photon spontaneous decay of electron to the ground state. c.) Electron is in the ground state and a photon has been emitted.

2.2.4 Amplified Spontaneous Emission

The ASE cascade of emission from dye molecules in the excited state is stimulated by the spontaneous emission from other molecules' decay from an excited state. ASE is not, then, a purely spontaneous phenomenon, but spontaneously emitted photons that are amplified by further coherent stimulated emission. The emitted photons will be of the same frequency centered around the wavelength of maximum gain. In materials with high gain, the laser-like amplified spontaneous emission (ASE) occurs without the aid of multiple pass gain build up of a cavity with mirrors. It can require relatively high pump powers in the single pass gain geometry. A signature of amplified spontaneous emission is gain narrowing of the fluorescence spectrum. As the pump intensity increases the spectrum changes from a normal fluorescence to pure ASE. In Figure 2.8 the increase in ASE is seen to grow out of the fluorescence spectrum as a function of incident intensity.
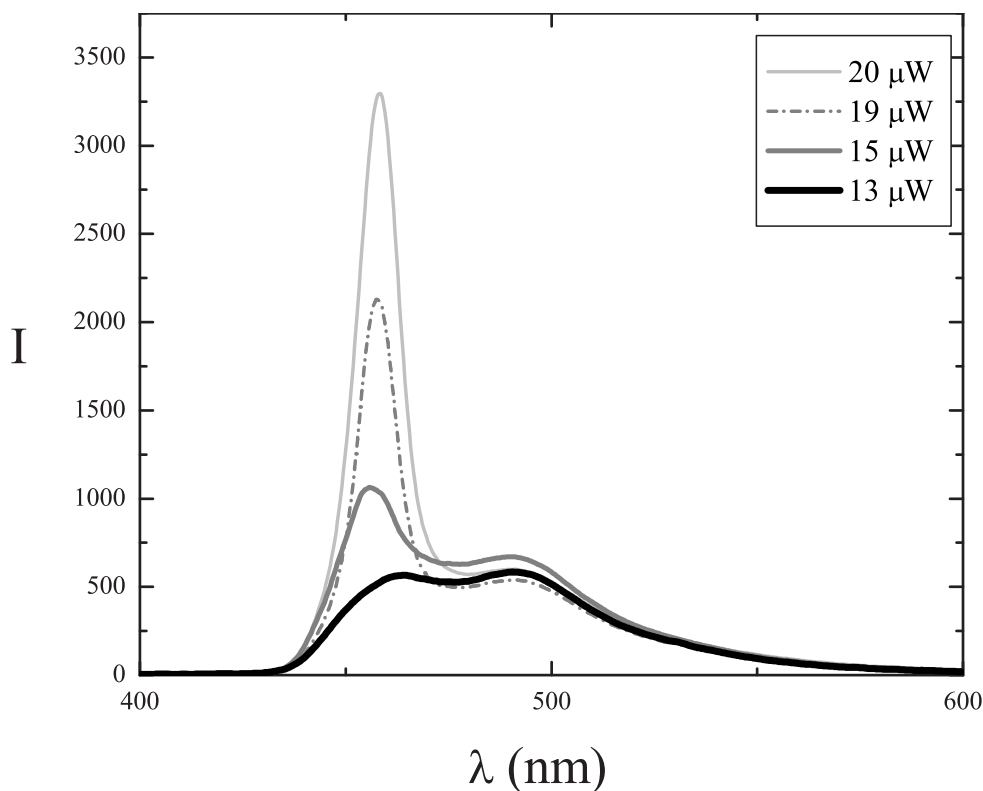
Figure 2.8: ASE as a function of increasing pump power.

The ASE is emitted perpendicular to the polarization of the incident intensity. If the energy of the photon is changed after scattering then it is considered Raman scattering. Photons excite a molecule which loses energy to vibrational or geometric reorientation of the molecule prior to a photon being emitted. The directionality of the emitted ASE due to the dipole nature of the dye molecules is illustrated in Figure 2.9.

2.3   Gain

Gain occurs when the stimulated emission of photons exceeds the reabsorption or loss due to scattering. Laser (Light Amplification by Stimulated Emission of Radiation) light is produced by atoms or molecules in an excited state that are stimulated to emitted coherent "monochromatic" directional light upon returning to the ground state. But, we must have gain (amplification) to lase. When gain exceeds the loss the gain material will lase. So gain is the increase in the number of emitted photons. If the gain is greater than zero then
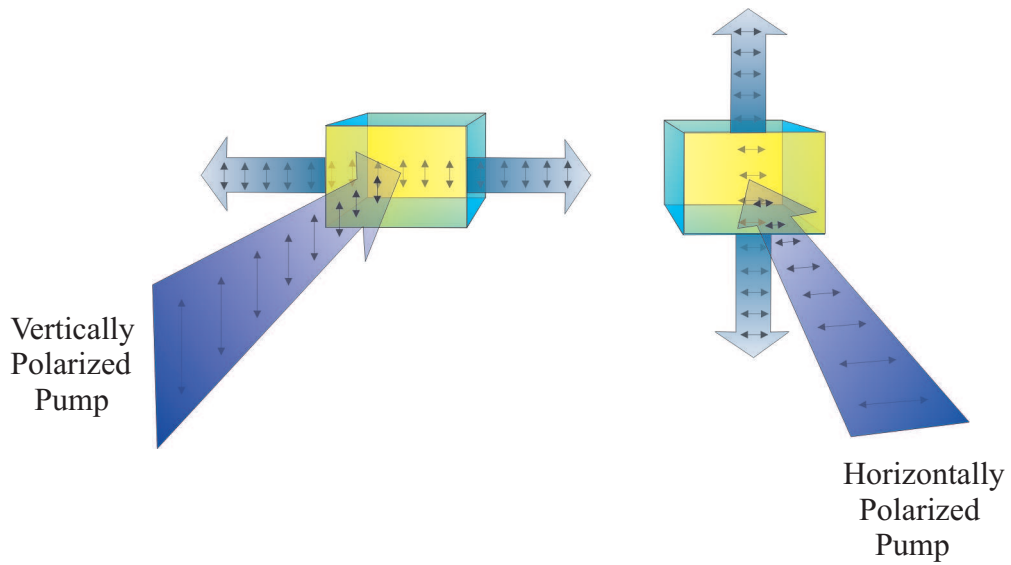
Figure 2.9: Directional ASE output for pump polarization.

(a)   (b)
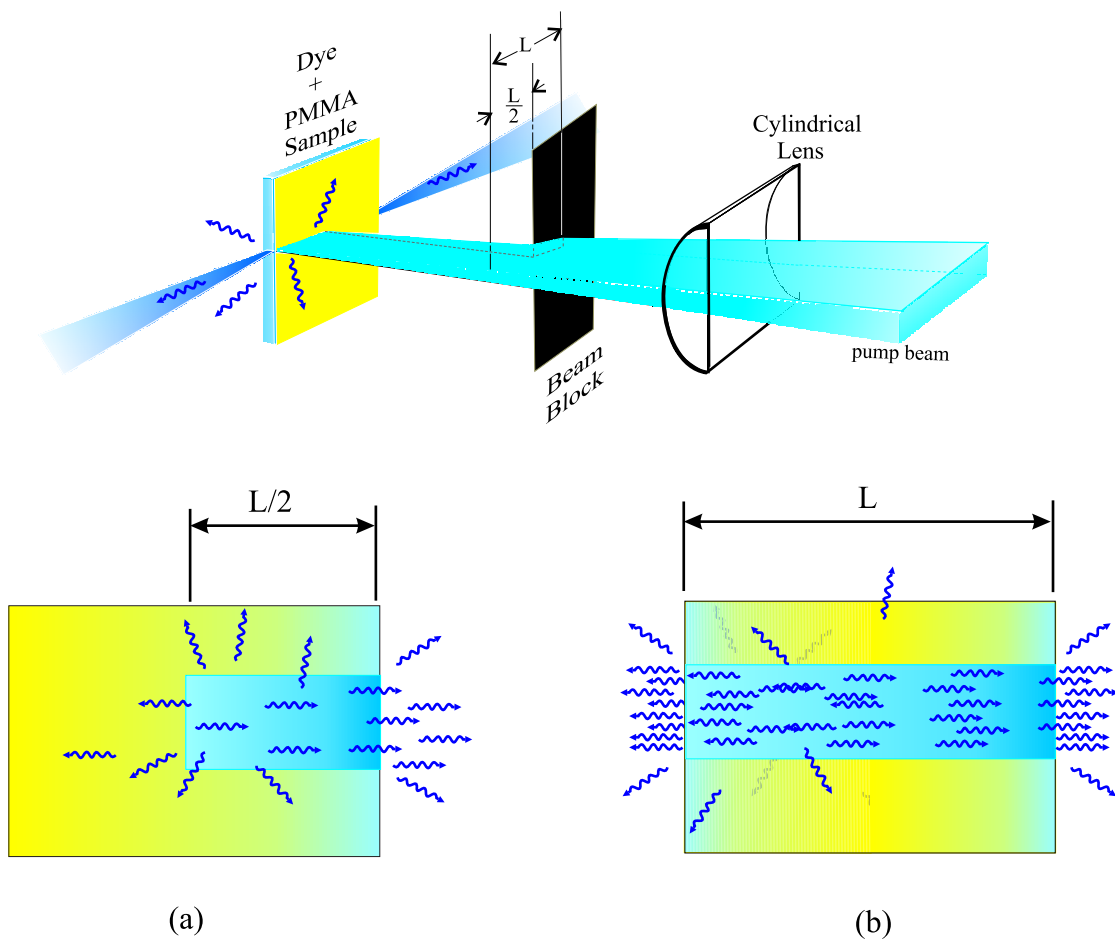
Figure 2.10: Gain for pump lengths of L and half L at constant intensity. a. Half the total pump length, emission in all directions but less amplification than in longer pump length. b. Whole length of incident pump.

photons are emitted while a gain less than zero implies net absorption. Gain is the natural logarithm of the ratio of photons emitted divided by the number of absorbed photons. The gain is dependant on both wavelength and incident intensity.

The gain is measured by detecting the ASE intensity for two different beam intensities, keeping all other beam parameters fixed. ASE gain is the increase in the ratio of light intensity emitted to incident intensity per unit length of the gain material that is pumped. We use the method by Shank to measure gain.[9] In this technique the laser is focussed on the sample with a cylindrical lens to form a line. The gain is determined by measuring the ASE power when pumped with a line length of L and then $\frac{L}{2}$ as shown in Figure 2.10. It should be noted that this is the average gain not a time dependent gain associated with the pump pulse temporal profile. For completeness the derivation of the gain equation is given Section 2.3.1.

2.3.1 Derivation of the Equation for gain

The references do not derive the gain equations. For completeness it is derived here. P is the distance to the detector, γ the gain, and z is the length along the sample surface illuminated by the pump (see Figure 2.11).
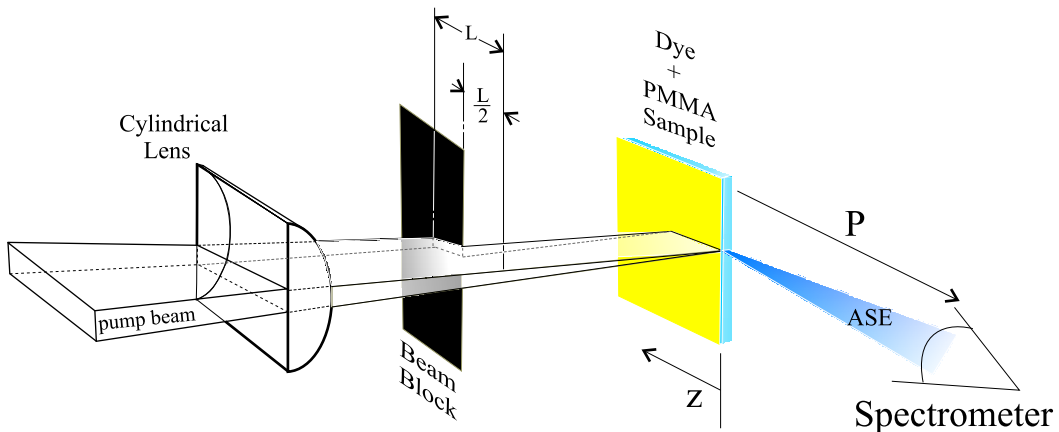
Figure 2.11: Gain Measurement Setup.

The intensity of the light I, entering a pinhole at a distance p from the sample as defined by Shank [9] is given by

$$I(\lambda) = \int_0^L \frac{e^{\gamma z}}{(p+z)^2} \, dz. \tag{2.5}$$

Since p $\gg$ L, then Equation 2.5 becomes

$$I(\lambda) = \int_0^L \frac{e^{\gamma z}}{p^2} \, dz. \tag{2.6}$$

Integration of Equation of 2.6 gives:

$$\int_0^L \frac{e^{\gamma z}}{p^2} \, dz = \frac{e^{\gamma L} - 1}{\gamma p^2}. \tag{2.7}$$

The ratio between the output intensity recorded by the spectrometer of the dye's ASE from a pump line length of L (I_L) and of half of L ($I_{\frac{L}{2}}$) is given by,

$$\frac{I_L}{I_{\frac{L}{2}}} = \frac{\frac{1}{\gamma p^2}\left(e^{\gamma L} - 1\right)}{\frac{1}{\gamma p^2}\left(e^{\gamma \frac{L}{2}} - 1\right)}. \tag{2.8}$$

Upon factoring the numerator, we get:

$$\frac{I_L}{I_{\frac{L}{2}}} = e^{\gamma \frac{L}{2}} + 1. \tag{2.9}$$

Solving for the gain, γ we find,

$$\gamma = \frac{2}{L} \ln\left[\frac{I_L}{I_{\frac{L}{2}}} - 1\right], \tag{2.10}$$

which is the standard definition of laser gain as given by Shank. [9]

2.4   Efficiency

Efficiency is the ratio of output to input energy. The ASE efficiency is therefore the ratio of the ASE to pump power or the measure of the ability of the dye to convert pump energy to ASE at a different wavelength. The ASE is emitted in both directions along the pump axis as in Figure 2.9. The measured value of the ASE intensity is then multiplied by two to

account for the fact that the experiments usually only measure the output at one end.

The fluorescence efficiency ϕ_f, also known as the quantum yield, indicates the fraction of pump photons that are converted to fluorescence photons per dye molecule. $\phi_f \equiv$ (the number of events)/(the number of absorbed photons) where the maximum value is unity. The ASE efficiency and the fluorescence quantum yield will both be considered in this work.

2.5 Two Photon Processes

2.5.1 Two Photon Absorption (TPA)

Elementary processes with two quantum jumps were shown theoretically from solution of Dirac dispersion by Gopper-Mayer[12] in 1931. When the energy of two light quanta matches a transition energy in an atom, TPA proceeds as shown in Figure 2.12. It was not demonstrated experimentally until 1961 by Kaiser and Garrett.[11]

As with linear absorption, an electron is promoted from the ground state to an excited state, not by absorbing one but two photons at the same time given they are both within the absorption band gap of the dye molecule. Similarly, two-photon absorption has an absorption coefficient α_2 and absorption cross section σ_2, given by

$$\alpha_2 = \frac{3\omega}{2\varepsilon_0 c^2 n_0^2} \mathrm{Im}[\chi^{(3)}], \tag{2.11}$$

where n_0 is the linear index of refraction, ε_0 is the permitivity of free space, ω is the frequency of light, $\chi^{(3)}$ is the third order nonlinear optical susceptibility and c is the speed of light.

Two-photon absorption is of interest for a number of applications, including optical limiting, 3-D fluorescence imaging, 3-D microfabrication, and optical data storage. The designing of dye molecules (chromophores) with large two-photon cross sections (σ_2) will offer lower pump energies with less optical damage to the host materials.

Dye design has been such that either symmetric D-D and A-A or asymmetric A-D chromophores are separated with π bridges. Studying a variety of these combinations should give insight to how electronic structure affects the optical properties. Future design of the high

17

efficiency chromophores depends on such understanding.[14] NRL303 has a π-center flanked by two electron-acceptors, 2-phenyl-5-(4-ter-butyl)-1,34-oxadiazole, which appears to be a promising molecule design.

This dye was not designed based on Donor-Donor or Acceptor-Acceptor structural symmetry of a stilbene moiety π- center or structural asymmetry of a Donor-Acceptor pair with a fluorene π-center. An appropriate π-center is paired with an Acceptor pair to achieve an electronic balance between the two. It has been shown that it is not Donor-Donor vs Acceptor-Acceptor pairs that have the higher TPA cross section (σ_2), but the dye with the π-center best electronically balanced between the electron Donor/Acceptor and the electron relay (π-center). Planar rigid π-centers also tend to have greater σ_2.
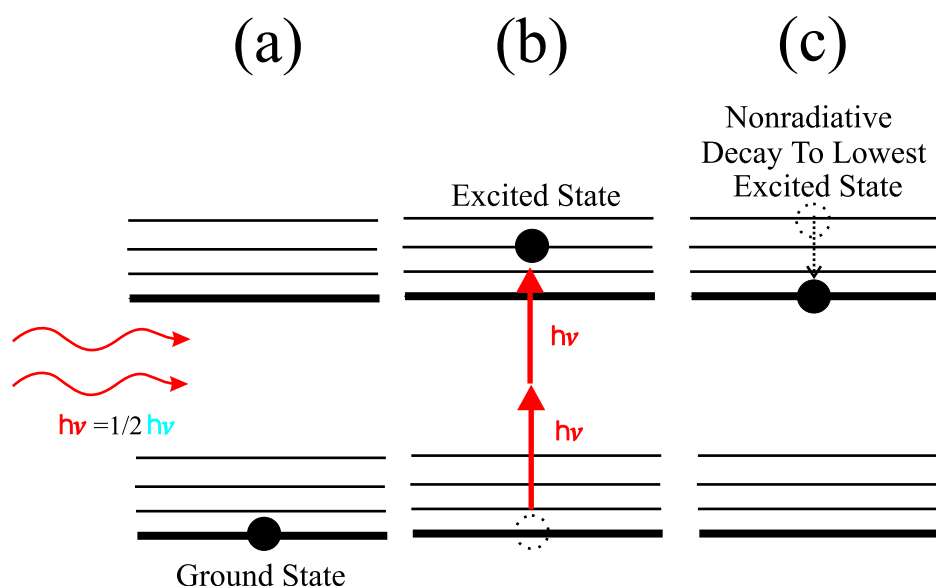
Figure 2.12: Two-photon Absorption. a.) Electron in the ground state. b.) Electron is promoted to an excited state with the energy difference equal to the sum of the energy of two photons. c.) Non-radiative decay of the electron to the lowest excited state.

2.5.2 Two photon cross section (σ_2)

The method outlined by Albota, Xu and Webb [18, 19, 20] were used for determining the two photon cross section σ_2, from either the two photon absorption or fluorescence. Measuring the absorption is a simpler experimental setup than that required for fluorescence measurements; however, decay and photobleaching of the sample can make absorption measurements

difficult as well since high pump powers are required. Obtaining $\sigma_2(\lambda)$ as a function of pump wavelength is therefore not practical with most tunable laser systems. The Spectra Physics Hurricane Ti:Saphire laser system used for measurements in this work is well suited to two photon fluorescence measurements with the large peak pump power and wide tunability with dual OPAs.

Since the properties of a new chromophore are largely unknown, σ_2 can not be measured directly. The detector response (quantum efficiency) and the geometry of the setup must be taken into account to give an absolute value of $\sigma_2(\lambda)$. Dye doped PMMA disks were made of NRL303 and Rh6G as the reference standard. Both were made to the same dimensions. Care was taken to keep the experimental setup in the same geometry for measurements of the two photon induced emission (TPE) of both unknown and reference samples. σ_{TPE}, the two photon emission cross section, is related to σ_2 by the chromophore's fluorescence quantum efficiency ϕ_f:

$$\sigma_{TPE} = \phi_f \sigma_2. \tag{2.12}$$

We used the method by Albota, Webb and Xu [18, 19] to determine the two-photon cross section. The fluorescence, F(t), is related to the detector's quantum efficiency η_2, and experimental geometry , the chormophore's fluorescence quantum efficiency ϕ_f, and the number of photons absorbed as a function of time N(t) so that

$$F(t) = \frac{1}{2}\eta\phi_f N(t). \tag{2.13}$$

The factor of $\frac{1}{2}$ accounts for the fact that two photons are being absorbed for every one photon emitted as fluorescence. The spectrometer used to measure the fluorescence signal has a finite integration time giving a time averaged spectrum $\langle F(t) \rangle$ where,

$$\langle F(t) \rangle \approx \frac{1}{2}\eta\phi_f\sigma_2 C \frac{g_p}{f\tau} \frac{8\langle P(t)^2 \rangle}{\pi\lambda/n}, \tag{2.14}$$

where C is the dye concentration, g_p is dimensionless and depends on the pulse shape, f is the pump pulse repetition rate, τ is FWHM of the pump pulse and, n is the index of refraction.

It follows then that σ_2 is

$$\sigma_2 = \frac{2\langle F(t)\rangle}{\eta \phi_f C} \frac{f\tau}{g_p} \frac{\pi\lambda}{8n\langle P(t)^2\rangle}. \tag{2.15}$$

Equations 2.14 and 2.15 are not sufficient to determine σ_2 if the collection efficiency η_2 is not known for the experimental setup. The use of a reference standard with a known value of $\sigma_2(\lambda)$ allows the unknown dye's σ_2 to be calculated for the ratio of the two individual equations:

$$\frac{\langle F(t)\rangle_{ref}}{\langle F(t)\rangle^{unkn}} = \frac{\phi_{ref}\eta_{ref}\sigma_2^{ref}C^{ref}\langle P^{ref}(t)^2\rangle n^{ref}}{\phi_f^{unkn}\eta^{unkn}\sigma_2^{unkn}C^{unkn}\langle P_{unkn}(t)^2\rangle n_{unkn}} \tag{2.16}$$

Solving for σ_2 we get,

$$\sigma_2^{unkn}(\lambda) = \frac{\phi_f^{ref}\eta^{ref}\sigma_2^{ref}C^{ref}}{\phi_f^{unkn}\eta^{unkn}C^{unkn}} \frac{\langle P^{ref}(t)^2\rangle}{\langle P^{unkn}(t)^2\rangle} \frac{\langle F(t)\rangle^{unkn}}{\langle F(t)\rangle^{ref}}. \tag{2.17}$$

Equation 2.17 is solved at $\lambda = 700$nm, since there are values for both the unknown and Rh6G reference at that wavelength. Since f, τ, π, g_p, ϕ_f and n are all constants for the experimental setup, these values are folded into the K value. Assigning K the value of all these constants solve the equation for the unknown's K value where,

$$K = \frac{\sigma_2^{unkn}\phi_f^{unkn}C^{unkn}\langle P(t)^2\rangle\lambda}{\langle F(t)\rangle^{unkn}} \tag{2.18}$$

where K also contains the ratio

$$\frac{f\tau}{g_p} \frac{\pi}{8n\eta\phi_f}. \tag{2.19}$$

Substituting K into equation 2.15 we get,

$$\sigma_2^{unkn}(\lambda) = \frac{K}{\lambda} \frac{\langle F(t)\rangle}{\langle P(t)^2\rangle} \tag{2.20}$$

symbol	quantity
$\langle F(t) \rangle$	time averaged fluorescence
η	Experimental collection efficiency
ϕ_f	the dyes fluorescence quantum efficiency
σ_2	TPA cross section
C	Dye concentration $/cm^3$
$g^{(2)}$	second order temporal coherence of pump
$g^{(2)}$	$\equiv \langle I_0^2(t) \rangle / \langle I_0(t) \rangle^2$
$\langle I_0 \rangle$	= ave intensity at focal plane in sample
g_p	pulse shape parameter(dimensionless)
$\langle P(t) \rangle^2$	time averaged pump power (photons/s)
f	pump rep rate
τ	FWHM of pump pulse
λ	pump wavelength
n	index of refraction
GM	Goppert-Mayer unit
1 GM	$= 10^{-50} \ (cm^4 s)/$photon

Table 2.1: TPA symbol definitions.

Chapter 3

Experimental

3.1 Sample Preparation of the Dye NRL303

3.1.1 Thick slab samples

The dye under investigation, NRL303, was synthesized by Dr. Oh-Kil Kim of the Navy Research Laboratory (Figure 3.1). The dye was dissolved in methylmethacrylate (MMA) from Polyscience Inc. The MMA was filtered through an aluminum powder column prior to use. It should be noted that 0.0098 grams total were provided by O.Kim to the Nonlinear Optics research group at Washington State University. Part of this supply was sent to the the Air Force Research Laboratory for other measurements, leaving 0.0055 g for sample "b" and approximately 0.002 g for sample "a". The milligram quantity did not allow for any waste and presented extra difficulties in preparing dye doped polymer samples. The typical parallel analysis of the optical properties in various solvents had to be omitted.

The dye and MMA solution is heated to 90ºC in an oven for two days or until MMA
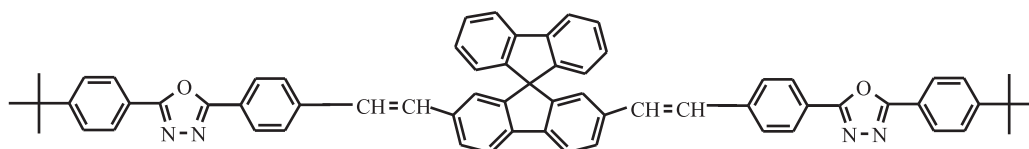
Figure 3.1: NRL303 Dye molecule structure. Molecular weight is 920amu.
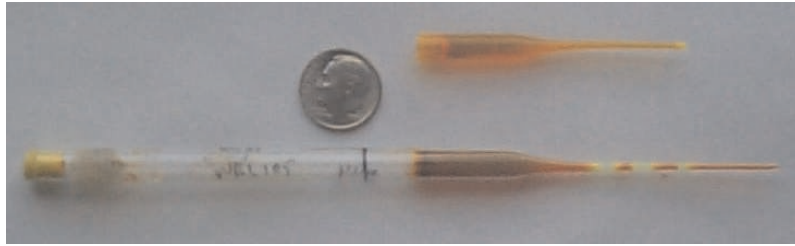
Figure 3.2: Sample preform in pipet mold.

Figure 3.3: Sample after being removed from mold.

becomes a solid matrix of polymethylmethacrylate (PMMA) with dye as a solute. Due to the very small amount of sample preforms had to be made in molds smaller than the standard test tube size. Glass pipets worked well to accommodate the unusually small sample volume (Figure 3.2). Polymerization of the dye doped MMA is catalyzed by heat. Each sample is prepared by determining the dye to MMA ratio for the desired dye concentration. To this solution $2.2\mu l$ of Tert-Butyl Peroxide per 1ml of MMA is added to initiate polymerization. The same amount of Butanethiol, as a chain transfer agent, is added to limit the chain length. When the PMMA and dye have cooled, the glass pipet is broken and the preform is removed (Figure 3.3, 3.4). This dye doped PMMA preform can then be pressed into or cut to the desired shape.

Once the preform is close to the required shape it can then be sanded and polished in preparation for optical experiments. Three types of samples were made, slabs and disks (Figure 3.5) approximately 1.5mm in thickness and fiber optics of various diameters of 2 to 4cm in length. The slabs were made by pressing the preforms between two quarter inch thick glass plates at 140°C till the desired thickness is reached. The polymer fibers were made by drawing the preforms while heating with a bunsen burner (Figure 3.7). Some fibers were made by extruding the heated PMMA through a mold block (Figure 3.6). One suitable fiber

23

Figure 3.4: NRL303b PMMA preform

Figure 3.5: Pressed sample of NRL303 Dye in PMMA. Sample (a) was made 1.3mm thick with a dye concentration of $1.3 \cdot 10^{18} molecules/cm^3$. Sample (b) was made 1.3mm thick with a dye concentration of $1.02 \cdot 10^{19} molecules/cm^3$.

was produced via this method. It proved to be ineffective due to the low volume of available material.

3.1.2 Fiber samples

PMMA fiber ranging in diameters from 200 to 800 μm and 2 to 4cm in length were made by heating the cylindrical preforms with a bunsen burner and pulling the fibers from the bulk material as shown in Figure 3.7. Micrographs of a typical fiber are shown in Figure 3.8.
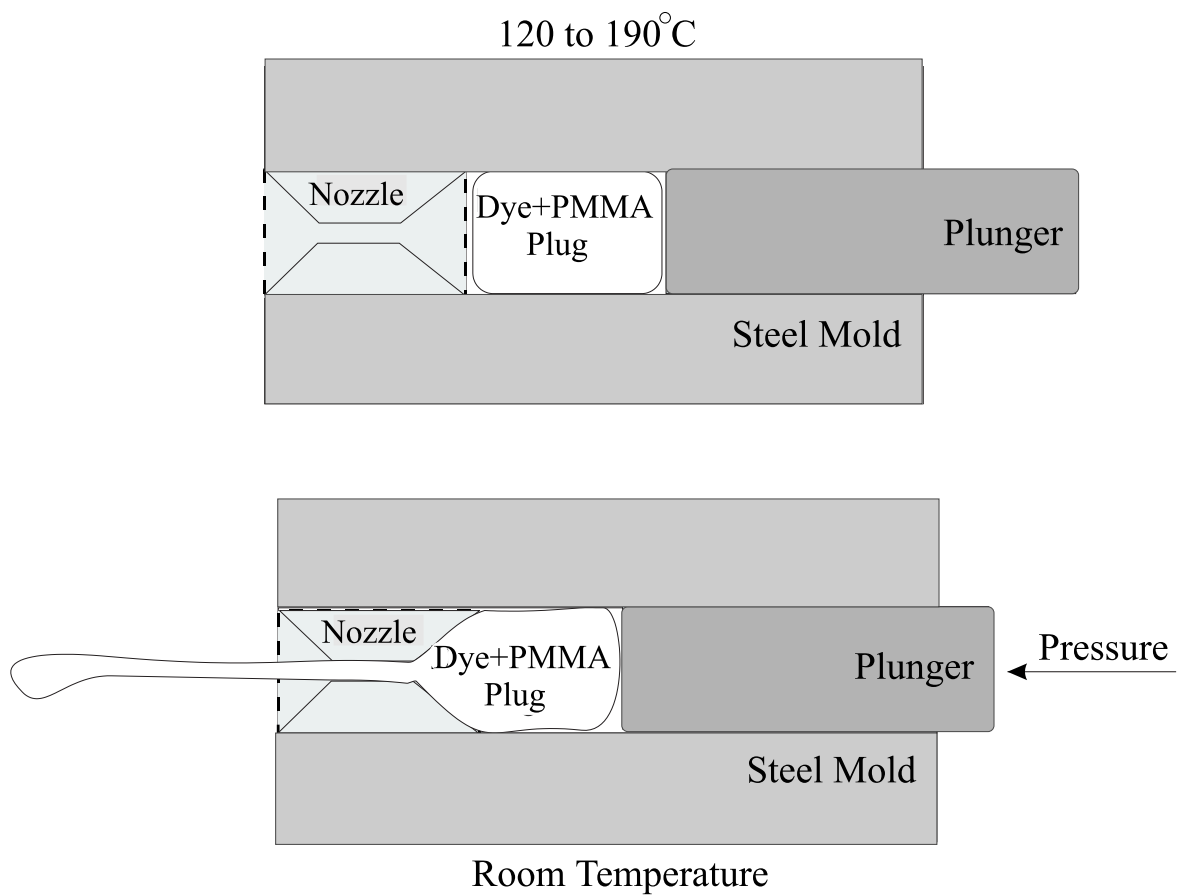
Figure 3.6: Fiber extruder.
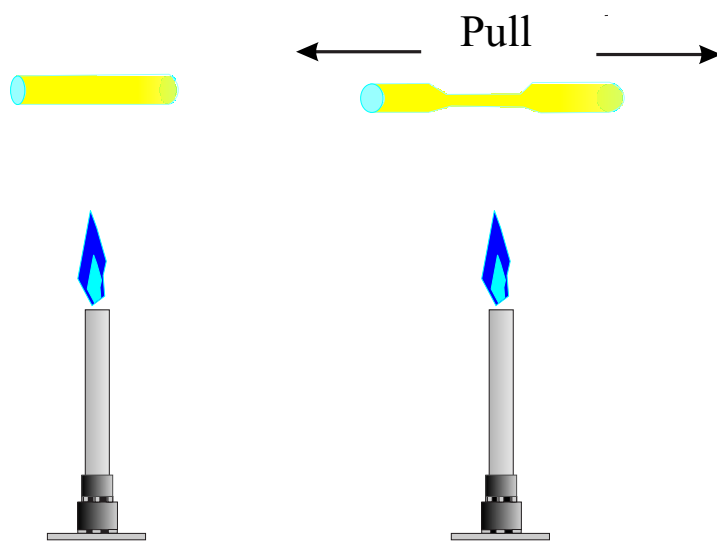
Figure 3.7: Drawing a polymer fiber by direct heating with a bunsen burner
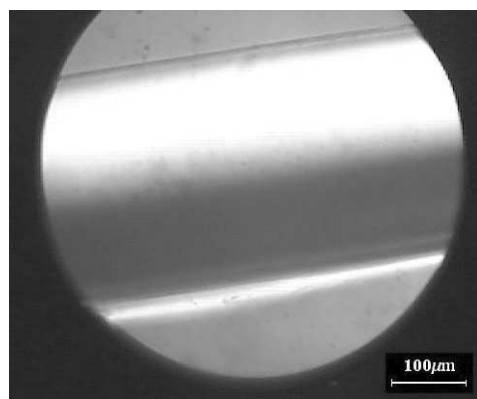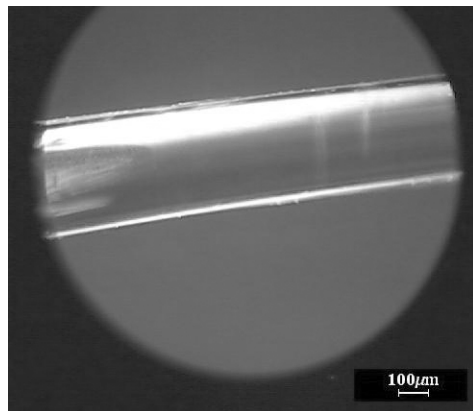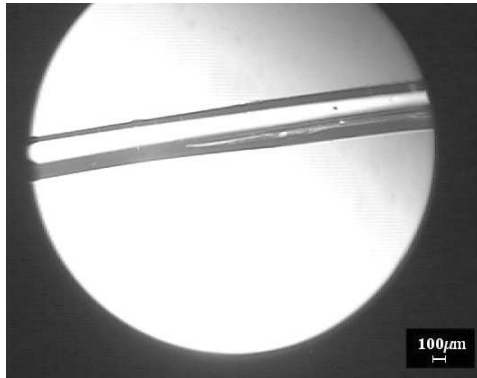
Figure 3.8: NRL303b PMMA fiber magnified 5x, 10x and 20x.

Dye	Geometry	Dimensions (cm)	Concentration
NRL303-a	thick film	3 x 2 x 0.1	2 x 10^{-3}M
	fiber	$2.5cm \times 500\mu m$	$(1.3$ x 10^{18} molec/cm^3)
	disk	1.4 x 0.125	
NRL303-b	thick film	1.35 x 1.75 x 0.08	1.6 x 10^{-2} M
	fiber	$2.5cm \times 400\mu m$	$(1.0$ x10^{19} molec/cm^3)
	disk	1.4 x 0.125	
NRL105-1	thick film	1.3 x 1.2 x 0.1	1.0 x 10^{-2} M
			$(6.38$ x10^{18} molec/cm^3)
NRL105-2	thick film	2.8 x 1.9 x 0.7	3 x 10^{-3} M
			$(1.80$ x10^{18} molec/cm^3)
NRL105-3	disk	1.45×0.14	5.3 x 10^{-3} M
			$(3.17$ x10^{18} molec/cm^3)
Fluorescein-1	disk	1.45×0.14	4.8 x 10^{-3} M
			$(2.93$ x10^{18} molec/cm^3)
Fluorescein-2	disk	1.45×0.14	9.9 x 10^{-4}M
			$(5.93$ x10^{17}molec/cm^3)
Rhodamine6G	disk	1.45×0.14	2.8 x 10^{-4} M
			$(1.7$ x10^{17}molec/cm^3)
Rhodamine6G	disk	1.45×0.14	4.33 x 10^{-5}M
			$(2.6$ x10^{16} molec/cm^3)

Table 3.1: Dye doped PMMA sample parameters.

3.2 Experimental Instrumentation

Standard optics were used for beam shaping and steering. All spectra were measured with an Ocean Optics USB spectrometer. Photodetectors and power meters were used for monitoring laser pump stability and the amplitude of the ASE generated from optically pumping the dye samples. Figure 3.9 shows the experimental setup for absorption measurements and Figure 3.10 shows the typical setup for fluorescence experiments.
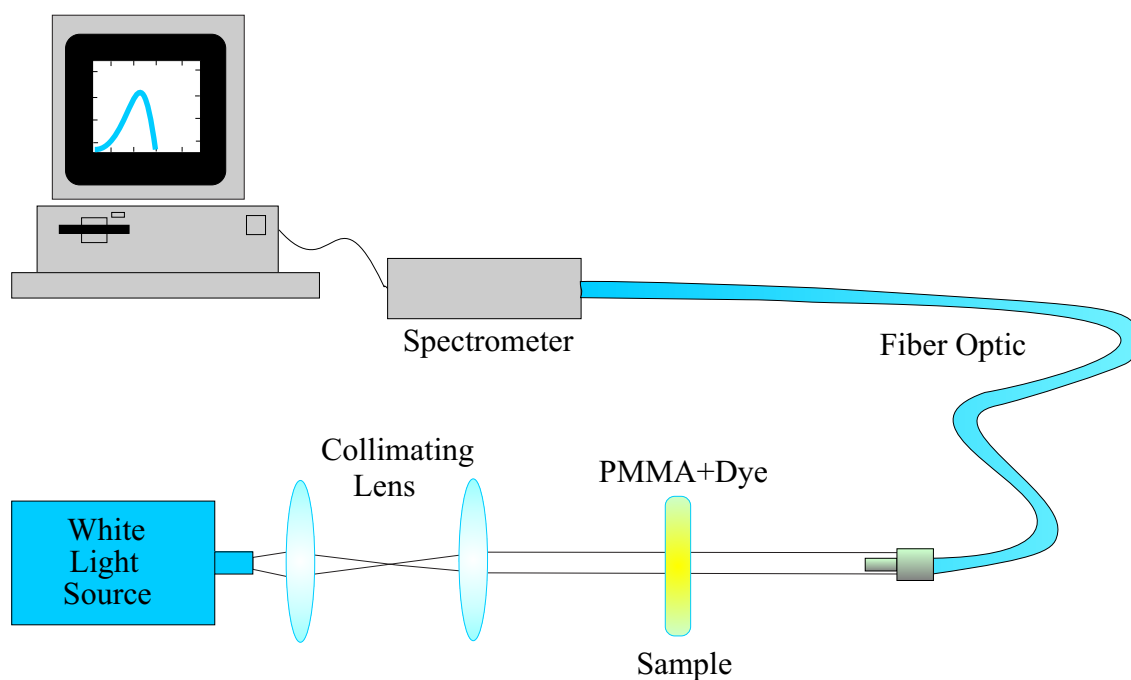
Figure 3.9: Experimental setup for optical absorption measurements.
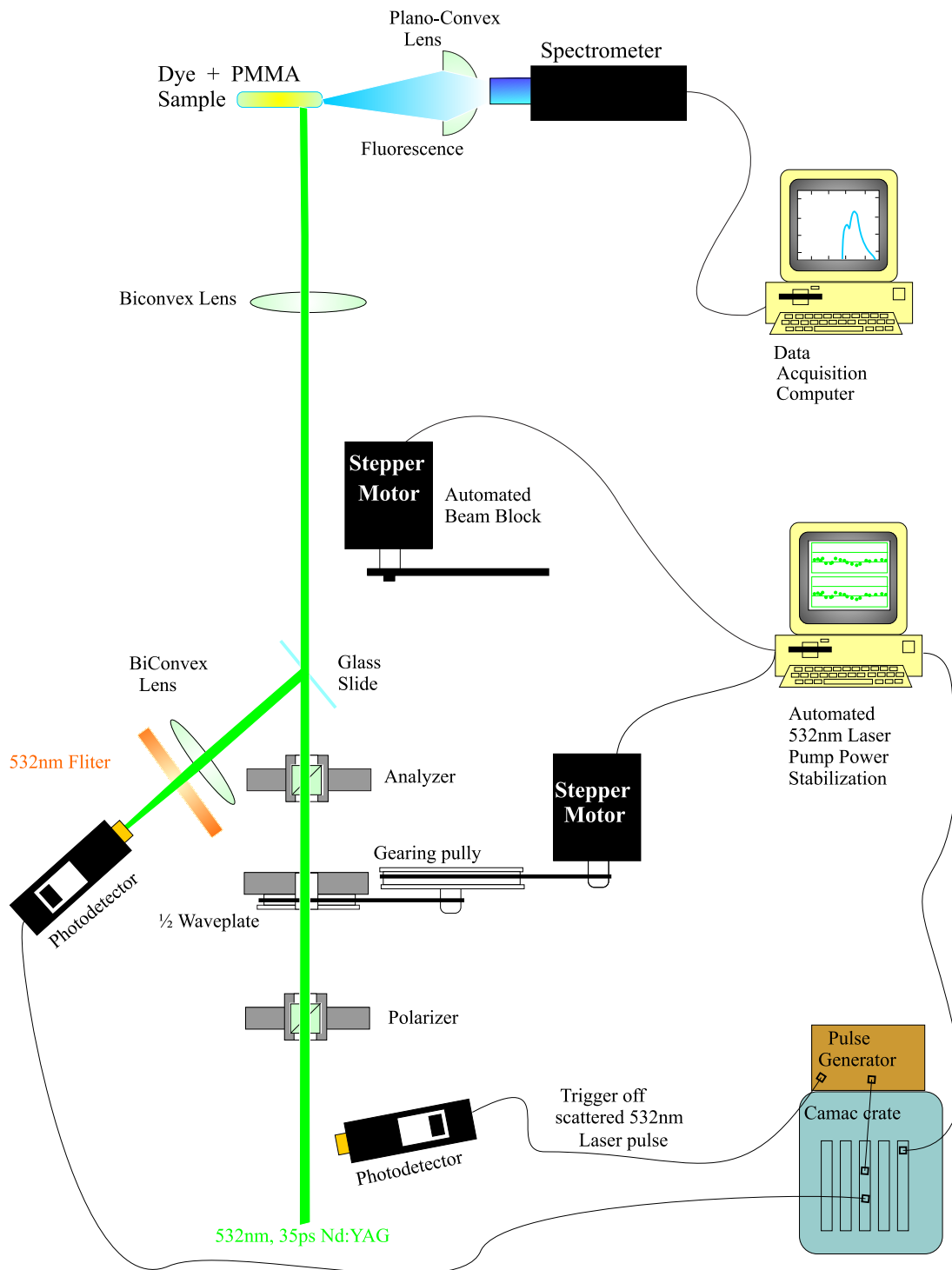
Figure 3.10: Experimental Setup for Fluorescence measurements from 532nm, 35ps laser pump pulses.

3.3 Linear Absorption and Fluorescence

3.3.1 Linear Absorption

The sample slabs a and b (NRL303 in PMMA) were used for absorbance and fluorescence measurements. The Ocean Optics USB spectrometer and model LS-1 white light source were used for the absorbance measurements. For the fluorescence measurements, the USB spectrometer was used for excitation pules at λ= 355nm and λ= 532nm (both 35ps laser pulses), and λ=400nm and λ=800nm (100fs laser pulses). The absorption maximum of the sample was measured to be at 395nm and the Fluorescence maximum at 491nm (Figure 3.11). The difference between the wavelength of maximum absorption and the fluorescence peak was found to be 96nm (the Stokes Shift). The difference from the absorption peak to the ASE peak is only 66nm which is comparable to but smaller than that for coumarin laser dyes.[10]
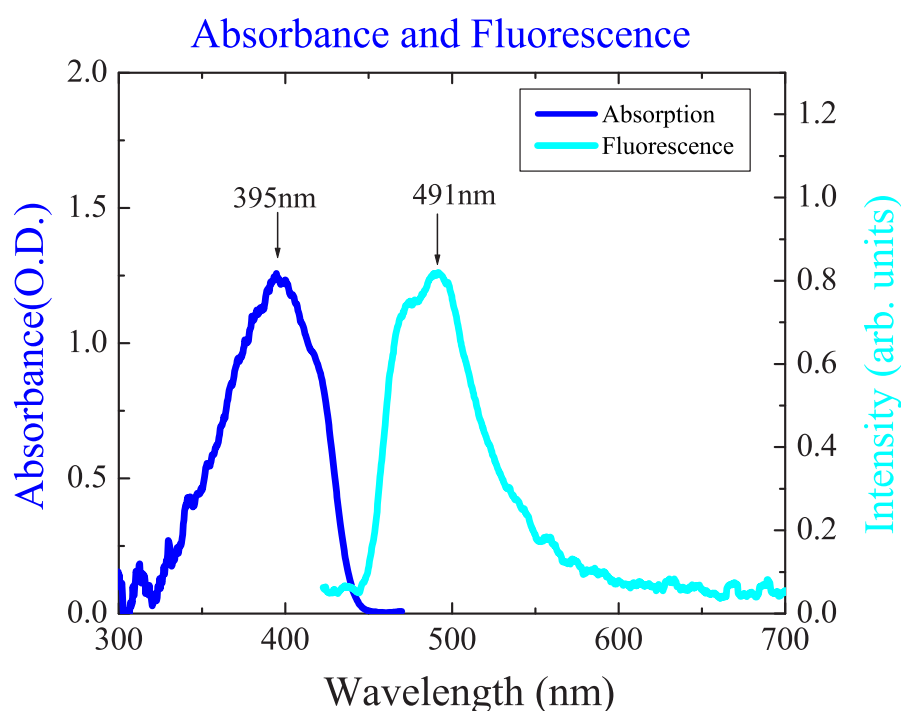
Figure 3.11: White Light Absorption spectrum and Linear Fluorescence spectrum for λ= 355nm and 35ps laser pump pulses for NRL303 in PMMA.
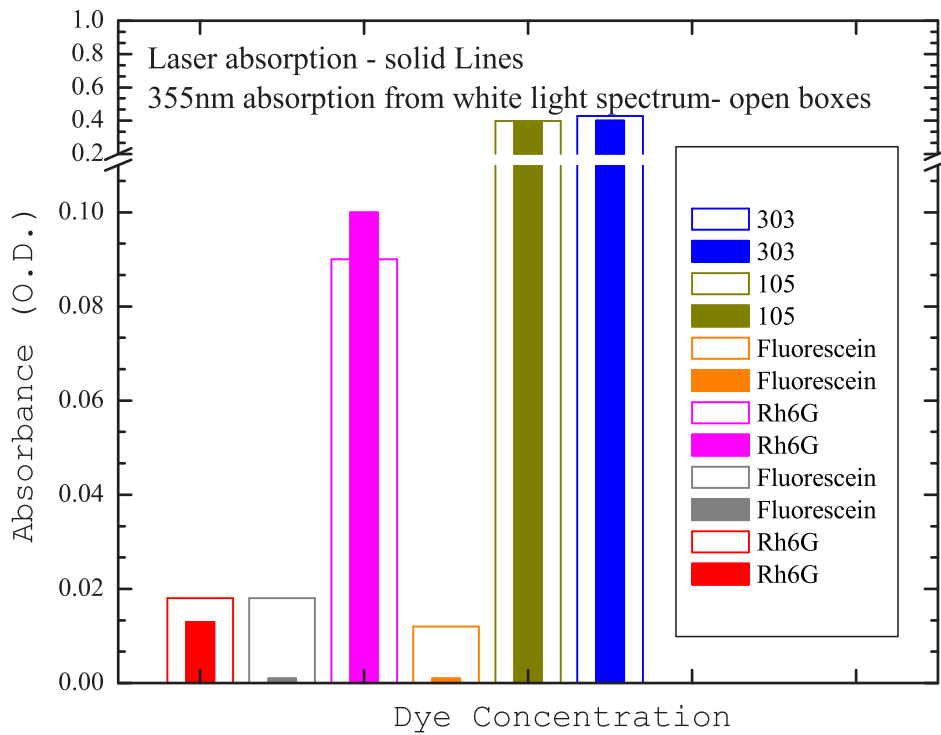
Figure 3.12: Linear absorption at 355nm determined from the white light spectrum (open boxes) and from 355nm laser light (solid lines).

The linear absorption value obtained from the white light absorption spectrum and from a 355nm 35ps 10Hz laser source are compared in Figure 3.12. The two methods for finding the linear absorbance at 355nm agree well for the concentrations of the NRL303 sample and the Rhodamine 6G reference.

3.3.2 Linear Absorption cross section

The linear absorption cross section σ was determined for NRL303 sample b. NRL303, sample b had a dye concentration of 1.02×10^{19} molecules/cm^3 and was 0.15 cm thick. From Equations 2.1 and 2.2, the absorbance A and the absorption coefficient α is used to determine the linear absorption cross section σ given by Equation 2.3. The result is a cross section of about 0.7 Å^2. This is lower than the geometric area of the molecule. Figure 3.13 shows the measured cross section as a function of wavelength.
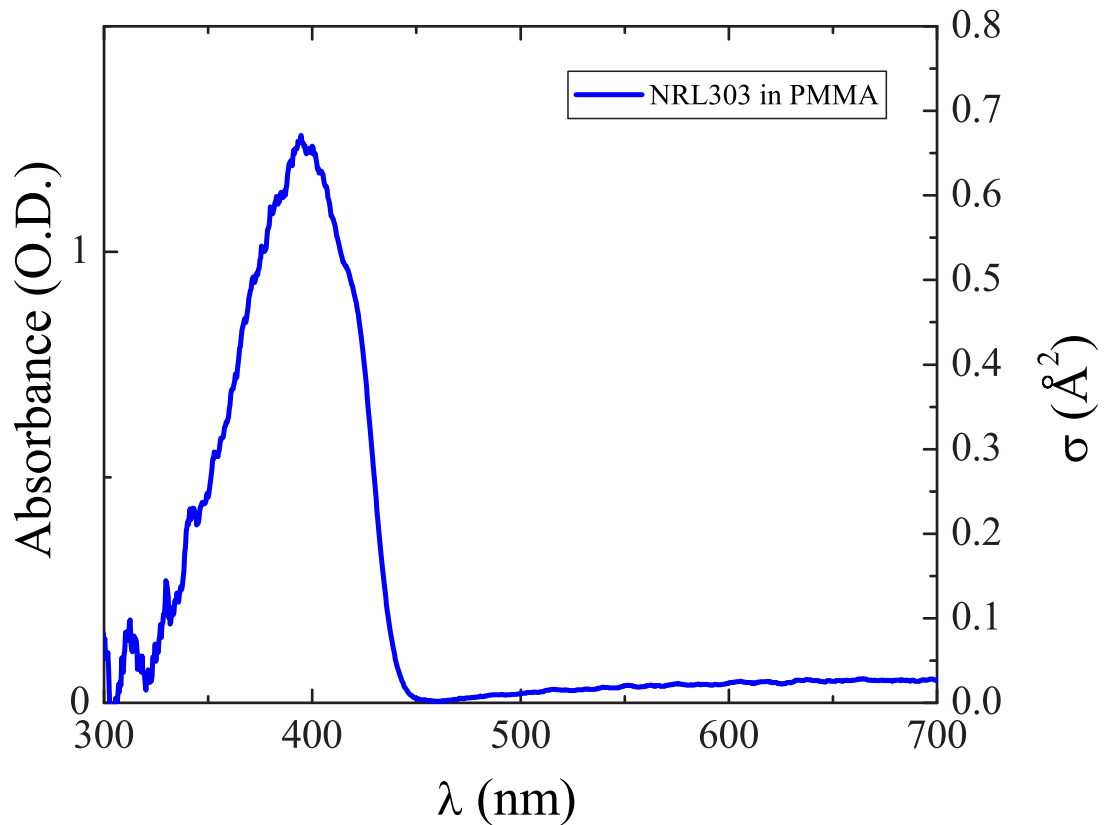
Figure 3.13: Optical absorbance of NRL303 doped PMMA.

3.4 Amplified Spontaneous Emission

ASE in NRL303 was produced by exciting the sample with 355nm, 35ps light generated from the third harmonic of an Nd:YAG laser and 400nm, 100fs light generated from the second harmonic of a Ti:saphire laser that optically pumped the NRL303 samples.

The ASE produced from the dye doped polymer optic fiber was much more intense than the ASE light generated from the slab, as seen in Figure 3.14. Both had emission maxima at 460nm. The fiber pumped with a wavelength of 355nm showed more gain narrowing, with a spectral width of 8.3nm FWHM, than in the bulk which had a spectral width of 12.3nm. A spectral width of 11nm FWHM was observed for the 303 sample in a thick film under 400nm excitation. ASE increases exponentially with increasing pump power as shown in Figure 3.15. Only fluorescence is observed, as in Figure 3.16, until the pump power reaches a threshold for the onset of amplified spontaneous emission or the pump line is increased in length beyond the critical path length for ASE. The distance travelled through the gain medium determines the amount of ASE output since ASE is the amplification by stimulated emission of a spontaneously emitted photon. The ASE emission is also enhanced preferentially along the axis of the polarization of the pump beam. Dye molecules whose largest polarizability axis is aligned with the incoming pump polarization are more likely to be excited, leading to dipole radiation that peaks in a direction that is perpendicular to the pump polarization. The fact that ASE's amplification comes from coherent stimulated emission explains the observed initial rise in fluorescence signal upon photodegradation followed by a decay that is in step with the ASE decay as shown in Section 3.7.
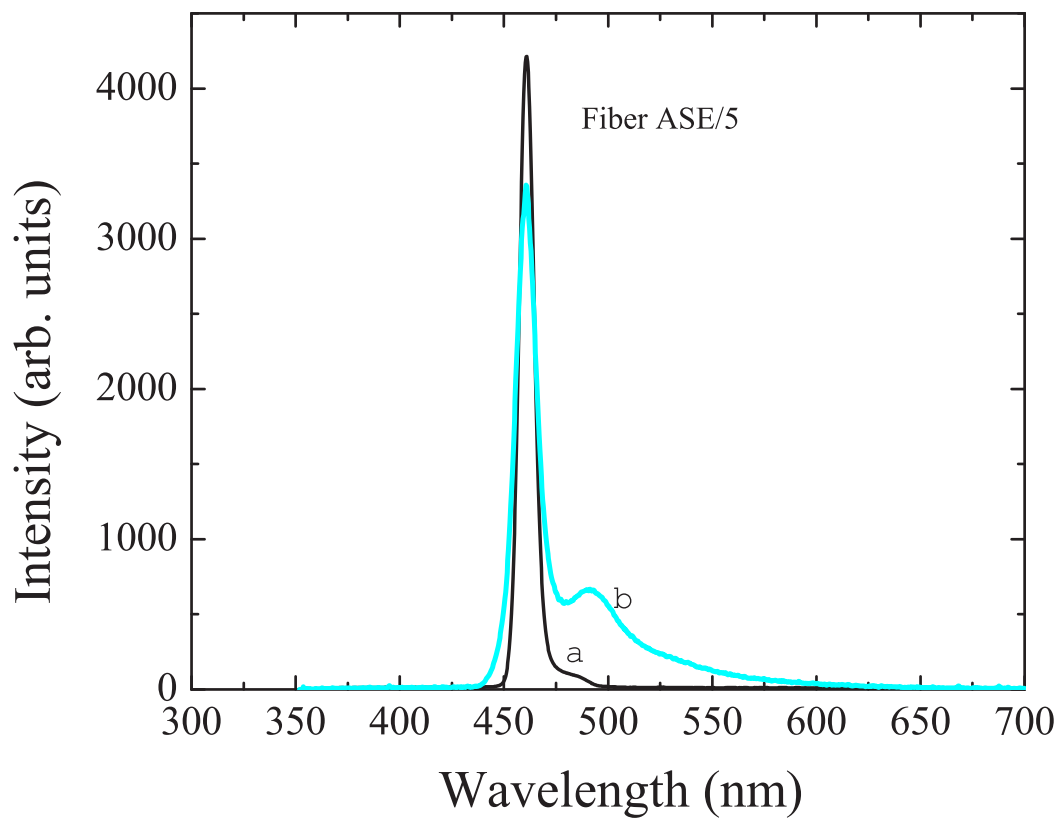
Figure 3.14: ASE in a slab and in a fiber under 355nm pump. a) 400μm fiber, b)1.3mm slab
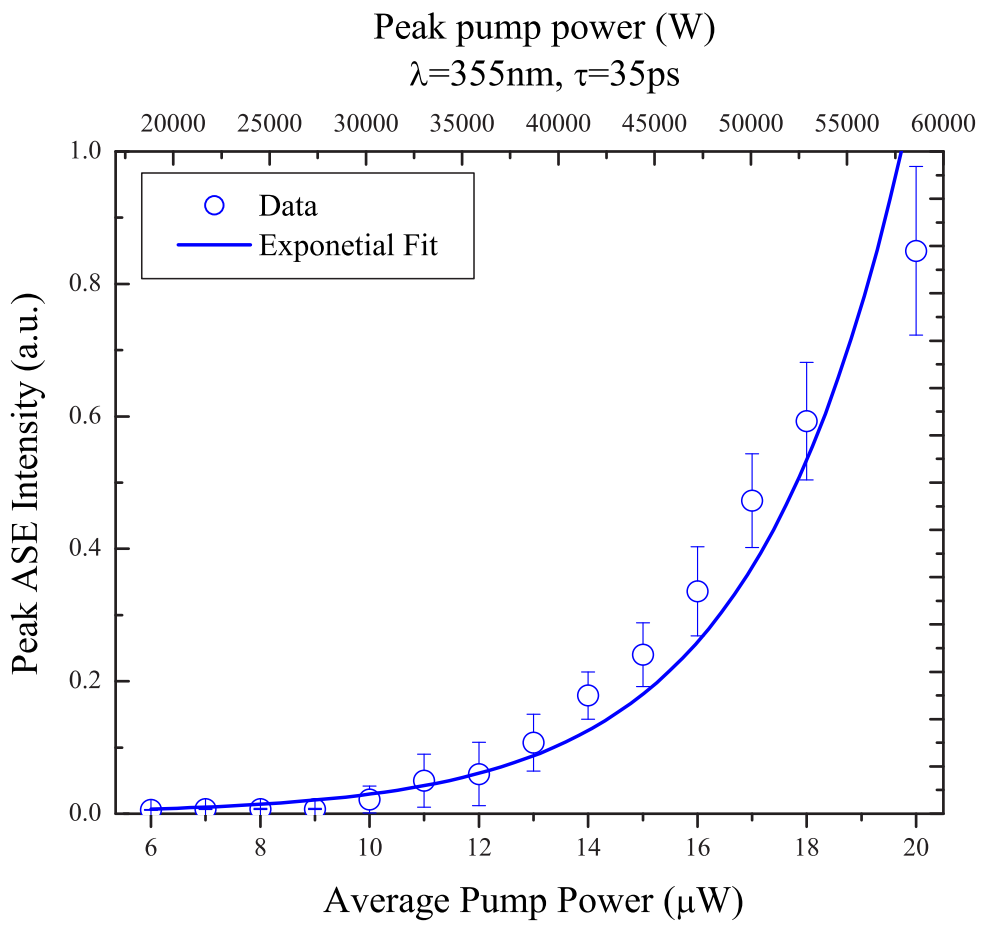
Figure 3.15: ASE intensity vs pump power. using a λ=355nm, τ=35ps laser source.
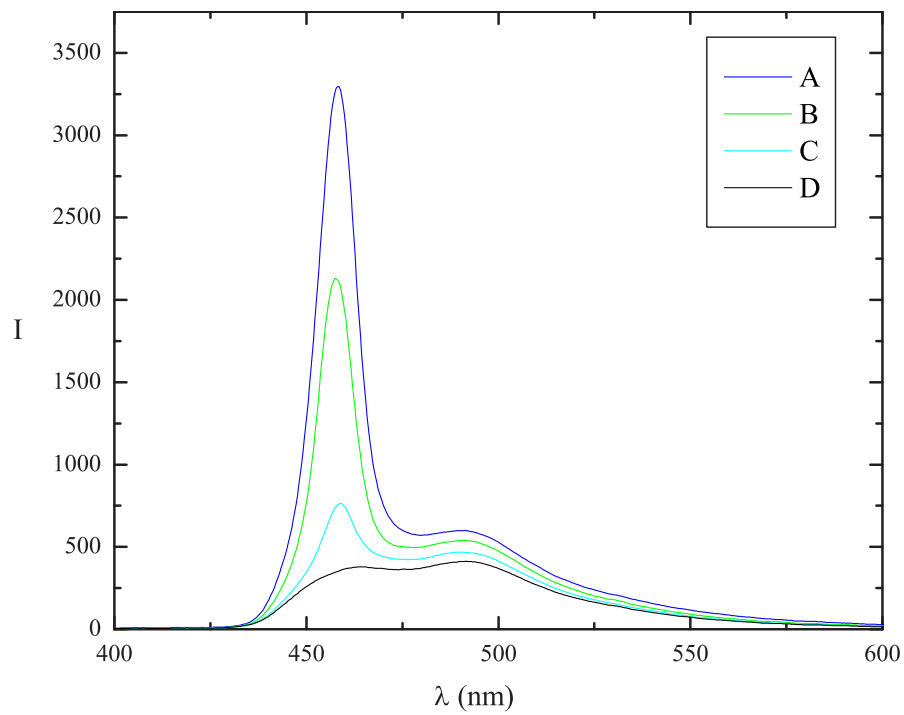
Figure 3.16: ASE spectrum as a function of pump power. A.)20μW, B.)19μW, C.)17μW, D.)17μW. A, B and C are from a 1cm pump line length of a 355nm, 35ps, 10Hz rep. rate laser pulse, while D is for a 0.05 cm diameter pump spot.

3.5 Gain (ASE)
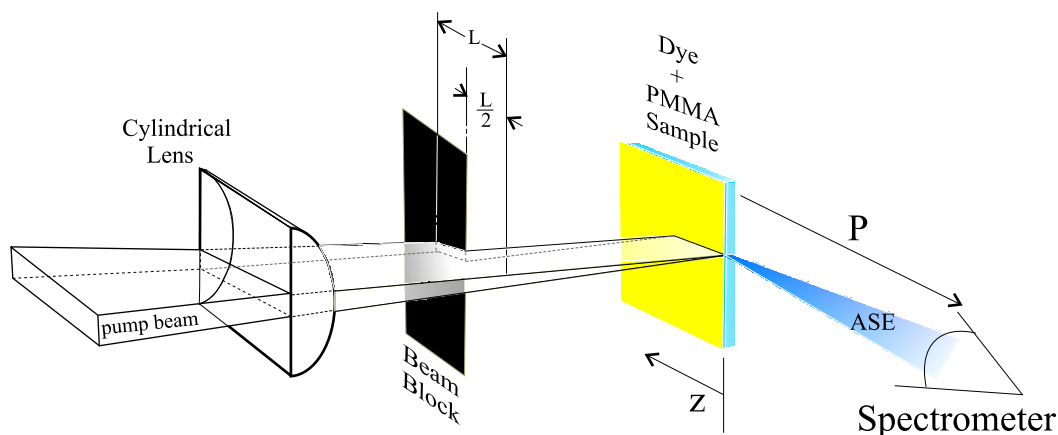
Figure 3.17: Gain Measurement Setup.

The gain was determined by measuring the ASE intensity from two different pump line length for the same pump power per unit length as described in Section 2.3.1 and shown in Figure 3.17. The 355nm, 35ps, 10Hz pump laser pulses were used for gain measurements. Figure 3.18 shows that the gain does not saturate as is commonly observed, but reaches a maximum value and decrease until the net gain turns negative. The gain maximum was found to be 2cm^{-1}(slab) and 4 cm^{-1}(fiber) for sample 303b and 7 cm^{-1} for sample 303a. It should be noted that sample A had a better optical surface quality. Both samples' gain compare favorably with Rh6G as shown it Table 3.2. [15]

Matrix	Rh6G	NRL303
	(Gain cm^{-1})	
PMMA (solid)	1.4, 3[†]	4, 7[‡]
MMA + EtOH (solution)	2.8	
EtOH	11	

Table 3.2: † Measured with SHG Nd:YAG excitation. All other Rh6G values were excited using a nitrogen laser(from Reference [15]. ‡ The higher NRL303 gain value was in a dye doped fiber.
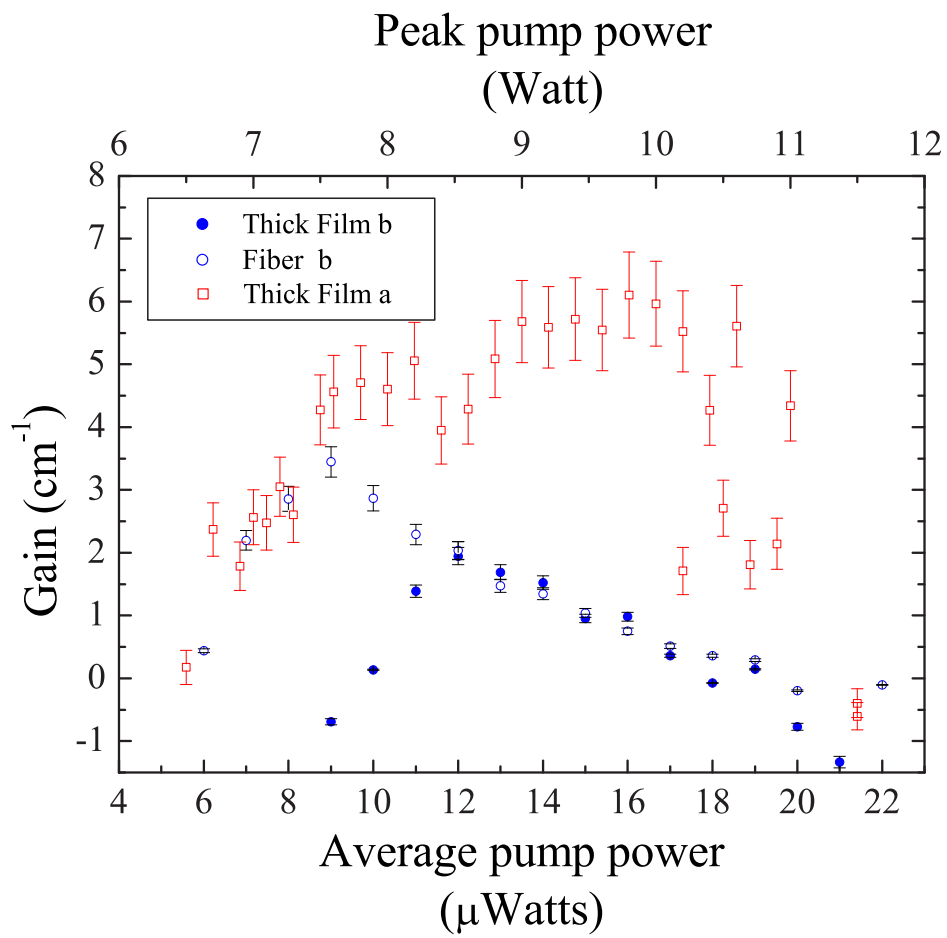
Figure 3.18: Measured gain for NRL303 doped PMMA as a function of pump power.

3.6   ASE Efficiency

PMMA doped slabs were pumped with 355nm, 35ps, 10Hz laser pulses as in the setup shown in figure 3.19
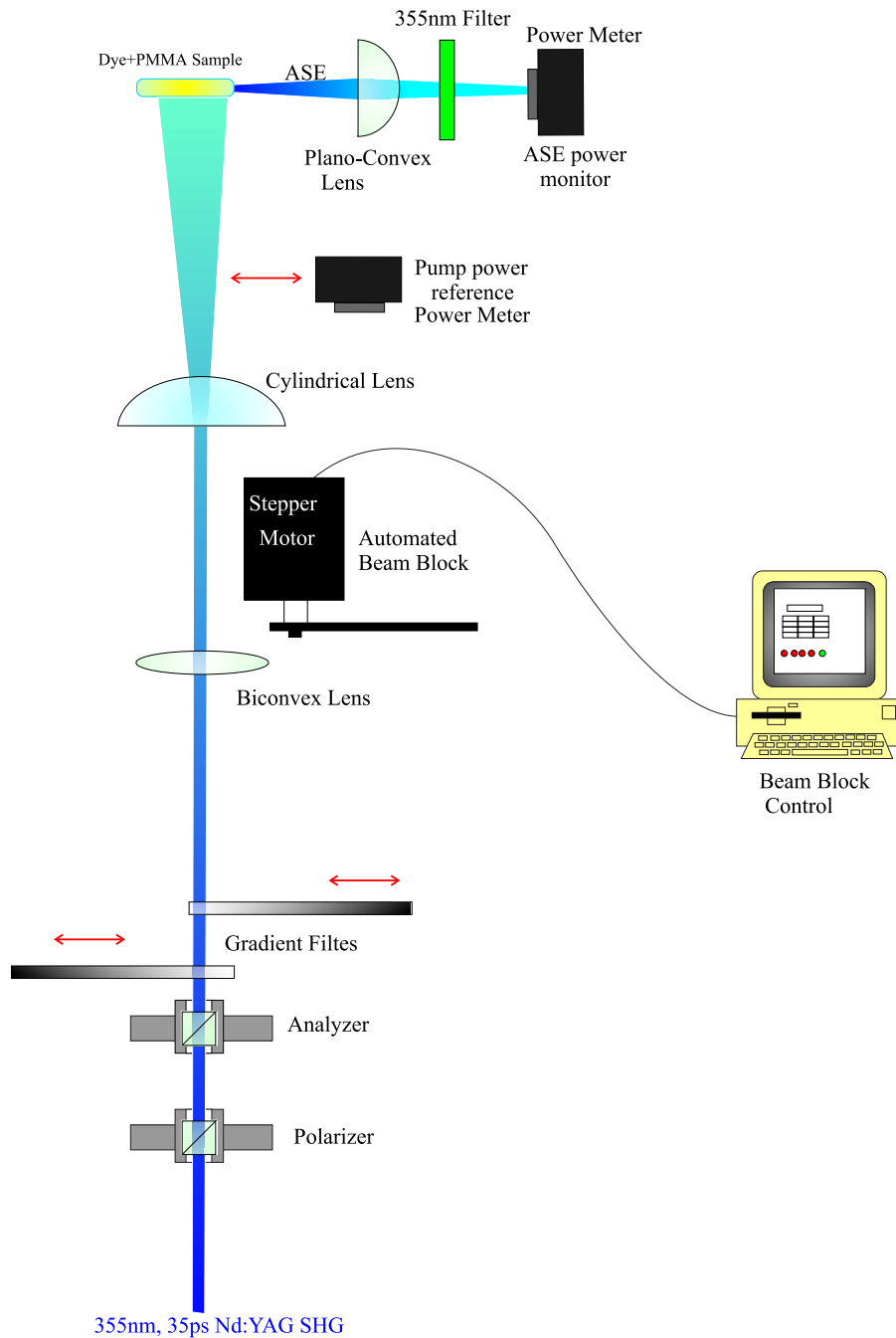
Figure 3.19: Efficiency setup.

The ASE conversion efficiency for NRL303 in PMMA is 25% (Figure 3.20), while for Rh6g in a pure polymer matrix (2-hydroxyethyl methacrylate (HEMA) and methyl methacrylate (MMA) 1:1) is reported to be 21.5 % and 26% in a modified organic-inorganic matrix [22]. Both values are relatively large considering they are for a solid matrix, which usually yields a much lower than in solution. Radiant Dye Laser Corporation's commercially available narrowscan model laser system specifies conversion efficiencies of 28 to 32 % in solution for the Nd:YAG SHG(532nm) pump configuration and 12 to 14% for the excimer (308nm) configuration.
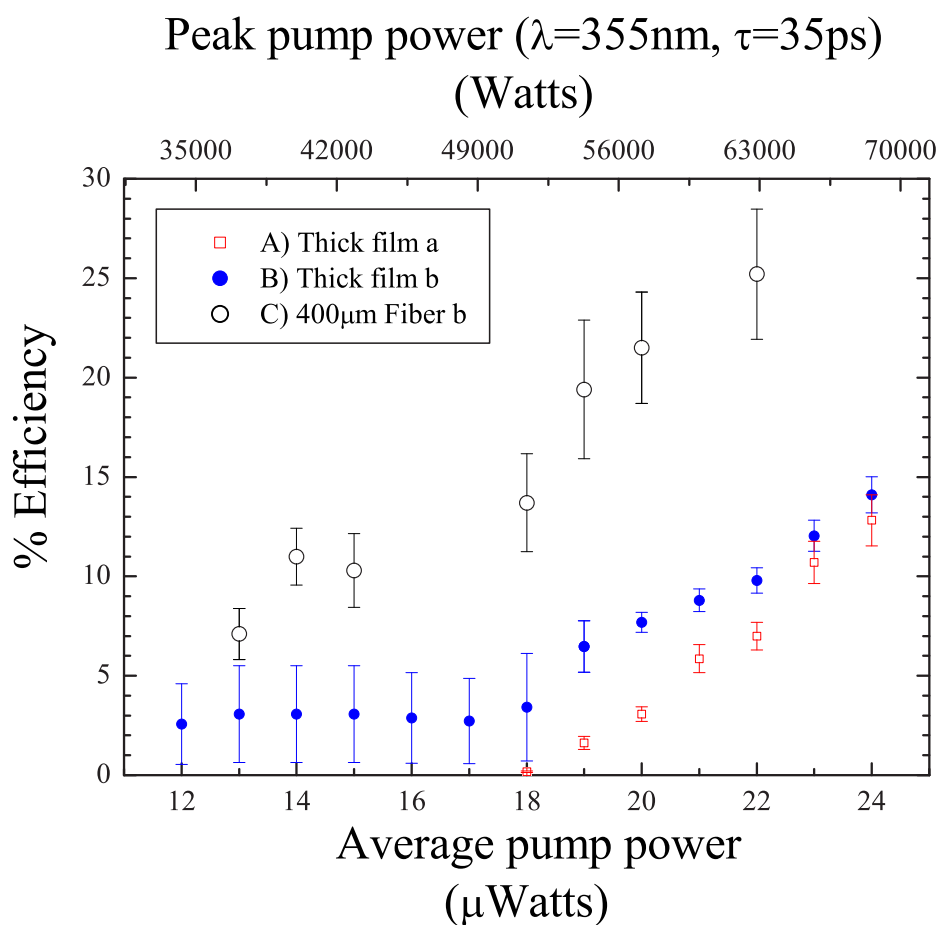
Figure 3.20: ASE conversion efficiency for NRL303 doped in PMMA.

3.7   Photobleaching

All decay measurement were taken with a Ocean optics USB spectrometer. Having a full spectrum of the light emitted form the samples makes it easy to distinguish between ASE and fluorescence. The numerical code in the appendix was used to automate the analysis of the decay data files. The peak intensity of the ASE and file header time could be read by the mathematica code to write a table file of ASE intensity vs time. Figure 3.21 shows a typical plot from a data file used to find the decay.
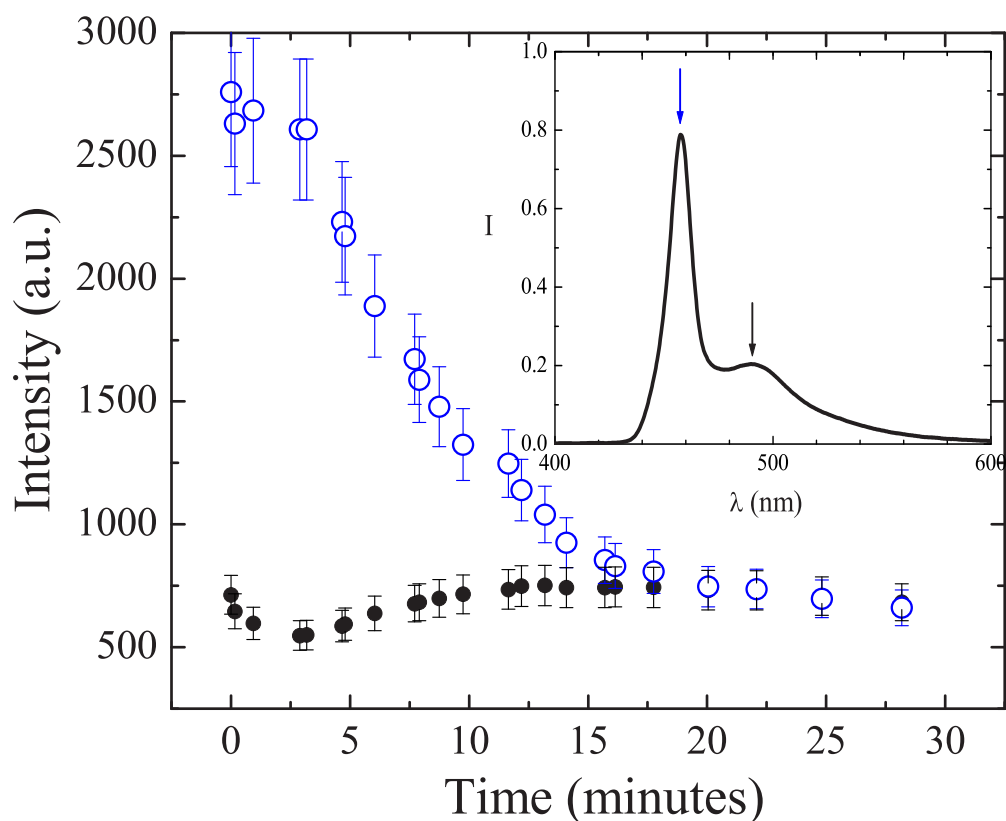
Figure 3.21: Fluorescence intensity at 490nm and ASE at 461nm as a function of time for NRL303, pumped with 35ps pulses at 355nm. The insert shows the typical spectrum with open and closed circles indicating the ASE and fluorescence values reflected in the decay plot.

3.7.1   ASE Decay and recovery

Reversible degradation of a material is uncommon, although there are some recent examples in which this is the case. [34] Unfortunately, no recovery was observed in our experiments with NRL303 as shown in Figure 3.22.
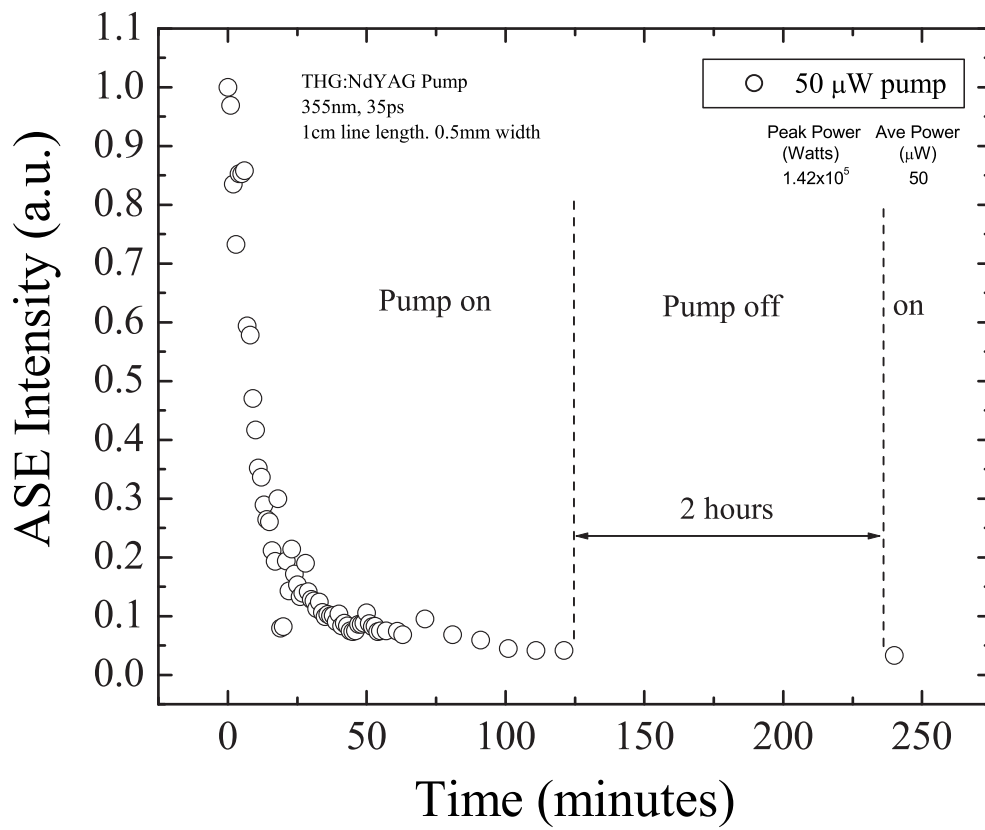
Figure 3.22: Decay of ASE intensity as a function of time for NRL303 using a 10Hz, 35ps, 355nm pump laser. Note that the process is not reversible.

3.7.2 ASE Decay
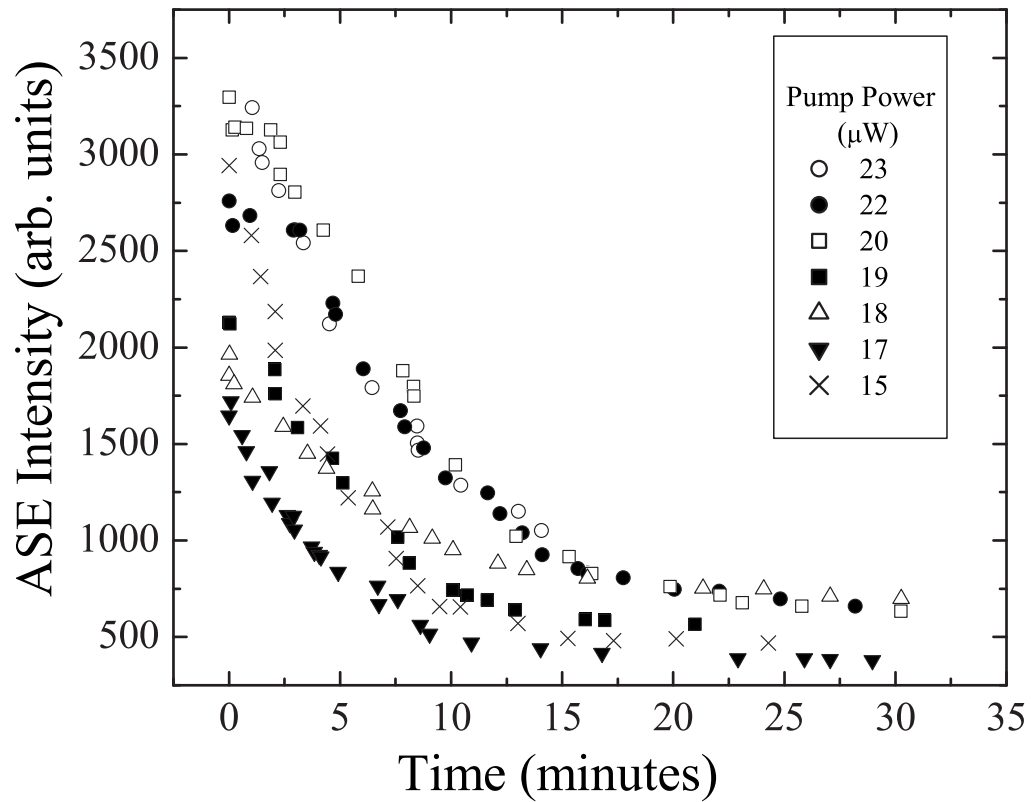
Figure 3.23: ASE decay of NRL303 in PMMA pumped with a 355nm, 35ps, 10Hz laser.

Figure 3.23 shows the ASE decay from NRL303 doped in PMMA for various pump powers of 355nm laser light. Figures 3.24-3.28 show the individual decays and curve fits. All curves have similar decay constants. It appears that there is only one process responsible for the ASE decay and it is nonrecoverable.
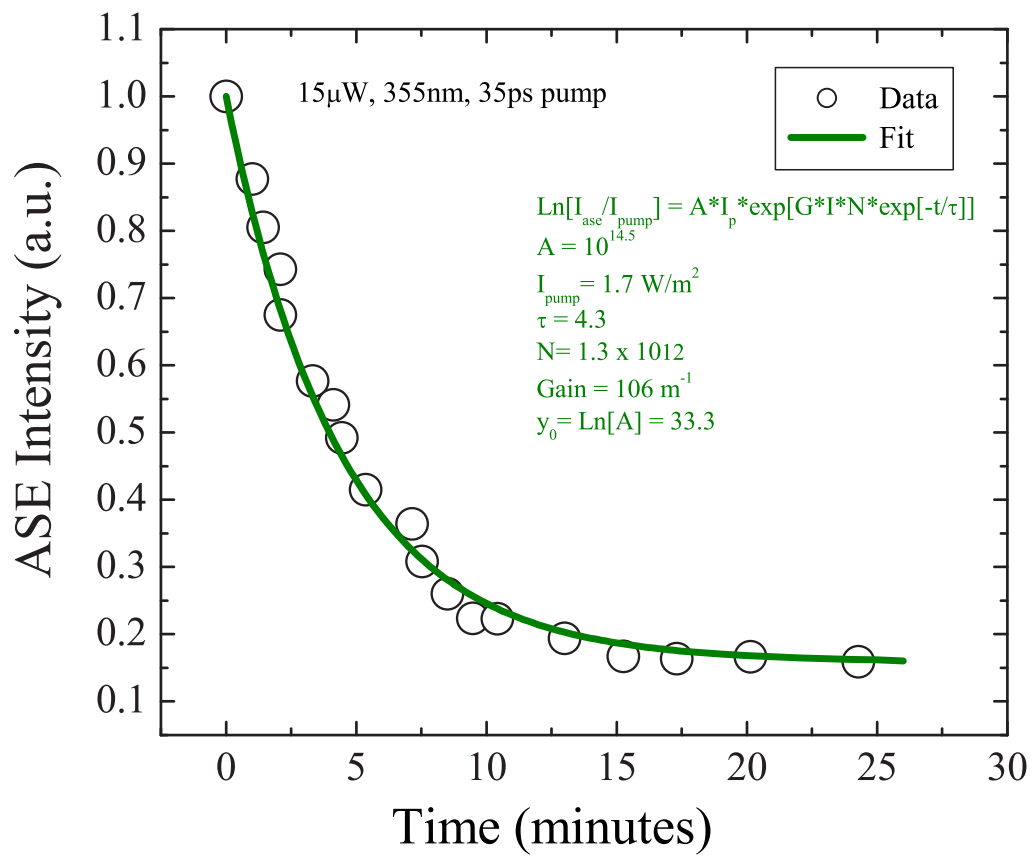
Figure 3.24: ASE decay of NRL303 in PMMA pumped with a 15μW, 355nm, 35ps, 10Hz laser.
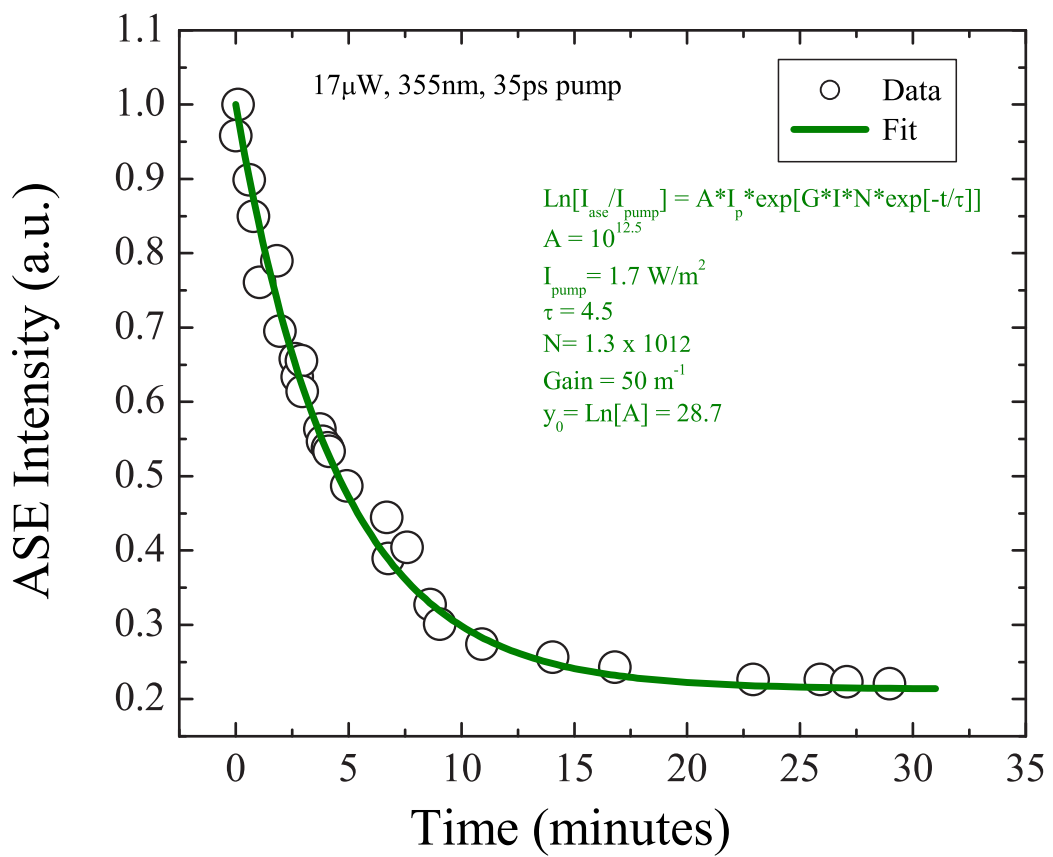
Figure 3.25: NRL303 decay in PMMA from $17\mu W$, 355nm, 35ps, 10Hz pump.

The figure contains the following annotations:

17μW, 355nm, 35ps pump

Data ○
Fit ——

$Ln[I_{ase}/I_{pump}] = A*I_p*exp[G*I*N*exp[-t/\tau]]$
$A = 10^{12.5}$
$I_{pump} = 1.7 \text{ W/m}^2$
$\tau = 4.5$
$N = 1.3 \times 1012$
$Gain = 50 \text{ m}^{-1}$
$y_0 = Ln[A] = 28.7$

Axis labels: ASE Intensity (a.u.), Time (minutes)
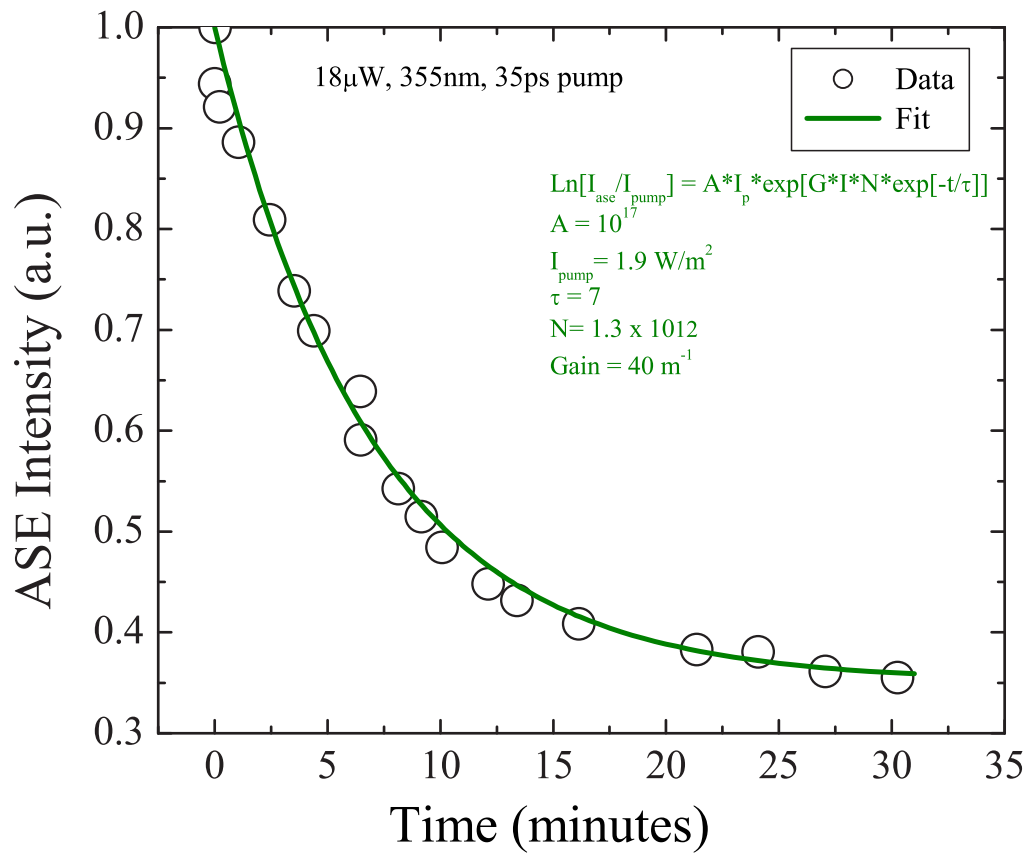
Figure 3.26: NRL303 decay in PMMA from 18μW, 355nm, 35ps, 10Hz pump.
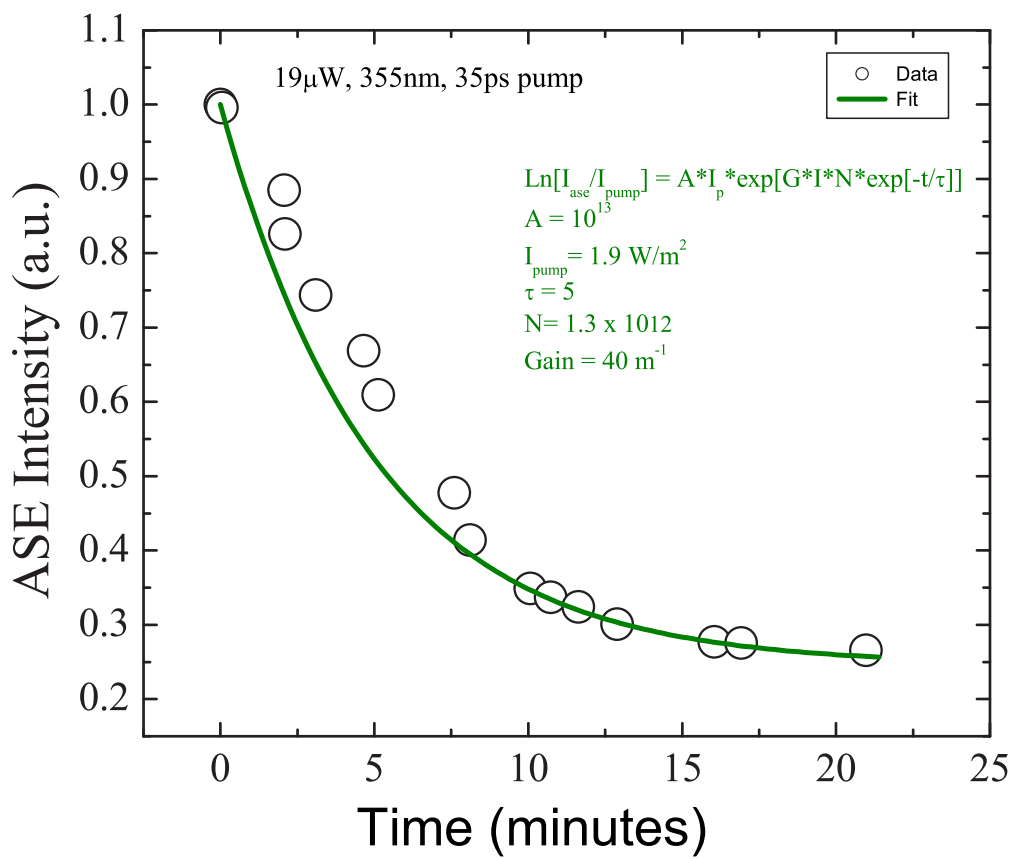
Figure 3.27: NRL303 decay in PMMA from 19μW, 355nm, 35ps, 10Hz pump.
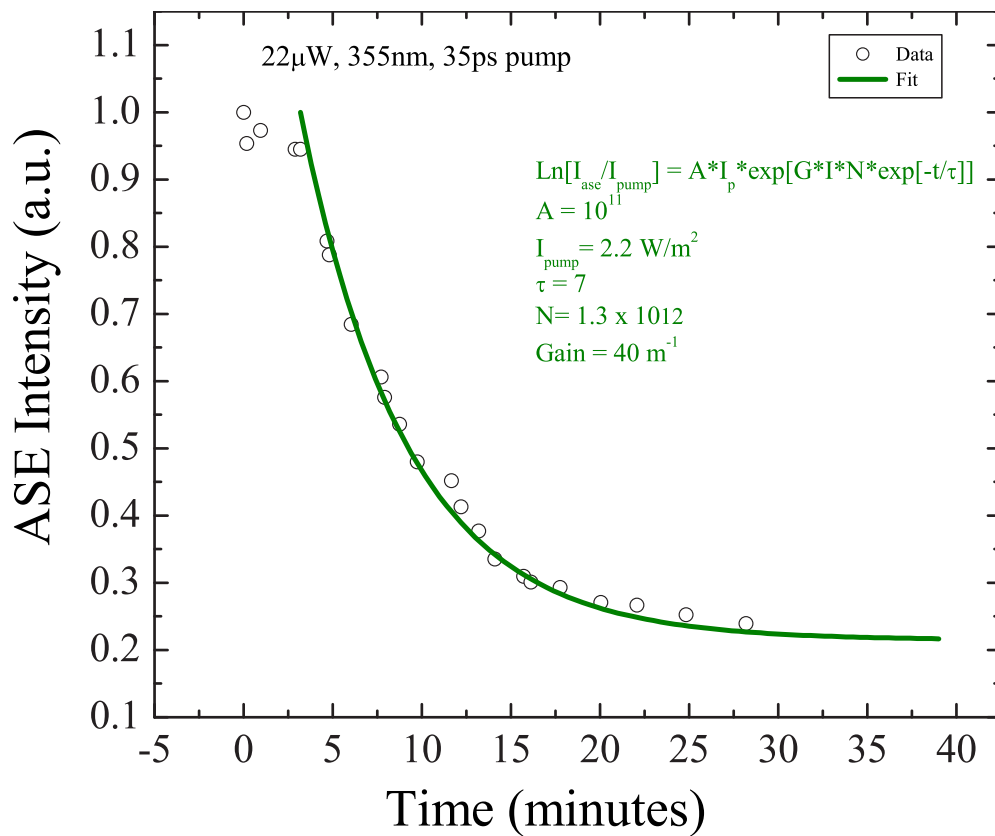
Figure 3.28: NRL303 decay in PMMA from 22μW, 355nm, 35ps, 10Hz pump.

3.8 Nonlinear Absorption and Fluorescence

Both the linear and nonlinear absorption spectra are shown in Figure 3.29. It should be noted that the one photon absorption spectrum was obtained from a continuous white light source while the two photon absorption was measured at a finite number of points using a 100fs Ti:saphire pumped optical parametric amplifier (OPA) that provides light wavelengths from 630nm to 790nm. As such, the resolution of the two photon spectrum is low. Since the TPA spectrum is obtained from the integrated intensities of the two-photon fluorescence spectrum, and the two-photon spectrum is the same as the one photon fluorescence spectrum (see Figure 3.30), it is clear that both fluorescence spectra result form de-excitation between the same states. The two photon absorbance induced fluorescence spectrum is similar enough to the one photon spectrum that the same fluorescence states are excited by both. [17] Figure 3.31 gives a qualitative look at the effectiveness of various pump wavelengths. Pump wavelengths near or twice the linear absorption maximum produces high fluorescence while the 532nm pump is far enough from the linear and two-photon absorption peaks that is has a much smaller fluorescence spectrum.
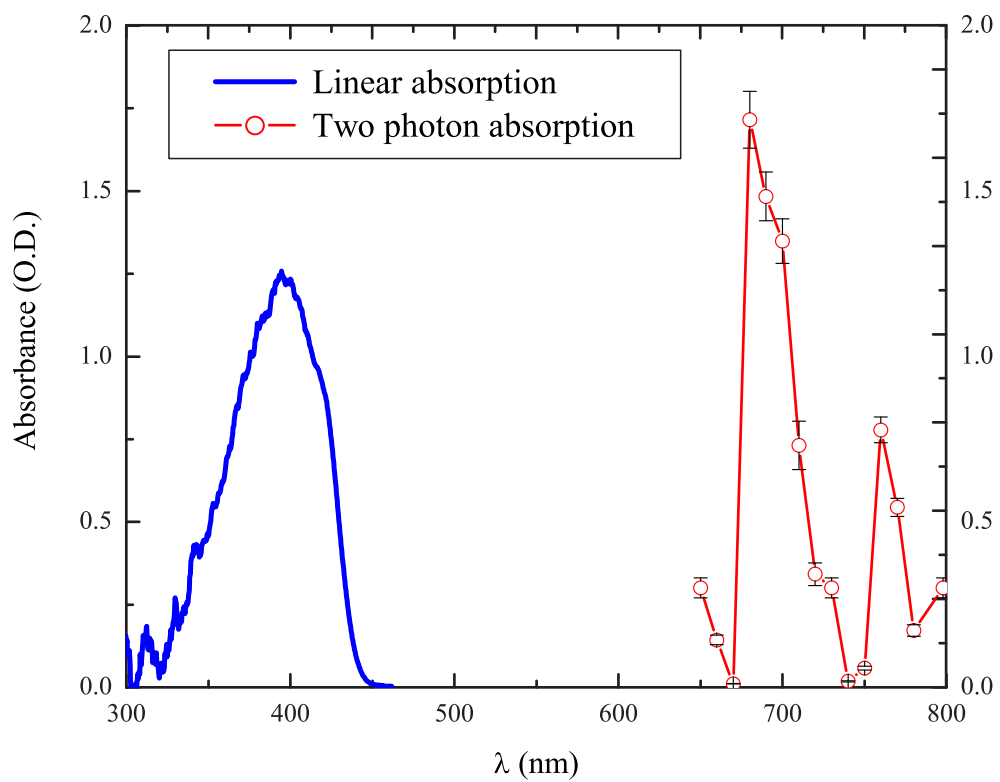
Figure 3.29: Linear absorption and two-photon absorption spectra for NRL303 doped in PMMA.
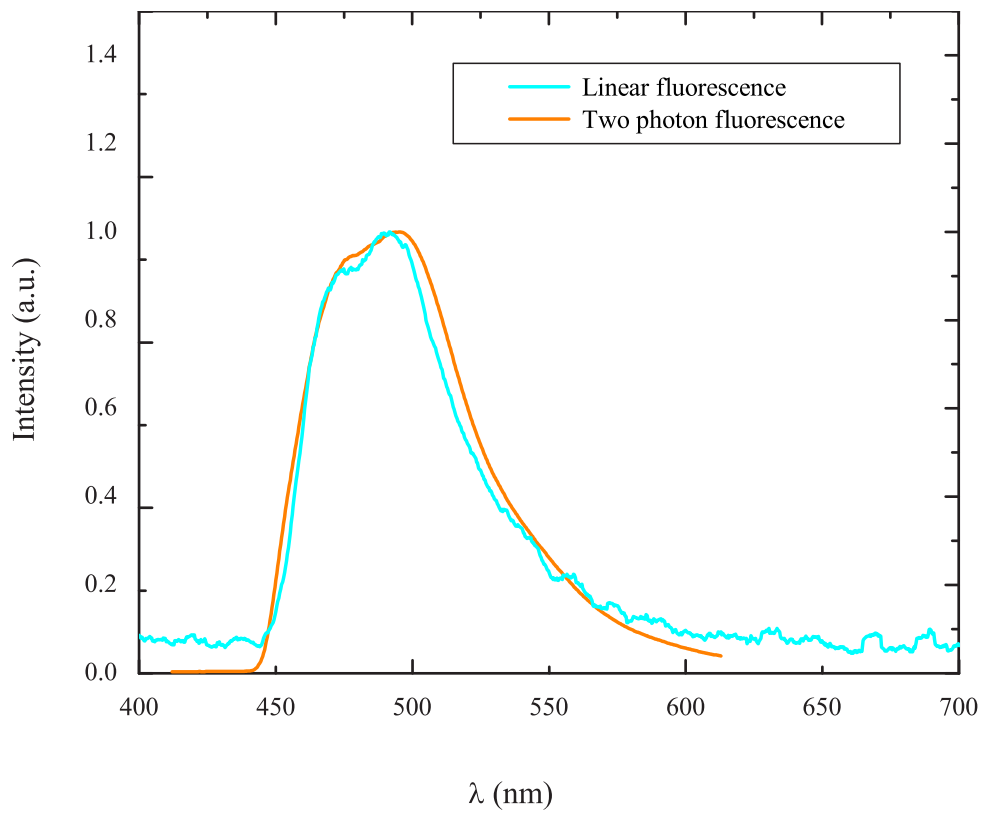
Figure 3.30: One and two photon fluorescence spectra of NRL303 doped in PMMA.
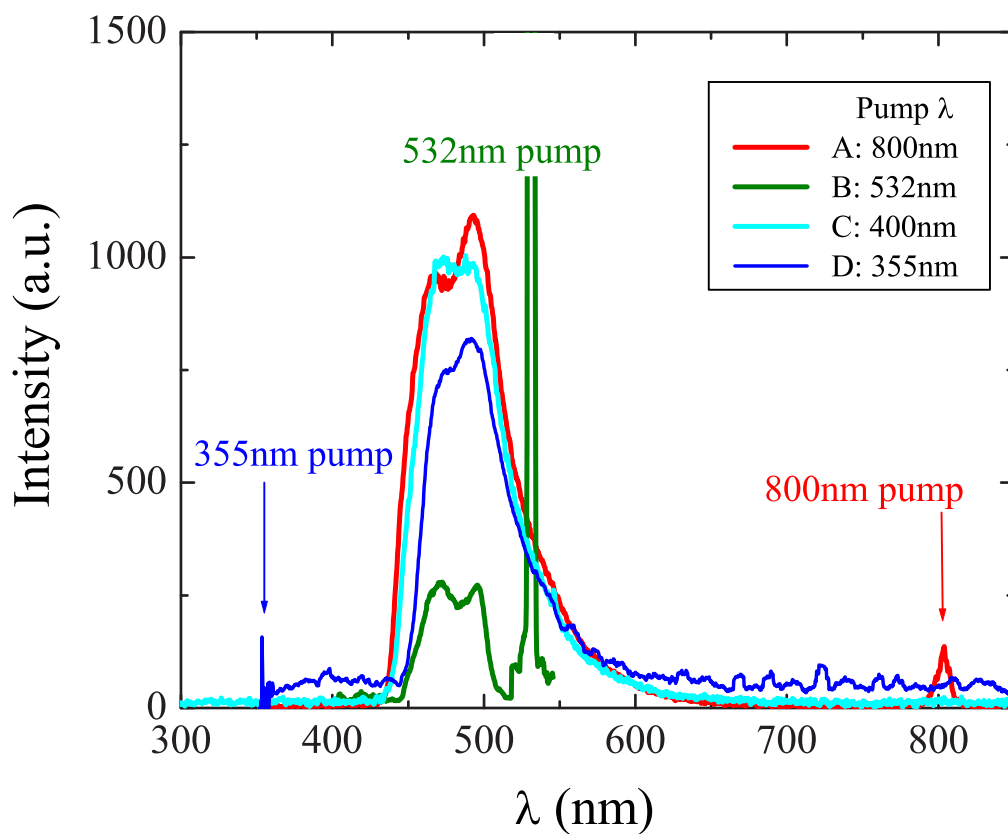
Figure 3.31: Two-photon fluorescence spectra of NRL303 in PMMA excited by four different laser sources: 800nm, 532nm, 400nm and 355nm. The 400nm and 800nm sources provide 100fs pulses while the others are 35ps pulses.

3.8.1   TPA cross section

Measuring the two photon cross section is a challenging process. [18, 19, 20] Being a well characterized molecule, [18, 21] Rh6G was used as reference to calibrate TPA cross section experiments (see section 2.5.2). Figures 3.32 and 3.33 shows the fluorescence spectrum of NRL303 in PMMA as a function of pump wavelength. The inset shows the ratio of NRL303's integrated two-photon fluorescence intensity to the integrated two-photon fluorescence of Rh6G. Figure 3.34 shows that the TPA fluorescence spectra areas as a function of wavelength for all three samples. 303a was used for the initial experiments and a new 303b sample was prepared for the two-photon cross-section experiments. (303a was likely damaged by previous degradation and photobleaching experiments. 303a was run merely for the author's own curiosity). Even after all the abuse from experimentation, 303a still had a higher fluorescence signal than the fresh Rh6G sample. Using Equation 2.20 we find that 303 indeed has a larger two-photon cross section than Rh6G as shown in Figure 3.35.
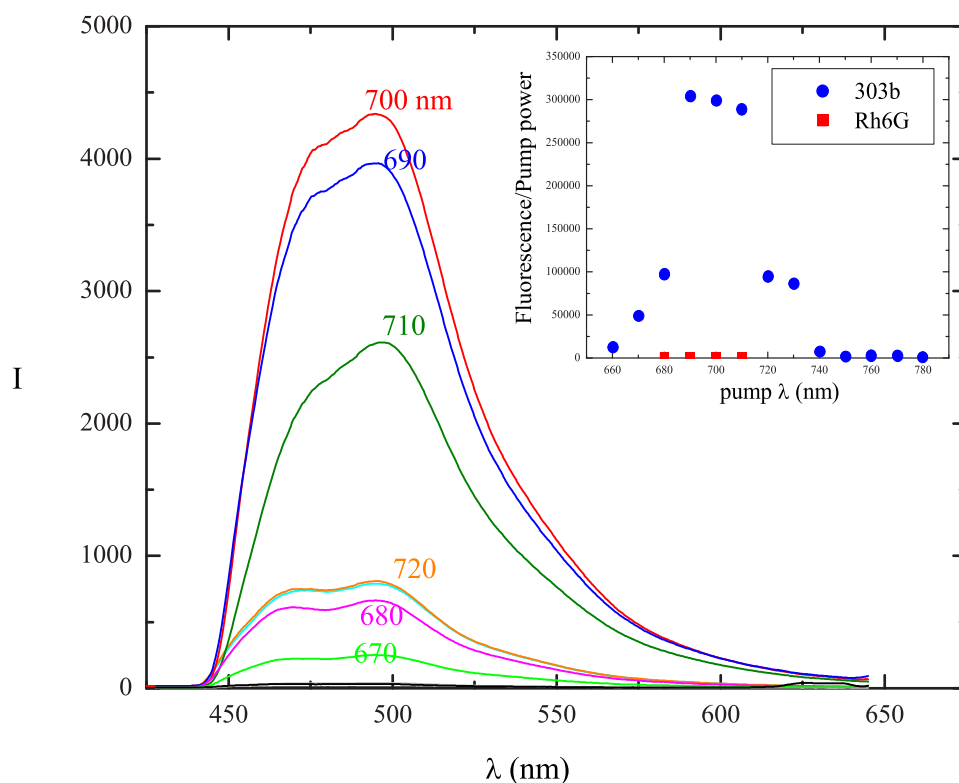
Figure 3.32: TPA fluorescence of NRL303 sample B as a function of pump wavelength. Each spectrum is normalized to the incident pump power. The inset shows the ratio of the integrated fluorescence from NRL303 to the integrated fluorescence from Rh6G.
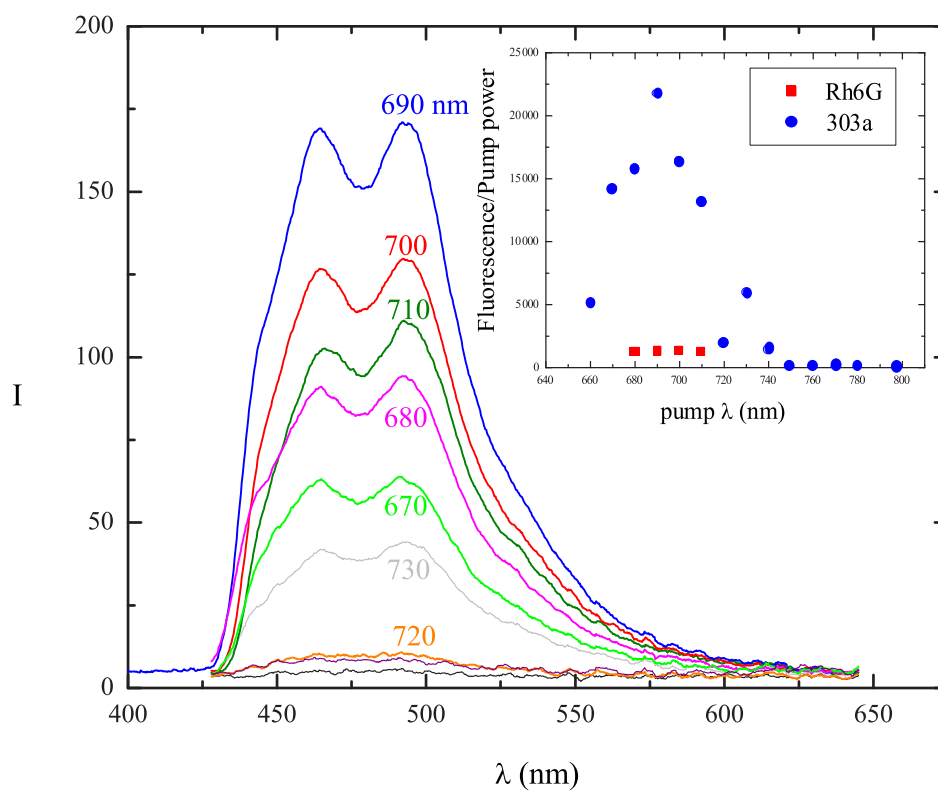
Figure 3.33: TPA fluorescence of NRL303 sample A as a function of pump wavelength. Each spectrum is normalized to the incident pump power. The inset shows the ratio of the integrated fluorescence from NRL303 to the integrated fluorescence from Rh6G.
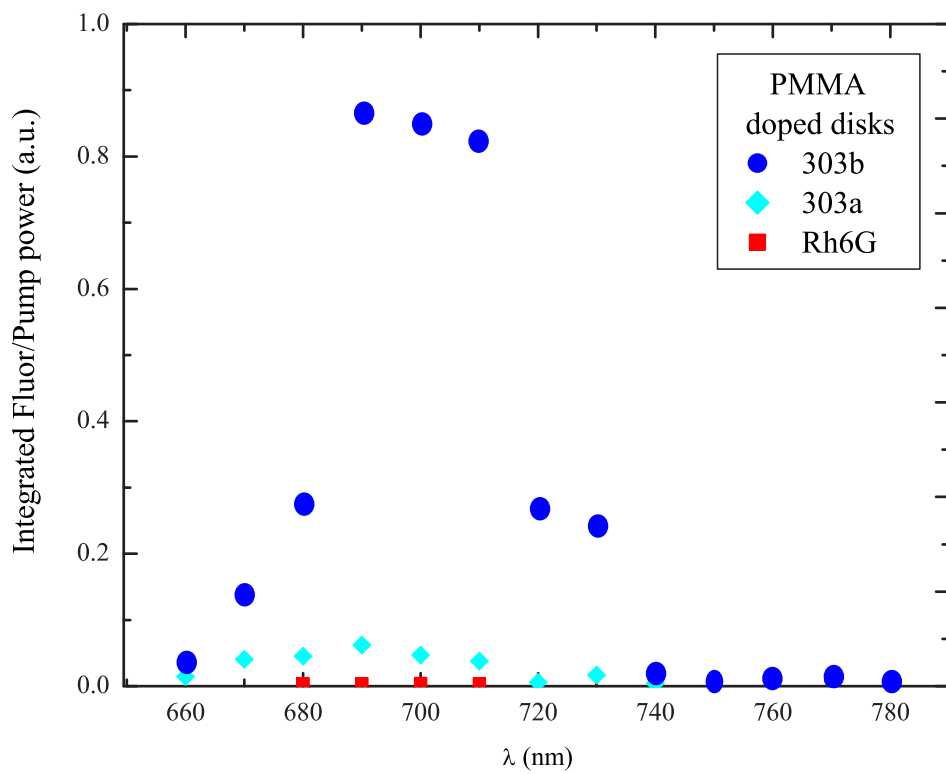
Figure 3.34: Integrated TPA fluorescence divided by pump power as a function of wavelength.
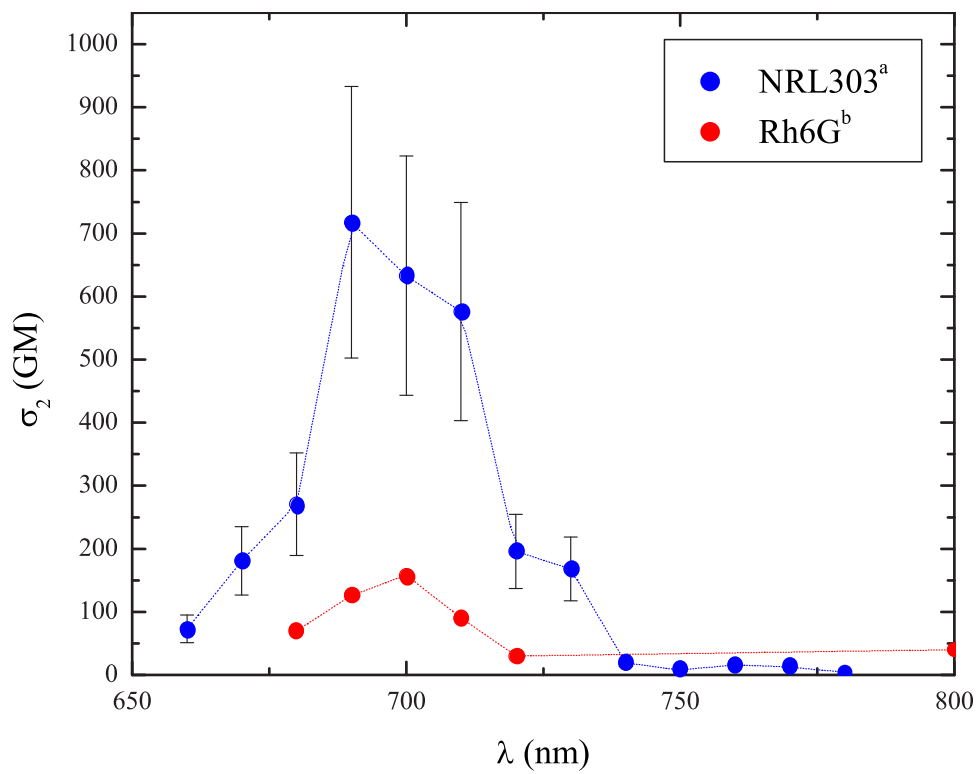
Figure 3.35: Two-photon cross section for NRL303b and Rh6G. a) 303 value measured by the author. b) Rh6G from reference[18].

3.8.2 TPA ASE

Figure 3.36 shows the onset of two-photon induced ASE. This was not seen in either of the other samples. The reason is not clear. The damage to the surface of the 303a sample may have introduced enough scattering and reflections to effectively increase the gain length without surpassing the damage threshold of the sample. Due to the limited amount of sample, further investigation is left for future work.
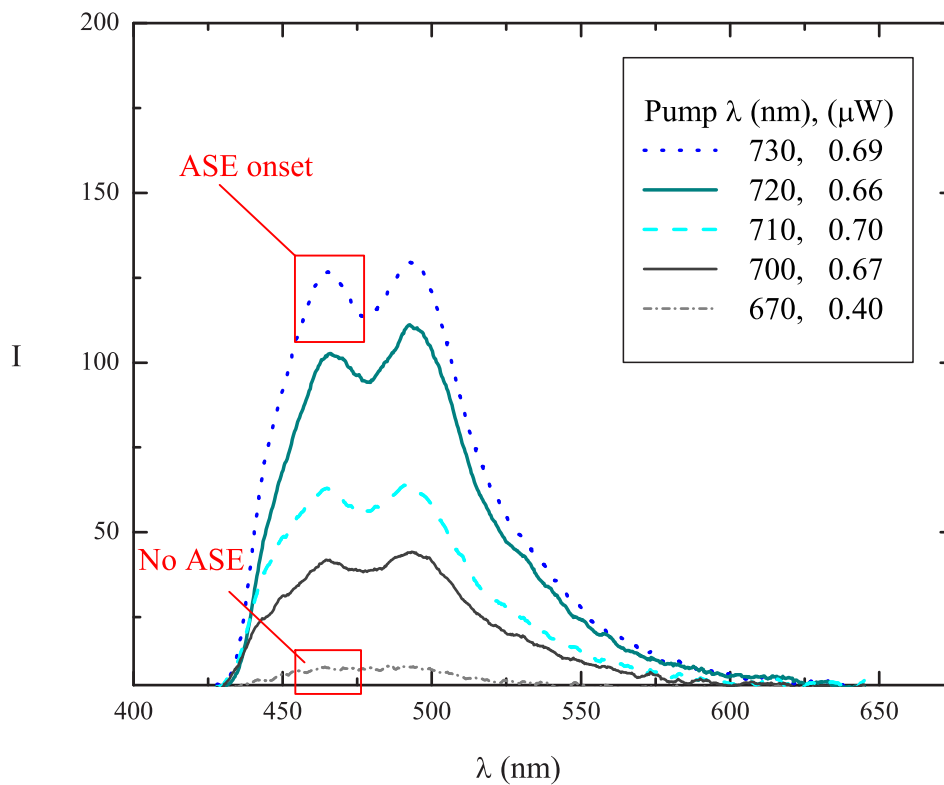
Figure 3.36: Two photon ASE in NRL303 doped PMMA as a function of pump wavelength.

Chapter 4

Discussion

4.1 Chromophore design strategy

The lack of commercially available chromophores with a large two photon absorption (TPA) cross-section or high lasing efficiency motivated this work to better understand how to make improved molecules. Particularly, research on blue light emitting materials has been and remains an area of great interest. Chemical synthesis, through molecular engineering, is a route to make molecules with large two-photon cross sections, high levels of stability, high gain and lasing efficiency. Results form the study of Naval Research Laboratory (NRL) chromophores demonstrates a design scheme leading to enhanced molecular properties for laser and TPA applications.

The ability to produce a solid state dye laser is hindered considerably due to limited availability of solid host matrices that do not quench emission efficiency. There is extensive data that dyes have higher gain and better efficiency in solution than in a solid matrix. [15, 23, 24, 25] A solid matrix acts to broaden the absorption and subsequent emission spectrum. In addition, the gain is inversely proportional to the square of the refractive index. Given that the refractive indices for EtOH (liquid) and PMMA (solid) are 1.36 and 1.45, the liquid's gain is expected to be greater than for a solid just based on the refractive index alone. Adding EtOH to dye doped MMA (the liquid monomer used to make PMMA polymers) prior to polymerization has been shown to increase the gain. The EtOH

allows for greater solubility of the dye and can then cause the formation of microcavities within the PMMA structure. Microcavities or metaloxide nano particles [27] suspended in the PMMA matrix both add light scattering centers that can increase the effective gain length of the medium. Since ASE output increases exponentially with distance propagated (gain length) in the gain material, even small increases in the propagation length lead to increased gain. Indeed, we observed increased gain for a striated NRL303 doped PMMA fiber since the striations along the fiber's long axis multiply scatter the pump laser and emitted light, effectively setting up many small resonators. Clearly, the design of a molecule is important but matrix properties and other polymer geometries should also be considered when maximizing the efficiency of the system.

Our approach to design photo active chromophores is to consider geometry, properties of the π-center (electron relay) and the strength of electron donor or acceptor groups attached to the π-center, which are described below.

4.1.1 Known Dyes

First we consider two well known groups of laser dyes, xanthenes (of which Rh6G is an example) and coumarins. The absorption maximum for Rh6G is at 530nm due to electron transfer between the nitrogen atoms. Note that there is no static dipole, μ_{00}, along the long axis of the molecule due to the symmetric π-electron structure. It is μ_{01}, the transition dipole moment (also along the long axis of the molecule) that is responsible for the large peak in the absorption spectrum. The fluorescent maximum at 557nm yields a Stokes shift of $\sim$30nm for Rh6G, while the ASE peak is found at 590nm. NRL303's maxima are at 395nm and 491nm for absorption and fluorescence, yielding a Stokes shift of 96nm. Less overlap in the absorption and fluorescence bands is good for a gain material's efficiency since there will be less self absorption of the fluorescence emission by the sample. As we will see, this is not the dominant or only factor. Since both have good fluorescence efficiencies (0.95 for Rh6G and 0.88 for NRL303), clearly other parameters are involved. Both molecules are highly planar; however, the conjugated links from the π-center to the A/A pairs of the NRL303 are not
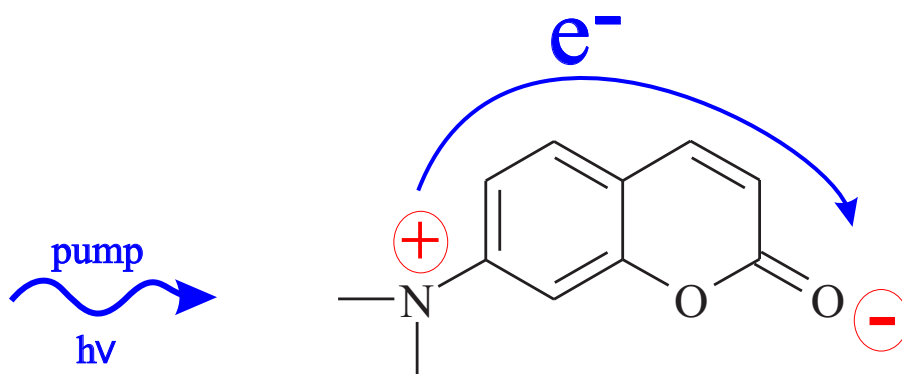
Figure 4.1: Absorption in coumarin

as rigid as the substituted three ring structure of Rh6G. A less rigid structure will have a greater loss of efficiency due to non-radiative decay. [30] On the other hand, a rigid structure does not imply that there will be efficient fluorescence, if any. The coumarins can have good gains and fluorescence efficiencies of up to 16cm^{-1} and 0.85.

If we look at the structure of electron transfer in a courmarin base structure, we get an idea of how the length of the molecule effects the absorption wavelength (see Figure 4.1). Electrons are free to move along a π conjugated structure. So, approximating this system as a particle in a box, the first excited state energy will be inversely proportional to the square of the length of the box. In the 1940's, Hans Kuhn showed that this was a good approximation for linear polyenes, the simplest conjugated system. [36]

4.1.2 Charge transfer

It is widely accepted that a rigid planar molecule tends to have a larger fluorescence efficiency than a non-rigid one. [10, p.158] A rigid planar geometry does not interfere with electron transfer across the molecule. It follows that useful molecular designs should start with a rigid planar π-centered system. Dye molecules were synthesized with either electron acceptors or electron donors linked to the π-center. For symmetric molecules (A-π-A or D-π-D) the strength of the donor/acceptor and the conjugation length have a greater impact on the nonlinear properties than the degree of asymmetry (A-π-D). [29] An example structure of
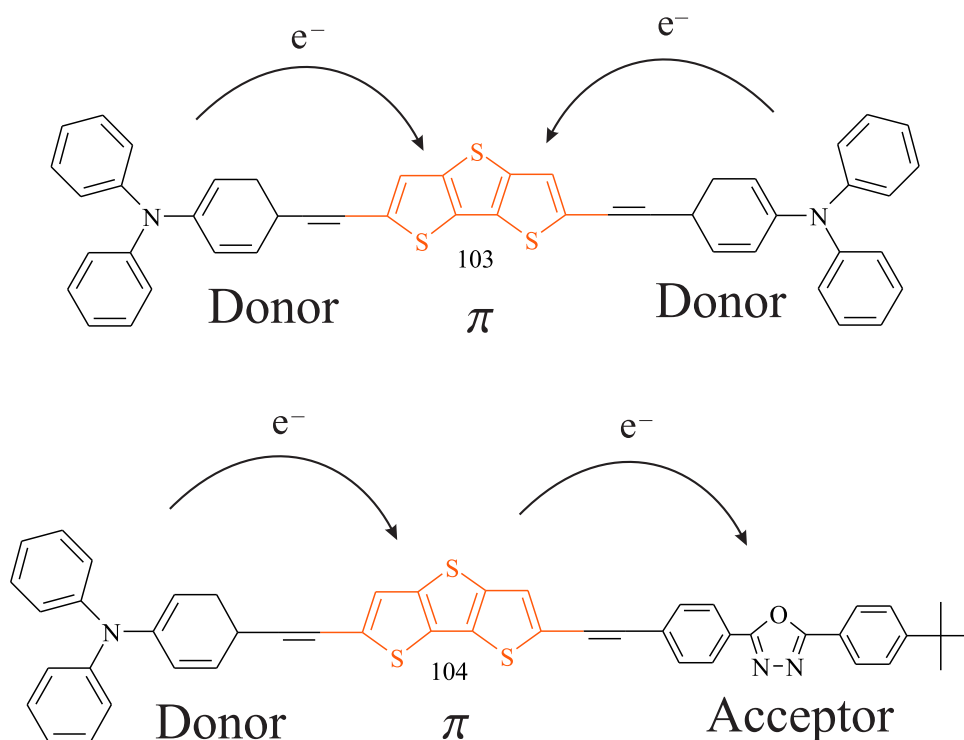
Figure 4.2: D/D and D/A charge transfer.

an A/A and A/D molecule are shown in Figure 4.2. Also, the planarity of the π-center is more important than conjugation length. [28, 38, 37]

4.1.3 Electronic Balancing of π-center and A/D moiety

The Chromophore design scheme produced molecules with varying acceptor/donor moieties linked to the same π-center (electron relay). Greater differences in energy between the moiety and the π-center should decrease the fluorescence efficiency. The less the electron transfer is impeded, the better the molecule should absorb and emit light. Fluorescence efficiency values for symmetric D/D, A/A and asymmetric A/D molecules with one of four π-centers were synthesized by Dr. Oh-Kil Kim at the Naval Research Laboratory and made available to us for study (see Figure 4.3 and 4.4).

101
$D_1 - \pi_1 - D_1$

102
$D_1 - \pi_1 - A$

103
$D_2 - \pi_1 - D_2$

104
$D_2 - \pi_1 - A$

105
$D_3 - \pi_1 - D_3$
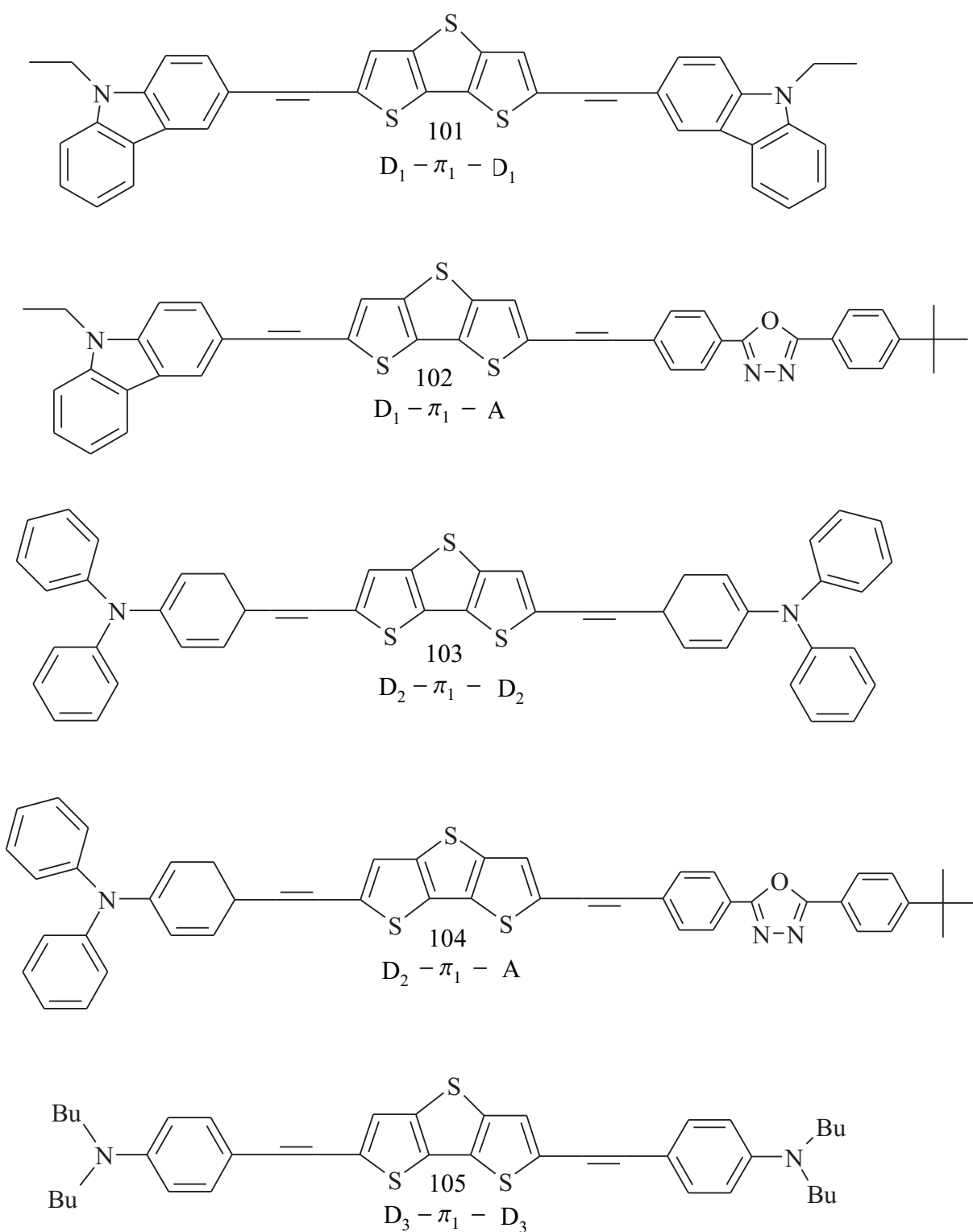
Figure 4.3: NRL100-series molecule structures

201
D$_2$ - π_2 - D$_2$

203
A - π_2 - A

301
D$_2$ - π_3 - D$_2$

302
D$_2$ - π_3 - A

303
A - π_3 - A
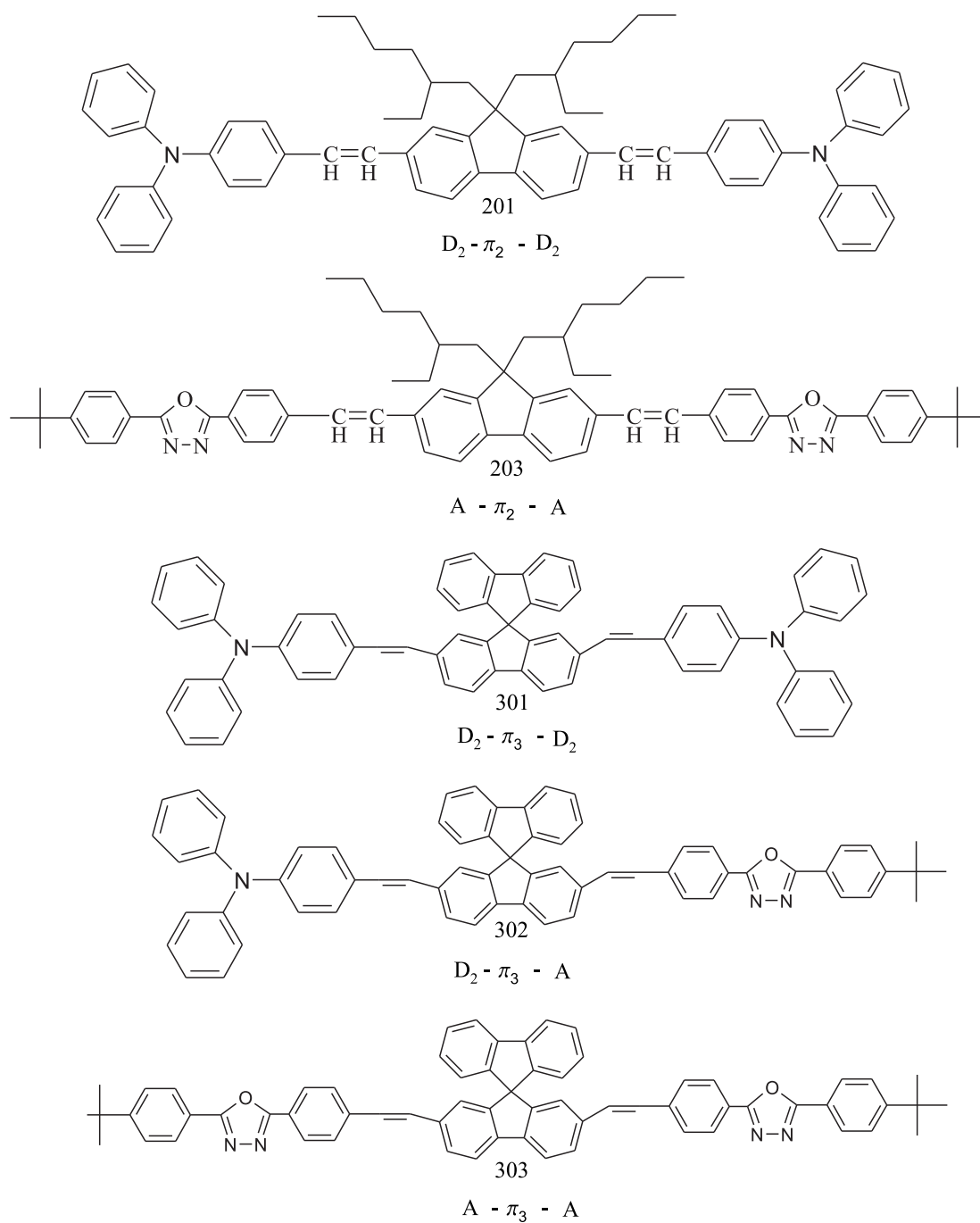
Figure 4.4: NRL200- and 300-series molecule structures

The NRL molecules were designed with the goal of enhancing the two photon absorption cross section, σ_2. In order to examine the effectiveness of the NRL design strategy, I introduce the design factor, σ_{DF}. Three weighted parameters are used to construct the design factor: the geometric planarity of the dye molecules structure, P, the quantum fluorescence efficiency, ϕ_f, and the difference in energy between the A/D pairs and the π-center, ΔE. The cross-section design factor is given by:

$$\sigma_{DF} = aP + b\phi_f + c\Delta E^{-1}. \tag{4.1}$$

The coefficients were determined empirically from the data to be $a = 3\,GM\,nm$, $b = 1\,GM$ and $c = 0.3\,GM\,eV$ respectively, where 1 GM=$10^{-50}cm^4$ s/photon. Each molecule was optimized for the lowest conformational energy state with the quantum computation software HyperChem 7.5. The value for the planarity was determined by the following equation applied to the optimized structures:

$$P = \left[\sqrt{\frac{\sum m_i h_i^2}{\sum m_i}} \right]^{-1}, \tag{4.2}$$

where m_i is the mass of the atom a distance h_i above or below the central plane of the π-center. The fluorescence efficiency and two-photon cross section are from values reported by Oh-Kil Kim [28]. The third parameter, ΔE was determined by semi-empirical self-consistent field method quantum calculations. AM1, the Austin Model 1 based on the Hartree-Fock model was used to calculate a potential energy surfaces with HyperChem 7.5. Iterative quantum calculations keep track of the electron repulsion energies for solutions of the Schrodinger equation. A wavefunction for the electron orbitals and electron repulsive forces is recalculated until the solution converges. The value for the calculated electronic energy is the entire potential energy surface for the structure, not that of just one electron.

All parameters were normalized then weighted to give the best linearity when plotted against the normalized two-photon cross-section, σ_2, as shown in Figure 4.5. Figure 4.6 shows that the planarity, P is the dominant factor for large two photon cross sections for
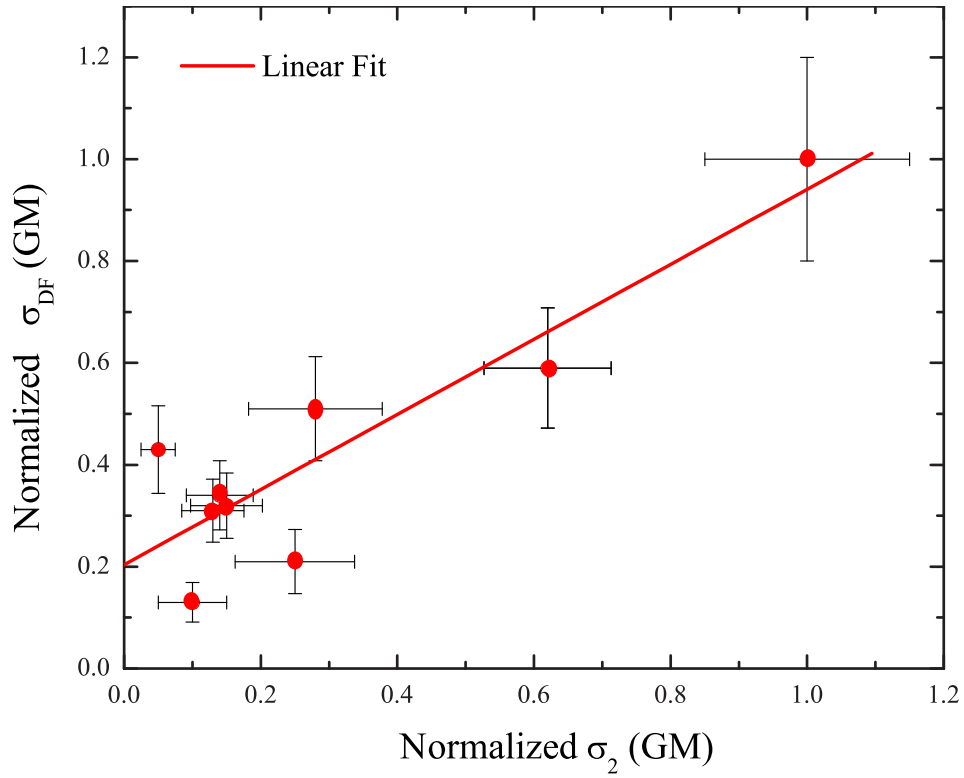
Figure 4.5: Cross-section design factor, σ_{DF} vs. the measured two photon cross section, σ_2.
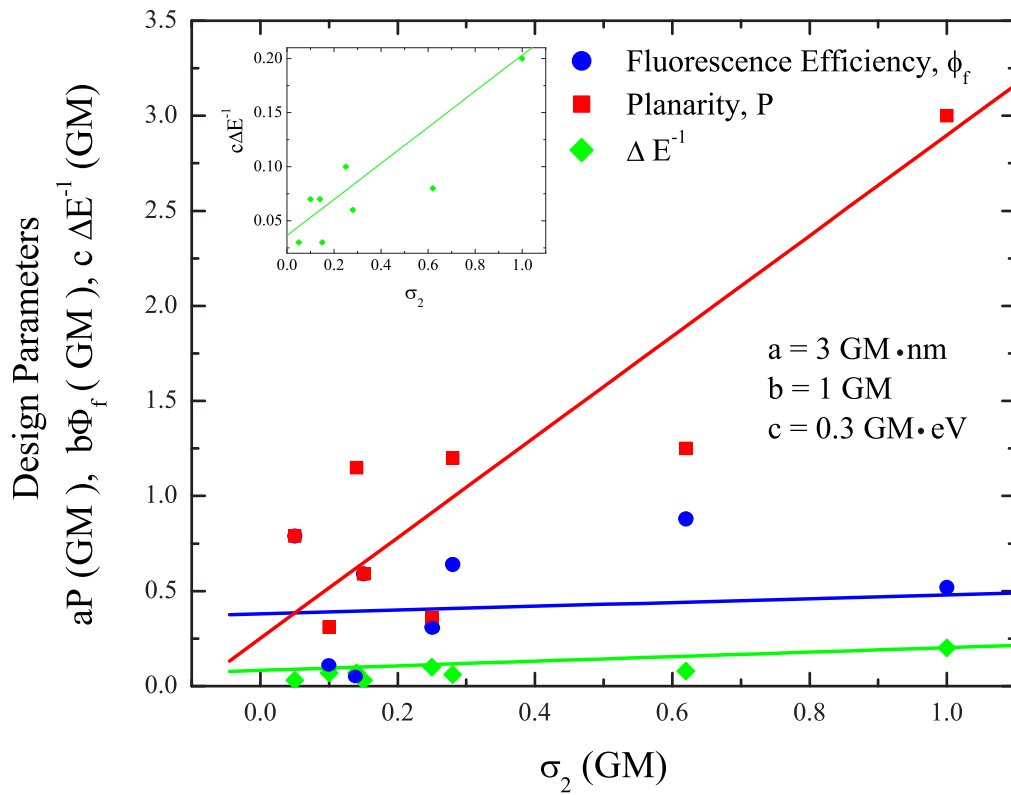
Figure 4.6: Design parameters vs. the two photon cross section, σ_2. The inset shows the energy parameter to highlight increasing trend.

the structures studied here. ΔE was seen to have a minor effect on the overall change in the two photon cross section. This is expected since these molecules were designed to electronically balance the energies of the π-centers with the A/D end pairs. Well balancing these should in turn further reduce the effect seen due to this parameter. Dyes of the same class that have not been designed with electronic balancing in mind would be expected to show a greater dependance of the two photon cross section on ΔE. Form Figure 4.6 we see that the fluorescence efficiency also impacts the overall value of the design factor. Knowing the contribution from each parameter is important for thoughtfully designing molecules with large two photon cross section. Optimizing each parameter independently should yield molecules with significantly higher two photon cross section than typically observed.

It is difficult to fully analyze all molecules since there are a large number of parameters to consider. Table 4.2 summarizes the results, which shows that lowering the barrier between the π-center and A/D moiety increases the two-photon cross section as seen in Figure 4.6. The following combinations all show the trend that the lower the difference in potential energy, ΔE of the moiety and the conjugated bridge, the higher the fluorescence efficiency, ϕ_f. For the molecules we have studied, the efficiencies follow this trend within groups with the same π-centers as follows, A/A linked $\pi_{2,3}$-centers 203 and 303, D/A linked π_1-centers 102 and 104, D/D linked π_1-centers 101, 103 and 105, which can be seen in Table 4.2.

Attributing TPA values to efficiency or potential difference of π-centers and A/D moieties is difficult. The two photon cross section, $\sigma_2(\lambda)$, is dependent on the incident wavelength and power. The further the incident wavelength is from the TPA maximum the lower the σ_2 value. In the molecules measured in our studies, the resonance enhancement is comparable, so we can ignore this effect. Table 4.1 shows that D/D symmetry is better for TPA than asymmetric A/D molecules as seen in 101/102 and 103/104 (see Figure 4.7). Symmetric charge transfer is important to TPA. [28, 32, 33] As shown in Figure 4.7 the asymmetric molecule of each set with the same π-center has the lowest two-photon cross-section. While the highest overall is the only one listed in Table 4.1 that is centro-symmetric.
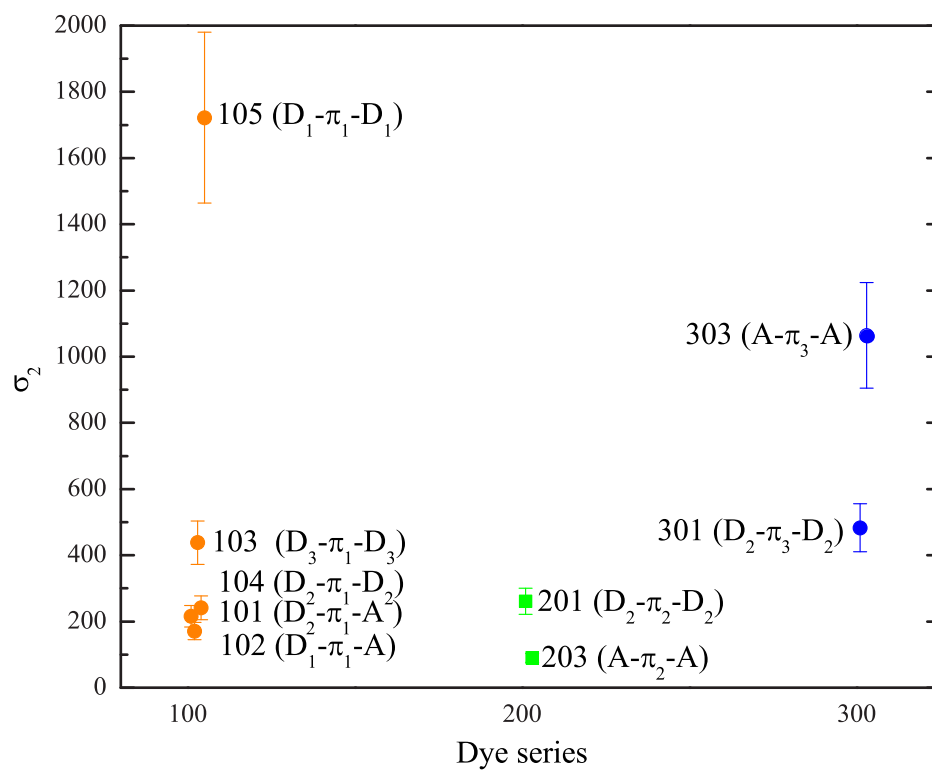
Figure 4.7: Symmetry effect on two photon cross section as a function of dye series (π-center).

NRL Dye	A/D moiety	Symmetry	σ_2 $(10^{-50}cm^4s/photon)^a$	Efficiency[a] ϕ_f
105	$D_1 - \pi_1 - D_1$	CS	1722	0.520
104	$D_2 - \pi_1 - D_2$	C1	241	0.055
103	$D_3 - \pi_1 - D_3$	C1	438	0.310
102	$D_1 - \pi_1 - A$	C1	171	0.095
101	$D_2 - \pi_1 - A$	C1	216	0.470
201	$D_2 - \pi_2 - D_2$	C1	261	0.590
203	$A - \pi_2 - A$	C1	90	0.790
301	$D_2 - \pi_3 - D_2$	C1	483	0.640
302	$D_2 - \pi_3 - A$	C1	-	0.250
303	$A - \pi_3 - A$	C1	1064	0.880

Table 4.1: Fluorescence efficiency vs electronic balancing. a. $\sigma_2 \pm 15\%$ measured by Kim et. al.

NRL Dye	σ_2 (normailized)[a]	Fluorescence Efficiency[a] ϕ_f	Planarity[b] P	Energy Difference[b] $\frac{1}{\Delta E}$	σ_{DF} (normailized)
105	1	0.52	3.00	0.20	1
303	0.62	0.88	1.25	0.08	0.59
301	0.28	0.64	1.20	0.06	0.51
103	0.25	0.31	0.36	0.10	0.21
201	0.15	0.59	0.59	0.03	0.32
104	0.14	0.06	1.15	0.07	0.34
101	0.13	0.47	0.38	0.30	0.31
102	0.1	0.10	0.31	0.07	0.13
203	0.05	0.79	0.79	0.03	0.43
302	-	0.25	1.07	0.06	0.37

Table 4.2: TPA cross-section design factor, (σ_{DF}) and parameters. a. $\sigma_2 \pm 15\%$ measured by Kim et. al., b. semi-empirical calculation

4.2 Chromophore properties
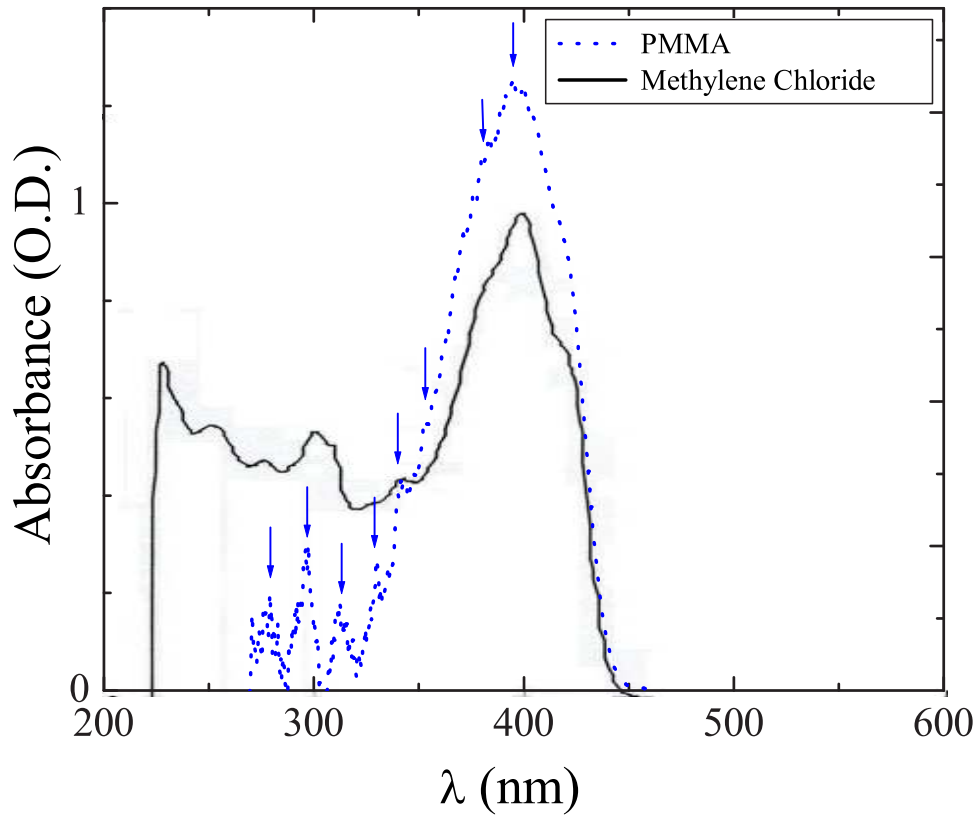
Figure 4.8: Absorption spectra of NRL303 in methylene chloride (measured by the Air Force Research Laboratory) and PMMA (measured at WSU).

NRL303 Absorption peaks										
Measurment	solvent / host	λ (nm)								
One-photon absorption(λ)	methylene chloride	248	272	297	-	338	340	382	**395**	418
	PMMA	238	278	295	311	328	340	382	**393**	415
Two-photon absorption($\frac{\lambda}{2}$)	PMMA					325*	**340**	380	400*	

Table 4.3: Wavelength of absorption peaks of NRL303 in methylene chloride, measured by AFRL and in PMMA measured at WSU, with largest peaks in bold. Wavelength of the TPA peaks measured in PMMA divided by two. *Values are approximate.

For NRL303, the main TPA peak is not at 800nm, which would be at twice the wavelength of the linear absorption peak of 400nm. Meshalkin et. al. [16] reports that some dyes have a TPA spectrum that is blue shifted up to 200nm, and never red shifted compared to the linear spectrum. Xu and Webb also have remarked on the lack of understanding of the origin of this blue shift. [17, 16] Closer examination of the absorption spectra sheds light. Figure 2.4 shows a series of small peaks super imposed on the larger main peak. These are the absorption peaks due to vibronic states, which are to the blue side of the main absorption peak. Table 4.3 compares the linear absorption peaks from Figure 4.8 with and nonlinear absorption peaks that are shown in Figure 4.9. The shape of the linear absorption spectra of NRL303 in both methylene chloride and PMMA are similar to the theoretical sketch plotted in Figure 2.4.

Figure 4.9 shows that the one and two photon fluorescence curves are identical. Identical fluorescence curves implies that the same initial and final states are involved in both fluorescence processes. As such, the conformational relaxation form the higher states excited by the light decays to the same lowest *excited state* leaving the molecule in the same geometry. The narrower fluorescence spectrum compared with the absorption spectrum when plotted as a function of energy implies that the exited states have steeper potential from torque ("torsional movement"). [10, 35] If molecules can undergo conformational changes, torsional movement and other vibrational non-radiative decays, then the fluorescence quantum yield clearly will be reduced. If a molecule's structure is rigid, then parasitic non-radiative decays,
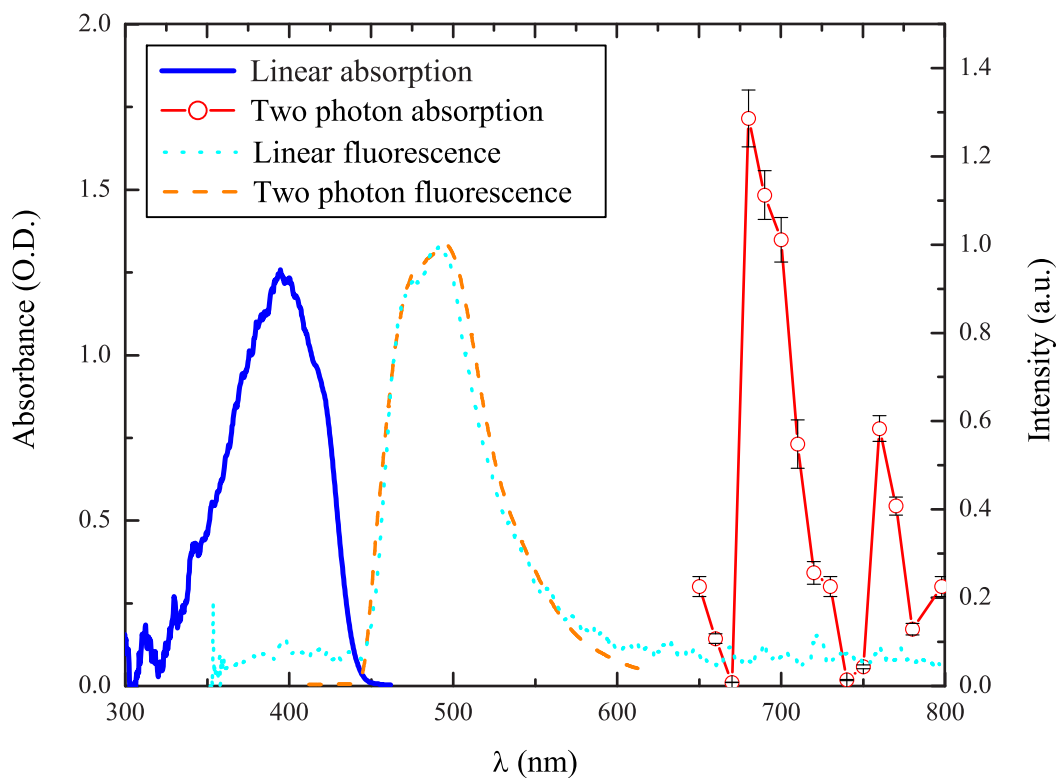
Figure 4.9: One- and two-photon absorption, and fluorescence spectra for NRL303 in PMMA.

from conformational relaxation will be reduced, improving the fluorescence quantum yield and ultimately σ_2 of the molecule; but, σ_2 is due to the states that are excited so fluorescence yield will not necessarily be perfectly correlated with σ_2. Similarly, if we compare the plot of the absorbance and fluorescence spectra, with the energy axis of the fluorescence spectrum inverted and shifted to coincide with the absorption spectrum peak, they coincide, showing that they are mirror images of each other of slightly different widths. It follows that the different vibronic levels of the same electronic states that are absorbing are in turn emitting, though different vibrational states are involved.
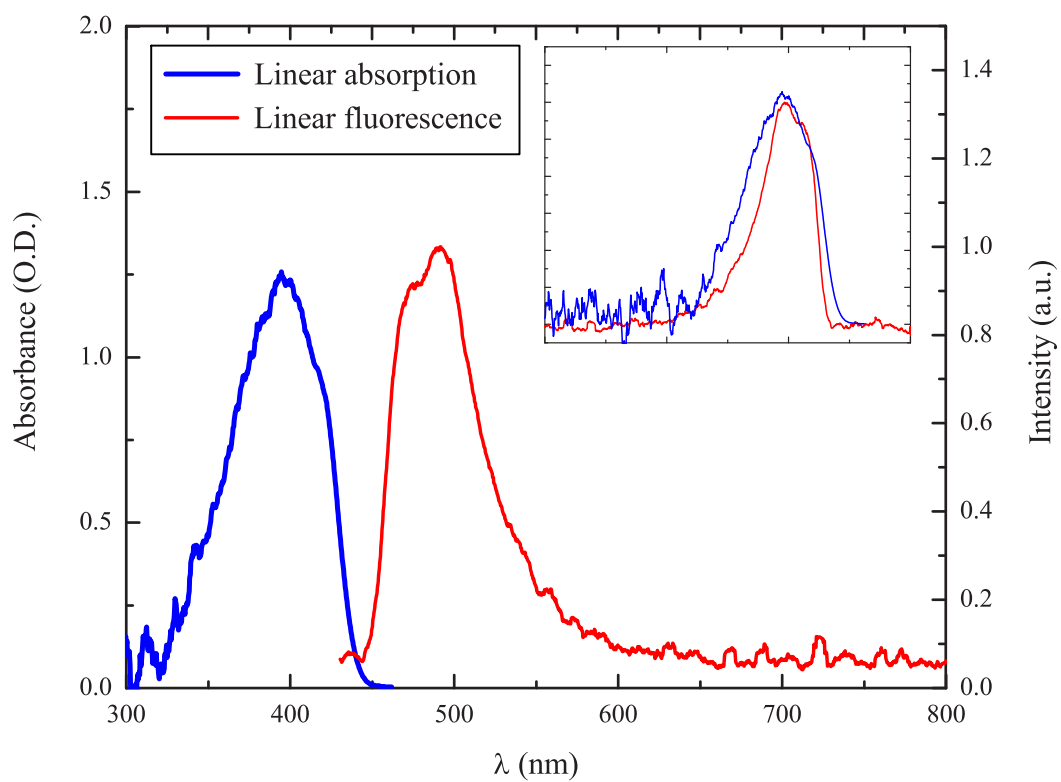
Figure 4.10: Absorption and fluorescence curves of NRL303 in PMMA. The inset shows the two peaks after they are overlapped with the fluorescence spectrum (wavelength axis) inverted.
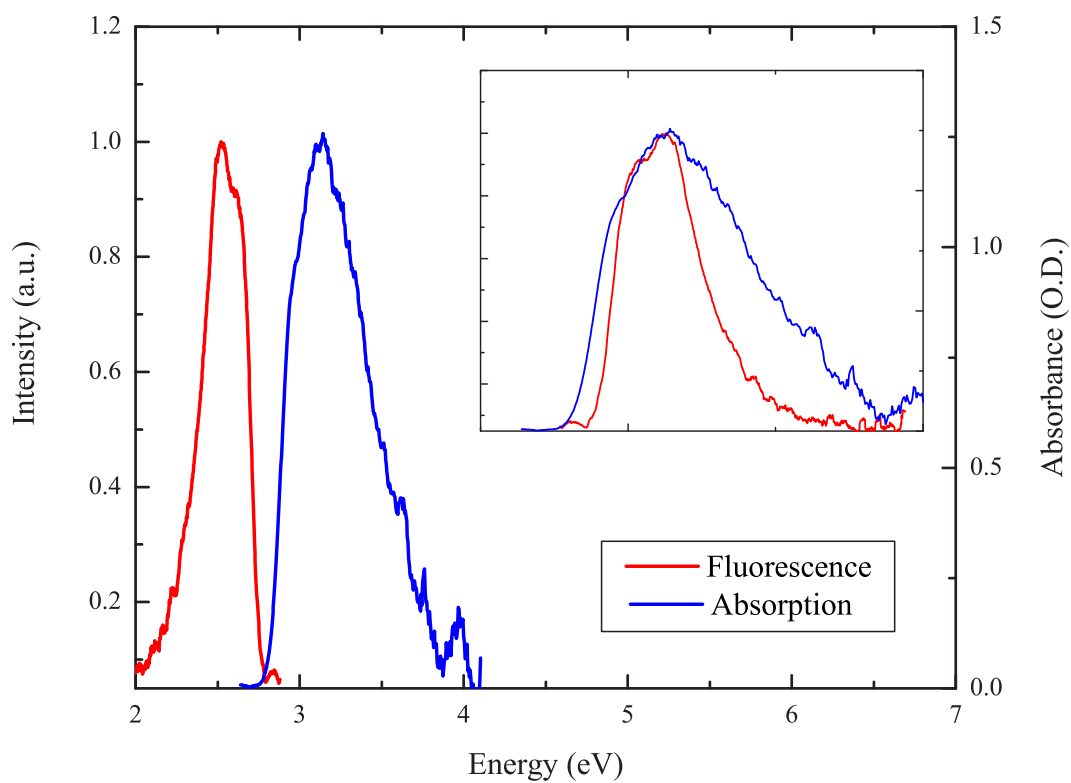
Figure 4.11: Absorption and fluorescence spectra of NRL303 in PMMA. The inset shows the two peaks after they are overlapped with the fluorescence spectrum (energy axis) inverted.

A narrow absorption band implies a rigid structure. [30] However the larger the width of the absorption band the greater the potential for a larger Stokes shift. These two effects thus compete with each other. The dominance of rigidity and planarity in a design scheme will give small Stokes shift and greater reabsorption.

Overall, each parameter of the two-photon cross-section design factor shows the trend of increasing with larger σ_2 as seen in Figure 4.6. However, all parameters do not contribute equally to the overall design factor. As such, the importance of each parameter should be weighted when designing new TPA molecules. While the increase of σ_2 with each parameter may not be linear, we find that a linear relationship approximates the trend in the data. The fact that the σ_{DF} has a better fit, within experimental uncertainty, than the fit of the individual parameters plotted against σ_2 leads us to believe that the design factor is valid for predicting relative two-photon cross-section values. Other factors not considered here may also contribute to fine tuning the successful engineering of large σ_2 molecules. Specifically we saw that the only centro-symmetric molecule had the largest σ_2.

Chapter 5

Conclusion

Experimental results have shown a blue emitting Chromophore (NRL303) made with symmetric acceptors and doped into PMMA surpasses the efficiency of Rh6G in PMMA, i.e. $\sim$25% v.s. 21%, respectively, when both are doped in polymer hosts.[31] The gain of NRL303 at 3 to 7 cm^{-1} is better than that of Rh6G which is measured to be 3 cm^{-1} and better than other emitters in the visible region of the spectrum listed in Table B.1, especially when compared with blue emitters. Rh6G has been the standard benchmark of laser dyes in efficiency and gain. It is evident that the electronic matching of the chromophore π-center and linked A/D moiety is important for efficient photoactivity.

Other issues should not be neglected, such as considering planar rigidity, A/D strength, conjugation length, dipole moment and atom substitution of the inner π-center ring structure. Drexhage's rule [10] predicts higher triplet populations if the π-electrons can move around the center of the chromophore when excited across the molecule. Populating the triplet state increases competition with the singlet state that quenches the singlet. The orbital magnetic moment induced by the circular path of electrons couples to the spin of the electron, increasing the probability of the triplet state being populated. Placing an atom in the center ring that hinders circular charge transfer around the bridge will lower the triplet state population.

Enhancement of each parameter and appropriate matching of energies will be required to continue improvements in molecular structures that will lead to an increase in the TPA cross

section, lasing efficiency, stability and possible recovery of degradation. A well designed dye in a robust solid matrix that enhances or at least does not quench fluorescence efficiency and gain will be vital to many applications. As such, efficient and stable absorbing and emitting molecules show promise of being synthesized.

5.1   Future work

The calculated values for the potential energies of A/D moieties and π-centers suggest that further calculations and experiments are needed to verify the relationship between energy matching and improved cross sections. Systematic synthesis of a larger set of slowly varying-strength A/D linked chromophores is in order. The insight could be applied to make better blue emitters and molecules with larger TPA cross-sections, two important applications that are becoming important to several technologies.

Photobleaching from pumping at λ=355nm, τ=35ps; and λ=400nm, τ=100fs pulses was seen in both NRL303 and NRL105. While NRL105 had the higher two photon cross-section, it's pump-induced emission decayed at a much faster rate that NRL303. No recovery was witnessed in either material. Determining a mechanism to promote recovery after pho-todegradition will be important to future work. Decay then subsequent recovery has been observed in disperse orange 11's ASE when pumped with 532nm 35ps pulses. [34] Clues as to the cause of this phenomena might be applicable to NRL dyes to make them more robust.

The goal of producing a recoverable, robust, wavelength tunable solid state dye doped system is motivated by many important applications. Increased theoretical work with the NRL design scheme is an exciting avenue for future work that could lead to even better molecules.

5.2   Applications

The recent interest in blue emitters and molecules with large two photon absorption cross sections is fuelled by applications such as optical limiting, underwater communications, 3D

imaging, data storage, two photon microscopy and analysis of chemical or biological samples. Further research on a dye doped fiber bundles could result in a disposable high-power blue source. A single dye doped fiber could be envisioned as a fluorescing sensor for detecting certain cancers within a patient or for chemical and biological agents in enclosed areas. Development of such technologies would undoubtedly have a large impact on society.

Appendix A

Definitions parameters and constants

Quantity	Symbol
Amplified spontaneous emission	ASE
Two-photon absorption	TPA
Absorption	A
Transmission	T
Intensity	I
Number density	N
Energy	E
Plank's constant $6.6260755 \cdot 10^{-34}$	h
Boltzman's constant	k
Absorption coefficient	α
Linear absorption cross section	σ
Two-photon absorption cross section	σ_2
Wavelength of pump laser	λ_p
Wavelength of emitted ASE signal	λ_{ASE}
Wavelength of emitted fluorescence	λ_{Fluor}

Table A.1: Definitions parameters and constants

Appendix B

Summary of the properties of blue-emitting dyes.

Dye	Absorption (nm)	Fluorescence (nm)	ASE (nm)	ASE Gain (cm^{-1})	Fluorescence Efficiency ϕ_f	Linear cross-sect σ (cm^2)	Two-photon cross-sect σ_2	Geometry	Dimensions	Concentration M (molec/cm^3)	Ref.
NRL303a	394	487	460	7	0.88^a	-	-	film	3cm x 2cm x 0.1cm	2x10^{-3}M	This Work
NRL303a	-	-	460	-	0.88^a	-	-	fiber	2.5cm x 500m dia	2x10^{-3} M	This Work
NRL303b	-	490	460	3	0.88^a	-	-	film	1.35 x 1.75 x 0.08	1.6x10^{-2}M	This Work
NRL303b	-	490	460	4	0.88^a	-	-	fiber	2.5 cm x 400m dia	1.6x10^{-2} M	This Work
Fluorescein	-	-	-	-	-	-	8 37 GM	water	-	1.45 x 10-5 M	[18]
Fluorescein	-	-	-	-	-	-	38 GM	water	-	100M	[19]
Fluorescein	-	-	-	-	-	-	0.075 GM	-	-	-	[19]
Fluorescein	-	-	-	-	-	-	0.23 ± 0.07 GM	-	-	-	[19]
Rh6G	530	556	-	-	-	-	-	-	-	-	This work
Rh6G	-	-	-	-	0.95	-	-	-	-	-	[47]
Rh6G	-	-	-	-	-	-	150GM	-	-	50-100M	[18]

Dye	Absorption (nm)	Fluorescence (nm)	ASE (nm)	ASE Gain (cm^{-1})	Fluorescence Efficiency ϕ_f	Linear cross-sect σ (cm^2)	Two-photon cross-sect σ_2	Geometry	Dimensions	Concentration M (molec/cm^3)	Ref.
BASF 339	526	605, 650	-	-	-	3.5×10^{-16}	-	slab	85x50x2.9mm3	10^{-4} M	[39]
KF241	577	535, 575	-	-	-	2.4×10^{-16}	-	slab	85x50x2.9mm3	10^{-4} M	[39]
C490 (pmma/etoh)	382	472	478	0.55	-	-	-	rod	3cm , 1cm dia.	2×10^{-2} M	[23]
C490 (MMA)	382	475	475	3.9	-	-	-	-	-	2×10^{-2} M	[23]
C490	380	460	476	6.1	-	-	-	-	-	2×10^{-2} M	[23]
C490 (mma/EtOH)	382	482	489	9	-	2.6×10^{-19}	-	EtOH	1cm	2×10^{-2} M	[23]
C490 (EtOH)	379	450	449	6.25	-	2.5×10^{-19}	-	EtOH	1cm	3×10^{-2} M	[24]
Coumarin 1 (EtOH) (Coumarin460)	410	448	458	1.2	-	-	-	Disk	1mm thick, 2cm x 1cm dia.	3×10^{-2} M	[24]
Coumarin 1 (PMMA +EtOH)	374	426	425	4	-	-	-	solution	1cm quartz cell	3×10^{-2} M	[24]
Coumarin 1 (MMA)	376	452	451	5.7	-	-	-	solution	1cm quartz cell	3×10^{-2} M	[24]
Coumarin 1 (MMA+EtOH)	406	424	425	0.9 cm^{-1}	-	-	-	Disk MMA solid	1mm thick,	3×10^{-2} M	[24]
Rh6G (PMMA/EtOH)	514	586	585	1.2	-	-	-	rod	3 cm x 1.5 cm dia.	6×10^{-3} M	[15]
Rh6G (PMMA)	526	566	-	-	-	-	-	rod	3 cm x 1.5 cm dia.	6×10^{-3} M	[15]
Rh6G (MMA/EtOH)	531	570	580	2.8	-	1.4×10^{-18}	-	solution	1cm	6×10^{-3} M	[15]
Rh6G (EtOH)	532	570	580	11	-	1.7×10^{-18}	-	solution	1cm	6×10^{-3} M	[15]
Coumarin 503 (PMMA+EtOH)	448	485	505	0.2	-	-	-	rod	-	3×10^{-2} M	[25]
Coumarin 503 (MMA+EtOH)	445	482	504	9.8	-	-	-	solution	-	3×10^{-2} M	[25]
Coumarin 503 (EtOH)	445	489	504	15.8	-	-	-	solution	-	3×10^{-2} M	[25]
Coumarin 503 (MMA)	443	470	473	8.2	-	-	-	solution	-	3×10^{-2} M	[25]
Coumarin 307 (PMMA+Dioxane)	387	467	491	3	-	-	-	rod	-	30×10^{-2} M	[26]
Coumarin 307 (MMA+Dioxane)	385	469	480	4.9 cm^{-1}	-	-	-	solution	-	-	[26]
Coumarin 307 (Dioxane)	380	476	480	3.6 cm^{-1}	-	-	-	solution	-	-	[26]
Coumarin 307 (MMA)	385	471	476	6 cm^{-1}	-	-	-	solution	-	-	[26]
Coumarin334	450	-	-	-	-	-	-	PMMA	film	0 by wt	[40]
C334 / TPB	-	455	-	-	-	-	-	PMMA	film	1/100 by wt	[40]
C334 / TPB	-	465	-	-	-	-	-	PMMA	film	1/32 by wt	[40]
C334 / TPB	-	480	-	-	-	-	-	PMMA	film	40% by wt	[40]
TPB	480	-	-	-	-	-	-	film	-	-	[40]
EtCz	-	370	-	-	-	-	-	film	700nm thick	-	[41]
5MeCz	-	380	-	-	-	-	-	film	700nm thick	-	[41]
EtCz2	-	420	430	-	-	-	-	film	700nm thick	-	[41]
ADD-1	371	425	-	-	-	-	-	rod	2.5cm dia.	1 to 7×10^{-4} M	[42]
ADD-2	364	420	-	-	-	-	-	rod	2.5cm dia.	1 to 7×10^{-4} M	[42]
ADD-3	374	443	-	-	-	-	-	rod	2.5cm dia.	1 to 7×10^{-4} M	[42]
m-LPPP	425	455	490	-	-	2.5×10^{-15}	-	film	100-200nm	conj. polymer	[43]
m-LPPP	450	490	-	-	-	-	-	solution	-	-	[42]
P1	265	425	455	-	-	-	-	film	-	-	[42]
PPV	440	460	455	-	-	-	-	ps fiber	1mm thick	2.8×10^{-3} M	[44]
SP35	-	-	494	36	0.85	-	-	ps film	0.5mm dia	1% by wt.	[42]
mppb	350-350	420	420	3.5 - 10	-	-	-	film	300-1000nm thick	-	[44]
PF3Cz	370	-	448	26	0.9	2.8×10^{-16}	-	film	200nm thick	(1.7×10^{17})	[45]
CBP	-	393	394	13	0.61	-	-	film	100nm	-	[46]
mCBP	-	400	401	4	0.49	-	-	film	100nm	-	[46]
dCBP	-	409	406	7.8	0.6	-	-	film	100nm	-	[46]
DPABP	-	419	423	13	0.44	-	-	film	100nm	-	[46]
TPD	-	424	424	12	0.41	-	-	film	100nm	-	[46]
α-NPD	-	445	-	-	0.29	-	-	film	100nm	-	[46]

Table B.1: Blue Emitting Dyes in PMMA

Appendix C

Mathematica Code for ASE decay analysis

```
■ Set Working directory

    (* Check working Directory *)
    << Statistics`NonlinearFit`
    Directory[]
    (***SetDirectory["C:\My Documents\Fits\TestFile"]
      C:\My Documents\Physics\Research Archive\NRL303\Data\a355Decay16July03\Decay02
        SetDirectory["D:\Documents and Settings\Administrator\My Documents\Fits\TestFile"]
        SetDirectory["D:\Documents and Settings\Administrator\My Documents\
          Research Archive\NRL303\Data\a355Decay16July03\Decay02"]***)

    SetDirectory[
      "D:\Documents and Settings\Administrator\My Documents\Research Archive\
        NRL303\Data\a355Decay16July03\Decay02"]

    D:\Documents and Settings\Administrator\My
      Documents\Research Archive\NRL303\Data\a355Decay16July03\Decay02
    D:\Program Files\Wolfram Research\Mathematica\5.0 Null

    FileNames["*"]

    {absFit.txt, NRL355Decay.0000000.Master.Scope, NRL355Decay.0000001.Master.Scope,
      NRL355Decay.0000002.Master.Scope, NRL355Decay.0000003.Master.Scope,
      NRL355Decay.0000004.Master.Scope, NRL355Decay.0000005.Master.Scope,
      NRL355Decay.0000006.Master.Scope, NRL355Decay.0000007.Master.Scope,
      NRL355Decay.0000008.Master.Scope, NRL355Decay.0000009.Master.Scope,
      NRL355Decay.0000010.Master.Scope, NRL355Decay.0000011.Master.Scope,
      NRL355Decay.0000012.Master.Scope, NRL355Decay.0000013.Master.Scope,
      NRL355Decay.0000014.Master.Scope, NRL355Decay.0000015.Master.Scope,
      NRL355Decay.0000016.Master.Scope, TestFile01.txt, TestFile02.txt,
      TestFile03.txt, TestFile04.txt, TestFile05.txt, test00I00.txt, test00I01.txt}
```

Import Files

Clear & Set File Names, Import and cut data to length.

```
Clear["dataset*"]; Clear["decaytimes*"]; Clear["datarevised*"]; Clear["datasetnames*"];
Clear["datasetnames"];
Clear["rawdata*"]; Clear["fluordata*"]; Clear["asedata*"]; Clear["dataplot*"]; Clear["fluorplot*"];
Clear["flrplot*"];
Clear["rawplot*"]; Clear["ASEplot*"]; Clear["nfits*"];
datasetnames = FileNames["NRL*"];  (** <- set file names to import **)
Length[datasetnames];
For[i = 1, i <= Length[datasetnames], i++,
    (*** Import DataFiles ***)
    Evaluate[ToExpression["datasetnames" <> ToString[i]]] = Import[datasetnames[[i]], "Table"];
    (*** Read Time, needs Extract[] to make time a real number and not a list of numbers length 1 ***)
    Evaluate[ToExpression["decaytimes" <> ToString[i]]] =
      Extract[ReadList[datasetnames[[i]], Record, RecordSeparators → {{"Date:", " "}, {"User:", "Valued"}}], 1];
    (*** raw data cut to length ***)
    Evaluate[ToExpression["rawdata" <> ToString[i]]] =
      Take[Evaluate[ToExpression["datasetnames" <> ToString[i]]],
        {22, Length[ToExpression["datasetnames" <> ToString[i]]] - 1}];
    (*** This   Take[Evaluate[ToExpression["datasetnames"<>ToString[i]]],
            Sets datsetnames to each file "table" values instead of {File1.txt, File2.txt} list in datasetnames[[]] ***)
    (*** Fluorescence peak from datafile ***)
    Evaluate[ToExpression["fluordata" <> ToString[i]]] =
      Take[Evaluate[ToExpression["datasetnames" <> ToString[i]]],
        {400, Length[ToExpression["datasetnames" <> ToString[i]]] - 1000}];
    (*** ASE peak from datafile ***) Evaluate[ToExpression["asedata" <> ToString[i]]] =
      Take[Evaluate[ToExpression["datasetnames" <> ToString[i]]],
        {35, Length[ToExpression["datasetnames" <> ToString[i]]] - 1720}];
    (** Print[i]   (* <-- For debugging purposes only! *) **)
    ]; (* <--- Closes For[] statement *)
(*** datasetnames (* This test for link between datasetnames[[i]] and "file name" *)
    decaytimes5 (* This test extraction of decay time from a file *) ***)
```

Null[7]

```
Length[datasetnames]
```

17

■ Test Import and size of tables

```
datasetnames;

datasetnames1 // TableForm;

fluordata1 // TableForm;
```

■ Import Absorbance File for Test Fit (x-axis inverted to match fluorescene)

cut imported data file to length & plot (absorb fit)

```
absorb = Import["absFit.txt", "Table"];
absorb // TableForm;
absorb2 = Take[absorb, {380, 780}];
absorbdataplot = ListPlot[absorb2, PlotRange → All, DisplayFunction → Identity];
```

```mathematica
For[i = 1, i <= Length[datasetnames], i++,
    (*** Import DataFiles ***)
    Evaluate[ToExpression["datasetnames" <> ToString[i]]] = Import[datasetnames[[i]], "Table"];
    (*** Read Time, needs Extract[] to make time a real number and not a list of numbers length 1 ***)
    Evaluate[ToExpression["decaytimes" <> ToString[i]]] =
      Extract[ReadList[datasetnames[[i]], Record, RecordSeparators -> {{"Date:", " "}, {"User:", "Valued"}}], 1];
    (*** raw data cut to length ***)
    Evaluate[ToExpression["rawdata" <> ToString[i]]] =
      Take[Evaluate[ToExpression["datasetnames" <> ToString[i]]],
        {22, Length[ToExpression["datasetnames" <> ToString[i]]] - 1}];
    (*** This  Take[Evaluate[ToExpression["datasetnames"<>ToString[i]]],
         Sets datsetnames to each file "table" values instead of {File1.txt, File2.txt} list in datasetnames[[]] ***)
    (*** Fluorescence peak from datafile ***)
    Evaluate[ToExpression["fluordata" <> ToString[i]]] =
      Take[Evaluate[ToExpression["datasetnames" <> ToString[i]]],
        {400, Length[ToExpression["datasetnames" <> ToString[i]]] - 1000}];
    (*** ASE peak from datafile ***) Evaluate[ToExpression["asedata" <> ToString[i]]] =
      Take[Evaluate[ToExpression["datasetnames" <> ToString[i]]],
        {35, Length[ToExpression["datasetnames" <> ToString[i]]] - 1720}];
    (** Print[i]  (* <-- For debugging purposes only! *) **)
    ]; (* <--- Closes For[] statement *)
(*** datasetnames (* This test for link between datasetnames[[i]] and "file name" *)
    decaytimes5(* This test extraction of decay time from a file *) ***)
```

Null^7

```mathematica
Length[datasetnames]
```

17

■ Test Import and size of tables

```mathematica
datasetnames;

datasetnames1 // TableForm;

fluordata1 // TableForm;
```


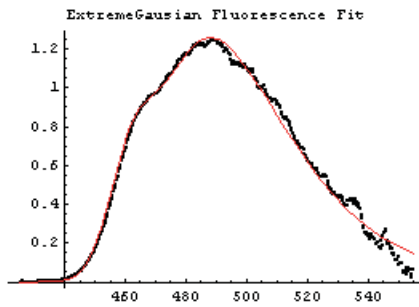## ■ Import Absorbance File for Test Fit (x-axis inverted to match fluorescene)

cut imported data file to length & plot (absorb fit)

```mathematica
absorb = Import["absFit.txt", "Table"];
absorb // TableForm;
absorb2 = Take[absorb, {380, 780}];
absorbdataplot = ListPlot[absorb2, PlotRange -> All, DisplayFunction -> Identity];
```

ExtremeGausian Fluorescence Fit

■ Convert Time string to number (from data file header)

```
Clear["thetime*"];
Clear["d1time*"];
Clear["d2time*"];
For[i = 1, i <= Length[datasetnames], i++ 1,
    Evaluate[ToExpression["d1time" <> ToString[i]]] =
        StringDrop[Evaluate[ToExpression["decaytimes" <> ToString[i]]], {3, 3}];
    Evaluate[ToExpression["d2time" <> ToString[i]]] =
        StringReplacePart[Evaluate[ToExpression["d1time" <> ToString[i]]], ".", {5, 5}];
    Clear[t2];
    Clear[t3];
    t2 = StringToStream[Evaluate[ToExpression["d2time" <> ToString[i]]]];
        t3 = Read[t2, Number];
                Evaluate[ToExpression["thetime" <> ToString[i]]] = t3;
    Close[t2];
    Clear[t2];
    (** Print[i]; **) (* <-- For debugging purposes only! *)
    ]; (* <--- Closes For[] statement *)
```

■ Test Corrected Time output

```
t2
t3
thetime1
thetime2
thetime3
thetime4
thetime5
```

t2

1135.12

1120.4

85

■ Extreme Gausian Fit to Fluorescence Data Table

```mathematica
datasetnames
```

{NRL355Decay.0000000.Master.Scope, NRL355Decay.0000001.Master.Scope,
  NRL355Decay.0000002.Master.Scope, NRL355Decay.0000003.Master.Scope, NRL355Decay.0000004.Master.Scope,
  NRL355Decay.0000005.Master.Scope, NRL355Decay.0000006.Master.Scope, NRL355Decay.0000007.Master.Scope,
  NRL355Decay.0000008.Master.Scope, NRL355Decay.0000009.Master.Scope, NRL355Decay.0000010.Master.Scope,
  NRL355Decay.0000011.Master.Scope, NRL355Decay.0000012.Master.Scope, NRL355Decay.0000013.Master.Scope,
  NRL355Decay.0000014.Master.Scope, NRL355Decay.0000015.Master.Scope, NRL355Decay.0000016.Master.Scope}

```mathematica
Clear["nfit*"];
Needs["Statistics`NonlinearFit`"]
For[i = 1, i <= Length[datasetnames], i++ 1,
    Evaluate[ToExpression["nfits" <> ToString[i] <> "[x_]"]] =
    NonlinearFit[Evaluate[ToExpression["fluordata" <> ToString[i]]],
```

$$\text{Amp} * E^{\left(-E^{(-x+488)/w} - (x-488)/w + 1\right)} + 0.33 * \text{Amp} * E^{-2\,(x-461)^\wedge 2/(w/1.5)^\wedge 2}, \{x\}, \{\text{Amp}, w\},$$

```mathematica
    MaxIterations -> 1000];
            (*** Print[i] ***)  (* <-- For debugging purposes only! *)
  ]; (* <--- Closes For[] statement *)
```

Show fits...

```mathematica
nfits1[x] // TableForm;
nfits2[x] // TableForm;
nfits3[x] // TableForm;
nfits4[x] // TableForm;
nfits5[x] // TableForm;


(*** nfitstable1 = Table[{i, nfits1[i]}, {i, 1, 20}]
nfitstable1//TableForm
Head[nfitstable1]
Head[nfits1]
FullForm[nfitstable1]
FullForm[nfits1] ***)
```

$$\text{Amp} * E^{\left(-E^{(-x+488)/w} - (x-488)/w + 1\right)} + 0.33 * \text{Amp} * E^{-2\,(x-461)^\wedge 2/(w/1.5)^\wedge 2}$$

■ Make Plots from fits

$$\text{Amp} * E^{\left(-E^{(-x+490)/w} - (x-490)/w + 1\right)} + 0.4 * \text{Amp} * E^{-2\,(x-470)^\wedge 2/(w/2)^\wedge 2}$$

```mathematica
Clear["nfit*"];
```

```
Clear["nfit*"];
Needs["Statistics`NonlinearFit`"]
For[i = 1, i <= Length[datasetnames], i++ 1,

  Evaluate[ToExpression["nfits" <> ToString[i] <> "[x_]"]] =
    NonlinearFit[Evaluate[ToExpression["fluordata" <> ToString[i]]],

      Amp*E^(-E^((-x+490)/w) - (x-490)/w+1) + 0.33*Amp*E^(-2 (x-461)^2/(w/1.5)^2), {x}, {Amp, w},

      MaxIterations -> 1000];

              (*** Print[i] ***) (* <-- For debugging purposes only! *)
  ]; (* <--- Closes For[] statement *)
Clear["fitplot*"];
For[i = 1, i <= Length[datasetnames], i++ 1,


    (*** Fit PLOT s ***)Evaluate[ToExpression["fitplot" <> ToString[i]]] =
      Plot[Evaluate[ToExpression["nfits" <> ToString[i] <> "[x]"]], {x, 430, 600}, PlotRange -> All,
        PlotLabel -> Evaluate[ToExpression["Fit" <> ToString[i]]], PlotStyle -> Hue[2],
        DisplayFunction -> Identity];


    Show[{Evaluate[ToExpression["fitplot" <> ToString[i]]], Evaluate[ToExpression["flrplot" <> ToString[i]]]},
      DisplayFunction -> $DisplayFunction];
    (** Print[i] (* <-- For debugging purposes only! *) **)
    ]; (* <--- Closes For[] statement *)
```
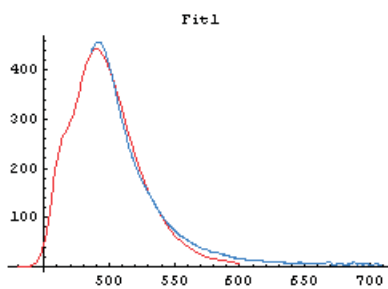
■ **Plot Raw Data: Whole File, Fluorescence, ASE.**

Clear["dataplot*"]; Clear["flrplot*"]; Clear["ASEplot*"];
For[i = 1, i <= Length[datasetnames], i++,

    Evaluate[ToExpression["dataplot" <> ToString[i]]] =
      ListPlot[Evaluate[ToExpression["rawdata" <> ToString[i]]], PlotJoined → True, Frame → True,
        PlotRange → All, Background → RGBColor[0, 0, 0], PlotStyle → Hue[.6], PlotLabel → "RAW Data",
   **AxesLabel → {"Wavelength", "Intensity"}, DisplayFunction → Identity];**

    Evaluate[ToExpression["flrplot" <> ToString[i]]] =
      ListPlot[Evaluate[ToExpression["fluordata" <> ToString[i]]], PlotJoined → True, Frame → True,
        PlotRange → All, Background → RGBColor[0, 0, 0], PlotStyle → Hue[.6], PlotLabel → "Fluorescence Data",
        AxesLabel → {"Wavelength", "Intensity"}, DisplayFunction → Identity];

    Evaluate[ToExpression["ASEplot" <> ToString[i]]] =
      ListPlot[Evaluate[ToExpression["asedata" <> ToString[i]]], PlotJoined → True, Frame → True,
        PlotRange → All, Background → RGBColor[0, 0, 0], PlotStyle → Hue[.6], PlotLabel → "ASE Data",
        DisplayFunction → Identity];

    (Print[i] (* <-- For debugging purposes only! *) **)**
    ]; (* <--- Closes For[] statement *)
Show[GraphicsArray[{dataplot1, flrplot1, ASEplot1}]];
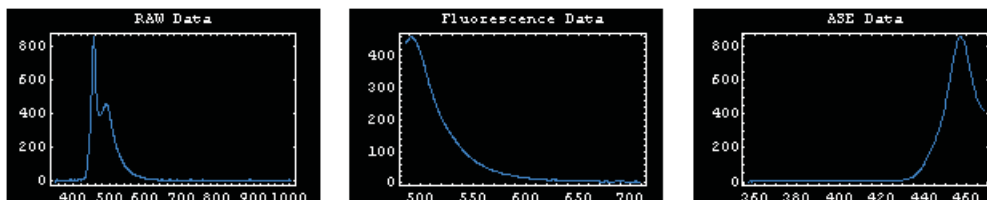
Show[{dataplot4, lastplot4}, DisplayFunction → $DisplayFunction];
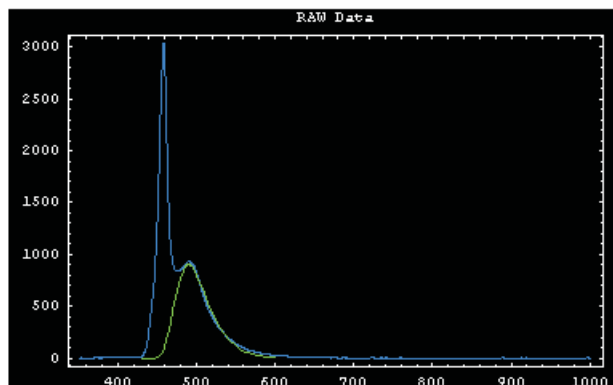
**Fits subtracted from data tables**

(∗∗∗ Fit Subtracted from data ∗∗∗)

```
Clear["dataminus∗"]
For[i = 1, i <= Length[datasetnames], i++ 1,
    Evaluate[ToExpression["dataminusfit" <> ToString[i]]] =
      Table[{Evaluate[ToExpression["rawdata" <> ToString[i]]][[k]][[1]],
          Evaluate[ToExpression["rawdata" <> ToString[i]]][[k]][[2]] −
            Evaluate[ToExpression["nfits" <> ToString[i]]][
              Evaluate[ToExpression["rawdata" <> ToString[i]]][[k]][[1]]]},
        {k, 1, Length[Evaluate[ToExpression["fluordata" <> ToString[i]]]]}];
    (∗ Print[i]; ∗)
  ];
```

ListPlot[dataminusfit1, PlotJoined → True, PlotRange → All]
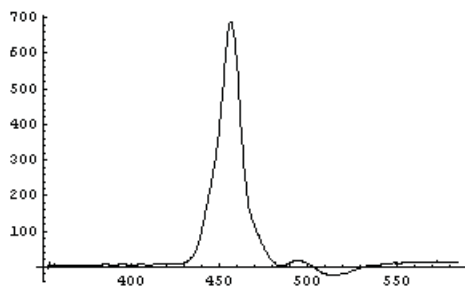
- Graphics -

Max[%]

DataMinusFit = Table[{rawdata1[[i]][[1]], rawdata1[[i]][[2]] − nfits1[rawdata1[[i]][[1]]]}, {i, 1, Length[fluordata1]}];

ASE = ListPlot[dataminusfit1, PlotRange → All, PlotJoined → True, PlotStyle → Hue[.1], DisplayFunction → Identity]

Show[{ASE, lastplot1, dataplot1}, DisplayFunction → $DisplayFunction];

- Graphics -

Show::gcomb : An error was encountered in combining the graphics objects in
    Show[{- Graphics -, lastplot1, - Graphics -}, DisplayFunction → (Display[$Display, #1] &)]. More...

◼ Make decay tables & Plots

```
Table[{decaytimes[i], Max[dataminusfit1]}]
```

```
(*** Gives max peak ve for corrected ASE ***)
Clear["peakmax*"];
For[i = 1, i <= Length[datasetnames], i++ 1,
    Evaluate[ToExpression["peakmax" <> ToString[i]]] =
      Max[Evaluate[ToExpression["dataminusfit" <> ToString[i]]]];
    (* Print[i] *)
    ;];
```

```
peakmax1
peakmax2
peakmax3
peakmax4
peakmax5
peakmax6
```

688.657

659.521

2869.65

2666.25

2602.58

2466.22

```
decaytable = {{thetime1, peakmax1}}
```

{{1120.4, 688.657}}

```
(** {Evaluate[ToExpression["thetime"<>ToString[i]]],Evaluate[ToExpression["peakmax"<>ToString[i]]]} **)
```

{1122.4, 14.6565}

```
(*** Combind Time and ASE Peak value  To Table == decaytable ***)
decaytable = {};
Clear["timetable*"];
For[i = 1, i <= Length[datasetnames], i++ 1,

  AppendTo[decaytable, {Evaluate[ToExpression["thetime" <> ToString[i]]],
      Evaluate[ToExpression["peakmax" <> ToString[i]]]}];

  (* Print[i]; *)];
```

■ Make decay tables & Plots

```mathematica
Table[{decaytimes[i], Max[dataminusfit1]}]
```

```mathematica
(*** Gives max peak ve for corrected ASE ***)
Clear["peakmax*"];
For[i = 1, i <= Length[datasetnames], i++ 1,
    Evaluate[ToExpression["peakmax" <> ToString[i]]] =
      Max[Evaluate[ToExpression["dataminusfit" <> ToString[i]]]];
    (*Print[i]*)
    ;];
```

```mathematica
peakmax1
peakmax2
peakmax3
peakmax4
peakmax5
peakmax6
```

688.657

659.521

2869.65

2666.25

2602.58

2466.22

```mathematica
decaytable = {{thetime1, peakmax1}}
```

{{1120.4, 688.657}}

```mathematica
(** {Evaluate[ToExpression["thetime"<>ToString[i]]],Evaluate[ToExpression["peakmax"<>ToString[i]]]} **)
```

{1122.4, 14.6565}

```mathematica
(*** Combind Time and ASE Peak value  To Table == decaytable ***)
decaytable = {};
Clear["timetable*"];
For[i = 1, i <= Length[datasetnames], i++ 1,

  AppendTo[decaytable, {Evaluate[ToExpression["thetime" <> ToString[i]]],
      Evaluate[ToExpression["peakmax" <> ToString[i]]]}];

  (*Print[i]; *)];
```

```
AppendTo[decaytable, {Evaluate[ToExpression["thetime" <> ToString[i]]],
    Evaluate[ToExpression["peakmax" <> ToString[i]]]}];

(* Print[i]; *)];
```

decaytable // TableForm

1120.4	688.657
1121.06	659.521
1122.1	2869.65
1122.41	2666.25
1122.56	2602.58
1123.3	2466.22
1124.03	2267.21
1124.4	2184.02
1124.4	2184.02
1125.58	1772.21
1127.5	1417.17
1129.52	1158.7
1129.54	1097.14
1129.58	1056.62
1131.49	860.729
1134.09	726.147
1135.12	645.867

■ Generate ASE peak emission vs Time Plot (ASE Decay)

ListPlot[decaytable, PlotRange → {0, 3000}]
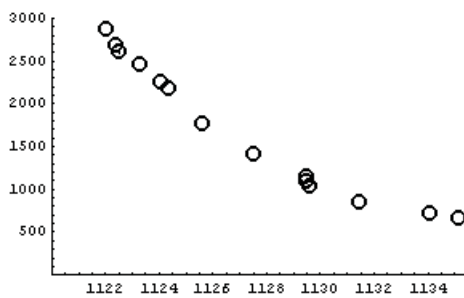
-Graphics -

Bibliography

[1] Mitsuo Maeda, *Laser Dyes, properties of Organic Compounds for Dye Lasers* (Academic Press, Orlando, 1984)

[2] G. Marowsky, *IEEE J.Quantum Electron.* **16**, 49 (1980).

[3] F.P.Schafer editor , *Topics in Applied Physics Vol1, Dye Lasers*, (Berlin, New York, Springer-Verlag, 1990) 3rd ed.

[4] P.P.Sorokin and J.R.Lankard, *IBM J. Res Dev.* **10**, 162, 1966

[5] P.P.Sorokin and J.R.Lankard, *IBM J. Res Dev.* **11**, 148, 1967

[6] N.E. Wolff and R.J. Pressley, "Optical maser action in an Eu+3 -containing organic matrix," *Appl. Phys. Let* **2**, 152 (1963)

[7] E.H. Huffman, "Stimulated optical emission of a terbium ion chelate in vinylic resin matrix," *Nature* **200**, 158 (1963)

[8] D.W.Gregg and S.J. Thomas, *IEEE J. QE5* **302**, 1969

[9] C.V. Shank, A. Dienes, W. Silfvast. *Applied Physics Letters* **17**, 307 (1970).

[10] K.H. Drexhage, *Structure and Properties of Laser Dyes in Topics in Applied Physics, Dye Lasers* (Springer-Verlang, Berlin, Germany 1990), pp.155-171.

[11] W. Kaiser, C.G.B. Garrett, D.L. Wood, *Phys. Rev.* **123**, 766 (1961).

[12] M. Goppert-Mayer. Ueber Elementarake mit zwei Quantenspruengen *Ann. Phys* **9**, 273-83 (1931).

[13] R.W. Boyd, *Nonlinear Optics* (Academic Press, San Diego, United States of America, 1992).

[14] O. Kim, K. Lee, Z. Huang, W. Heuer,C. Paik-Sung,*Optical Materials* **21**, 559-564 (2002).

[15] G. Somasundaram, A. Ramalingam. "Gain studies of Rhodamine 6G dye doped polymer laser." *J.Photochem & Photobio A:Chem* **125**, 93-98 (1999).

[16] Y. Meshalkin, V. Svetlichnyi, A. Reznichenko, A Myachin, S. Bakhareva, S. Dolotov, T. Kopylova, E. Ponomarenko "Two-photon excitation of dyes in polymer matrix by femtosecond pulses from a Ti:sapphire laser." *Quantum Electronics* **33**(9), 803-806 (2003).

[17] C. Xu, W. Zipfel, J. Shear, R. Williams, W. Webb, "Multiphoton fluorescence excitation: New spectral windows for biological nonlinear microscopy." *Proc. Narl. Acad. Sci. USA* **93**, 10763-10768 (1996)

[18] M. Albota, C. Xu, W. Webb,"Two-photon fluorescence excitation cross sections of biomolecular probes from 690 to 960nm" *Appl. Opt.* **37**, 7352-7356 (1998)

[19] C. Xu, W. Webb,"Measurment of two-photon excitation cross sections of fluorophores with data from 690 to 1050nm," *J.Opt. Soc. Am.B* **13**,(3), 481-491 (1996)

[20] C. Xu, J. Guild, W. Webb, W. Denk,"Determination of absolute two-photon excitation cross sections by in situ second-order autocorrelation" *Opt. Lett.* **20**, 23 2372-2374 (1995)

[21] A. Fischer, C. Cremer and E. Stelzer,"Fluorescence of coumarins and xanthenes after two-photon absorption with a pulsed titanium-sapphire laser", *App.Opt.* **l34**(12), 1989-2003 (1995)

[22] A. Costella, I. GarciaMoreno, C. Gomez, O. Garcia and R. Sastre,"New organic-inorganic hybrid matricies doped with rhodamine 6G as solidstate dye lasers", *App.Phys.B* **75**, 827-833 (2002)

[23] G. Somasundaram, A. Ramalingam. "Gain studies of Coumarin 490 dye-doped polymer laser." *Chem Phys Lett* **324**, 25-30 (2000).

[24] G. Somasundaram, A. Ramalingam. "Gain studies of Coumarin 1 dye-doped polymer laser." J*ournal of Luminescence* **90**, 1-5 (2000).

[25] G. Somasundaram, A. Ramalingam. "Gain studies of Coumarin 530 dye-doped polymer laser." *Optics and Lasers in Engineering* **32**, 157-163 (2000).

[26] G. Somasundaram, A. Ramalingam, "Gain studies of coumarin 307 dye-doped polymer laser," *Optics & Laser Technology* **31**, 351-358 (1999)

[27] W. Zhang, N. Cue, and K. Yoo, "Emission linewidth of laser action in random gain media." *Opt. Let.* **20**(9), 961-963 (1995)

[28] O.-K Kim, Z. Huang, E. Peterson, S. Kirkpatrick and C. Sung, "Novel Two-Photon Absorbing Conjugated Oligmeric Chromphores: Property Modulation by π-Center." *manuscript to be published* (2004)

[29] O.-K Kim, et. al., "New Class of Two-Photon-Absorbing Chromophores Based on Dithenophene." *Chem. Matter* **12**, 284-286 (2000)

[30] J. Mama. "Developments in the chemistry of long wavelength fluorescent dyes." *Advances in Colour Science and Technology* **2**, 3 (1999)

[31] S. Nonell, C. Marti, I. garcia-Moreno, A. Costela, R. Sastre, "Opto-acoustic study of tinuvin-P and rhodamine 6G in solid polymeric matrices." *Appl. Phys. B.* **72**, 255-360 (2001)

[32] M. Kuzyk, C. Dirk,"Effects of centrosymmetry on the nonresonant electronic third-order nonlinear optical susceptibility," *Phys. Rev. A.* **41**(9), 5098-5109 (1990)

[33] M. Albota, et. al., *Science* **281**, 1653-1656, (1998)

[34] B. Howell, M. Kuzyk, "Amplified spontaneous emission and recoverable photo degradation in polymer doped with Disperse Orange 11" *J OPT SOC AM B* **19**(8), 1790-1793 (2002)

[35] M. Stuke, *Topics in applied physics, Dye Lasers* (Springer-Verlang, Berlin, Germany, 1992), Vol.70

[36] O. Kuhn and H. Kuhn, "A quantum mechanical theory of light absorption of organic dyes and similar compounds." *J. Chem. Phys.* **17**, 1198 (1949).

[37] S. Pond, et. al. "One- and Two-Photon Spectroscopy of Donor- Acceptor-Donor Distyrlbenzene Derivatives: Effect on Cyano Substituted and Distorion from Planarity." *J. Am. Chem. Soc.* **106**, 11470-11480 (2002).

[38] M. Rumi, et. al. "Structrue-Property relationships for Two-Photon Absorbing Chromophores: Bis-Donor Diphenylpolyene and Bis(styrl)benzene Derivatives." *J. Am. Chem. Soc.* **122**, 9500-9510 (2000).

[39] H. Manaa, S.M. Al-Alawi , "Optical gain measurements in polymethyl methacrylate plastic doped with perylimide dyes," *Journal of Luminescence* **94-95**, 55-58 (2001).

[40] J. Huang, V. Bekiari, P. Lianos, S. Couris, "Study of poly(methyl methacrylate) thin films doped with laser dyes," *Journal of Luminescence* **81**, 285-291 (1999).

[41] Castex, Olivero, Fischer, Mousel, Michelon, Ades, Siove, "Polycarazoles microcavities: towards plastic blue lasers," *Applied Surface Science* **197-198**, 822-825 (2002)

[42] V. Thiagarajan, C. Selvaraju, P. Ramamurthy, "Excited behavior of dyes in PMMA matrix, inhomogeneous broading and enhancment of triplet," *Journal of Photochemistry and Photobiology A: Chemistry* **157**, 23-31 (2003)

[43] C. Zenz, G. Kranzelbinder, W. Graupner, S. Tasch and G. Leising, "Blue green stimulated emission of a high gain conjugated polymer," *Synthetic Metals* **101**, 222-225 (1999)

[44] T. Kobayashi and W. Blau, "Blue amplified spontaneous emission from a stilbenoid-compound-doped polymer optical fiber," Optics Letters **26**(24), (2001)

[45] X. Liu, et. al. "Low-threshold amplified spontaneous emission and laser emission in a polyfluorene serivative," *Appl. Phys. Lett.* **84**(15), 2722-2729 (2004)

[46] Y. Kawamura, et. al. "Ultraviolet amplified sponatneous emission from thin films of 4,4'-bis(9-carbazolyl)-2,2'-biphenyl and the derivates," *Appl. Phys. Lett.* **84**(15), 2724-2726 (2004)

[47] P. Kaantz, D. Shelton, "Two-photon fluorescence cross-section measruments calibrated with hyper-rayleigh scattering." *J. Opt. Soc. Am. B* **16** (6), 998-1006 (1999)